Supporting Information for
Random Subsets of Structured Deterministic Frames have MANOVA Spectra
arxiv.org/abs/1701.01211

Marina Haikin, Ram Zamir, Matan Gavish

Full results

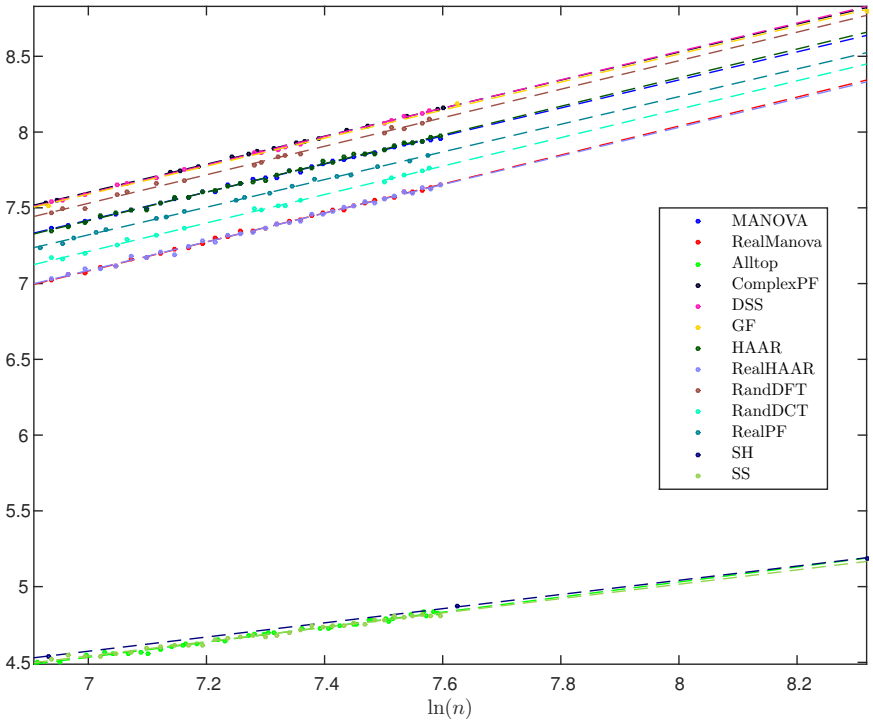

Figure 1: Test 1 for $\gamma = 0.5$ and $\beta = 0.8$. Plot shows $-\frac{1}{2}\ln Var_{K_n}(\Delta_{KS}(X_{K_n}^{(n)}; n, m_n, k_n))$ over $\ln(n)$.

Frame	R^2	$\hat{b}$	$SE(\hat{b})$	p-value $b = b_{MANOVA}$
MANOVA	0.99828	0.92505	0.00690	1
DSS	0.99858	0.93652	0.00911	0.32089
GF	0.99921	0.92474	0.02608	0.99082
ComplexPF	0.99950	0.92454	0.00535	0.95390
Alltop	0.98906	0.49660	0.00883	9.4651e-47
SS	0.98767	0.47354	0.00950	5.8136e-45
HAAR	0.99736	0.94421	0.00873	0.09019
RandDFT	0.99544	0.94127	0.01644	0.36788
RealMANOVA	0.99873	0.95610	0.00613	1
RealPF	0.99871	0.91244	0.00821	9.7174e-05
SH	0.99989	0.46822	0.00492	6.3109e-35
RealHAAR	0.99596	0.94456	0.01081	0.35675
RandDCT	0.99773	0.93859	0.01156	0.18737

Table 1: Results of Test 1 for $\gamma = 0.5$ and $\beta = 0.8$.

Frame	R^2	$\hat{b}$	$SE(\hat{b})$	p-value $b = b_{MANOVA}$
MANOVA	0.99993	0.85234	0.00126	1
DSS	0.99996	0.81176	0.00140	1.1392e-25
GF	0.99983	0.76518	0.00990	5.5733e-10
ComplexPF	0.99994	0.80178	0.00155	1.2255e-28
Alltop	0.99581	0.51708	0.00567	3.1903e-58
SS	0.99458	0.49792	0.00660	3.2466e-53
HAAR	0.99988	0.85488	0.00167	0.22822
RandDFT	0.99985	0.83460	0.00261	1.8531e-07
RealMANOVA	0.99996	0.85357	0.00101	1
RealPF	0.99996	0.82979	0.00131	7.8145e-19
SH	0.99999	0.49853	0.00144	2.9296e-51
RealHAAR	0.99975	0.85054	0.00243	0.25527
RandDCT	0.99992	0.84003	0.00189	9.9169e-08

Table 2: Results of Test 1 (MSE) for $\gamma = 0.5$ and $\beta = 0.8$.

Frame	R^2	$\hat{b}$	$SE(\hat{b})$	p-value $b = b_{MANOVA}$
MANOVA	0.98420	1.43554	0.03267	1
DSS	0.99108	1.40361	0.03439	0.50421
GF	0.99966	1.52986	0.02820	0.03630
ComplexPF	0.98611	1.44250	0.04421	0.89987
Alltop	0.98308	1.45646	0.03230	0.65043
SS	0.98659	1.49779	0.03137	0.17428
HAAR	0.98871	1.52271	0.02923	0.05117
RandDFT	0.98848	1.46925	0.04095	0.52317
RealMANOVA	0.99127	1.26008	0.02124	1
RealPF	0.99222	1.32138	0.02925	0.09656
SH	0.99990	1.33889	0.01308	0.00344
RealHAAR	0.98687	1.22579	0.02540	0.30443
RandDCT	0.98585	1.30063	0.04024	0.37744

Table 3: Results of Test 2 for Ψ_{AC}, $\gamma = 0.5$ and $\beta = 0.8$

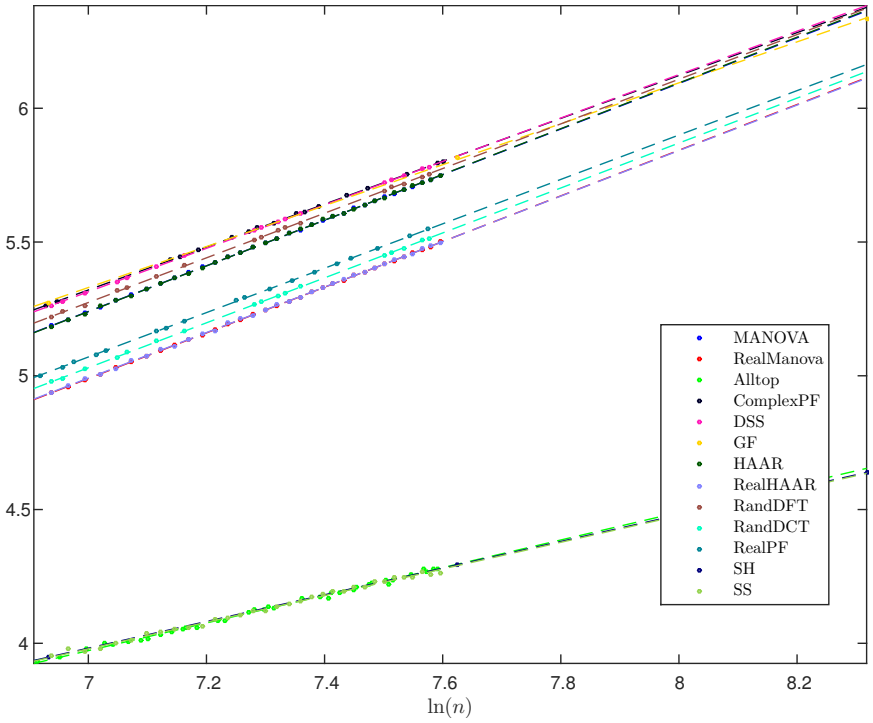

Figure 2: Test 1 for $\gamma = 0.5$ and $\beta = 0.8$. Plot shows $-\frac{1}{2}\ln \mathbb{E}_{K_n}(\Delta_{KS}(X^{(n)}_{K_n}; n, m_n, k_n)^2)$ over $\ln(n)$.

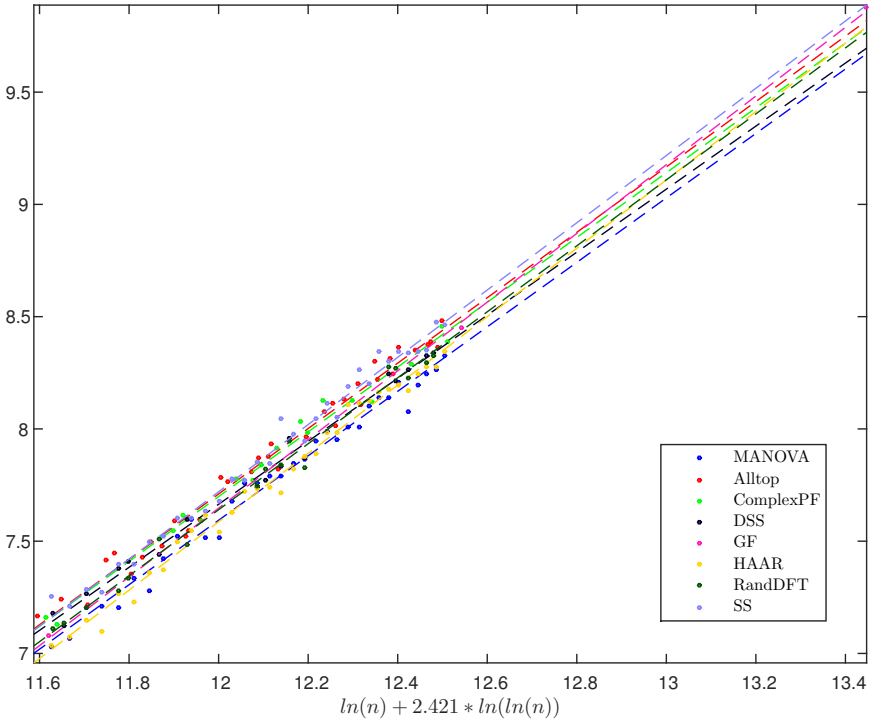

Figure 3: Test 2 for Ψ_{AC}, complex frames $\gamma = 0.5$ and $\beta = 0.8$. Plot shows $-\ln \mathbb{E}_{K_n}(\Delta_{\Psi}(X^{(n)}_{K_n}; n, m_n, k_n)^2)$

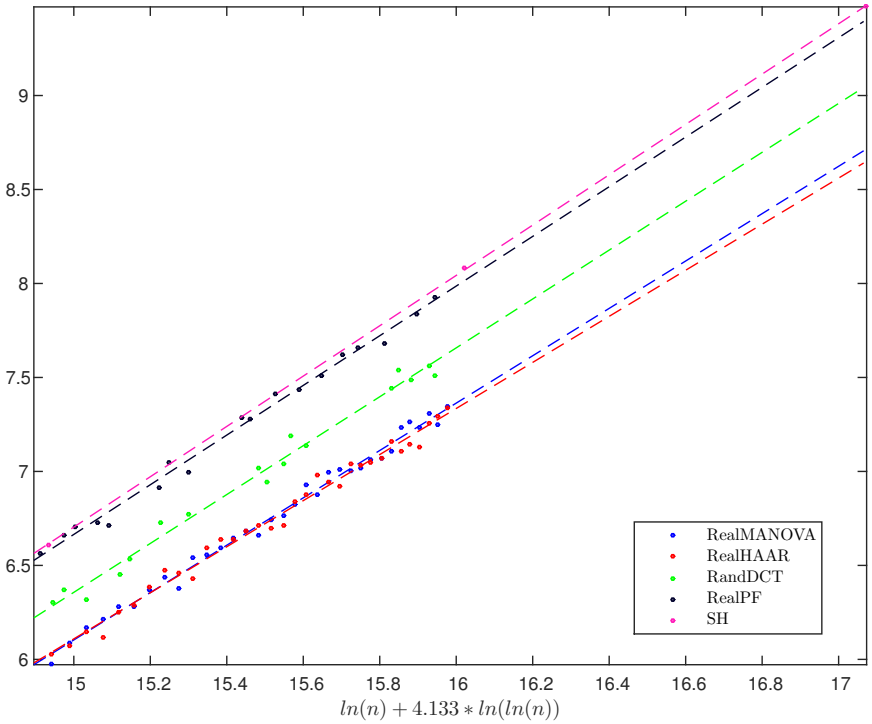

Figure 4: Test 2 for Ψ_{AC}, real frames $\gamma = 0.5$ and $\beta = 0.8$. Plot shows $-\ln \mathbb{E}_{K_n}(\Delta_\Psi(X_{K_n}^{(n)}; n, m_n, k_n)^2)$

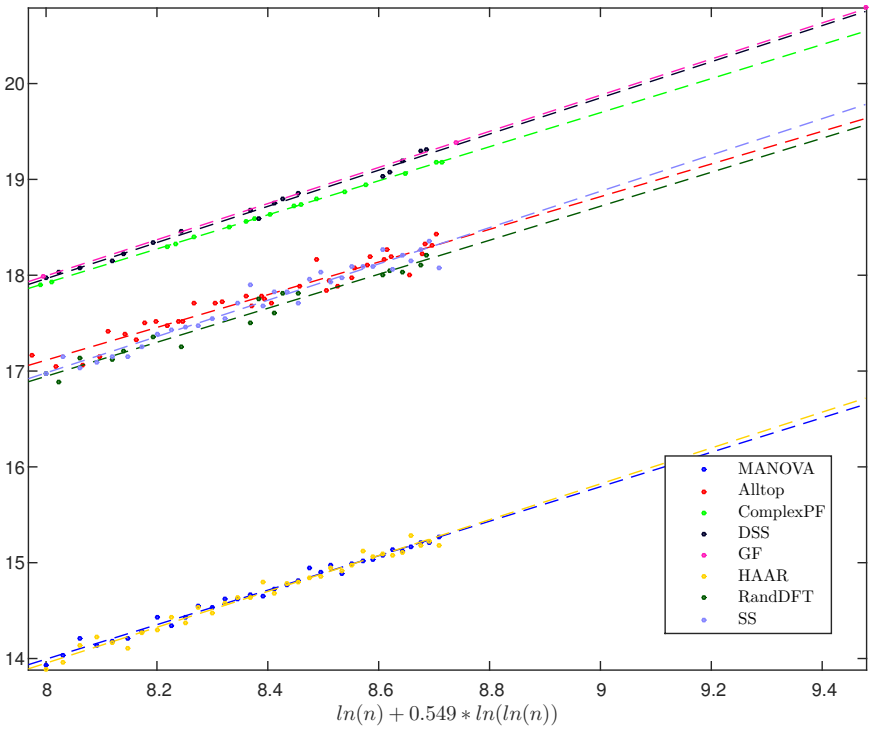

Figure 5: Test 2 for $\Psi_{Shannon}$, complex frames $\gamma = 0.5$ and $\beta = 0.8$. Plot shows $-\ln \mathbb{E}_{K_n}(\Delta_\Psi(X_{K_n}^{(n)}; n, m_n, k_n)^2)$

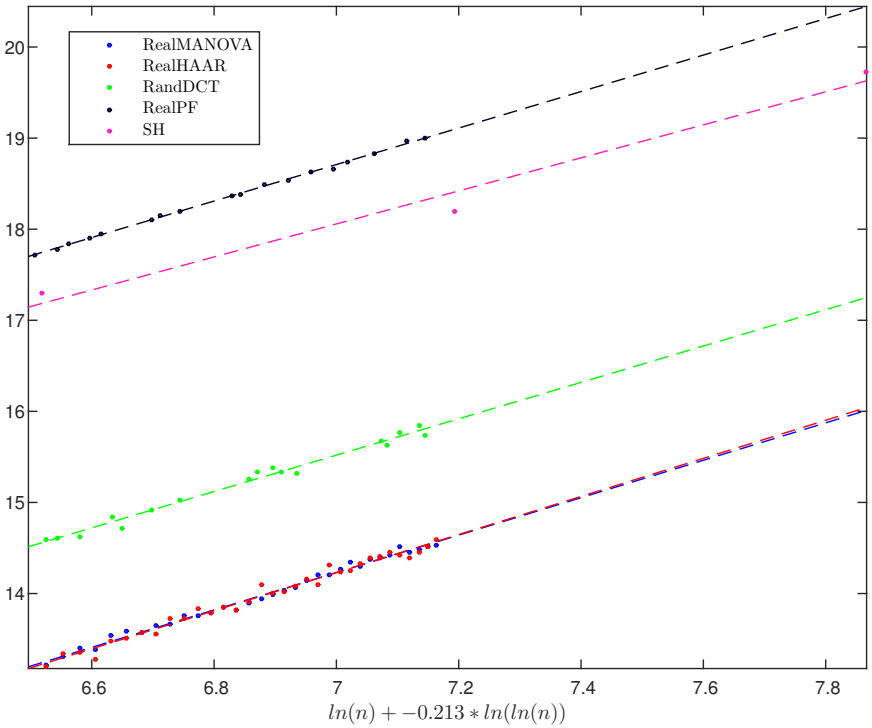

Figure 6: Test 2 for $\Psi_{Shannon}$, real frames $\gamma = 0.5$ and $\beta = 0.8$. Plot shows $-\ln \mathbb{E}_{K_n}(\Delta_\Psi(X_{K_n}^{(n)}; n, m_n, k_n)^2)$

Frame	R^2	$\hat{b}$	$SE(\hat{b})$	p-value $b = b_{MANOVA}$
MANOVA	0.98721	1.79936	0.03678	1
DSS	0.99110	1.88674	0.04615	0.14551
GF	0.99997	1.88548	0.01073	0.03161
ComplexPF	0.99977	1.77783	0.00701	0.56808
Alltop	0.93841	1.70618	0.07388	0.26297
SS	0.95539	1.89501	0.07355	0.24922
HAAR	0.97971	1.87082	0.04836	0.24400
RandDFT	0.96928	1.77454	0.08157	0.78270
RealMANOVA	0.99202	2.05451	0.03309	1
RealPF	0.99834	2.00345	0.02045	0.19576
SH	0.97850	1.81297	0.26874	0.37904
RealHAAR	0.98287	2.09078	0.04958	0.54503
RandDCT	0.98364	1.99663	0.06648	0.43977

Table 4: Results of Test 2 for $\Psi_{Shannon}$, $\gamma = 0.5$ and $\beta = 0.8$

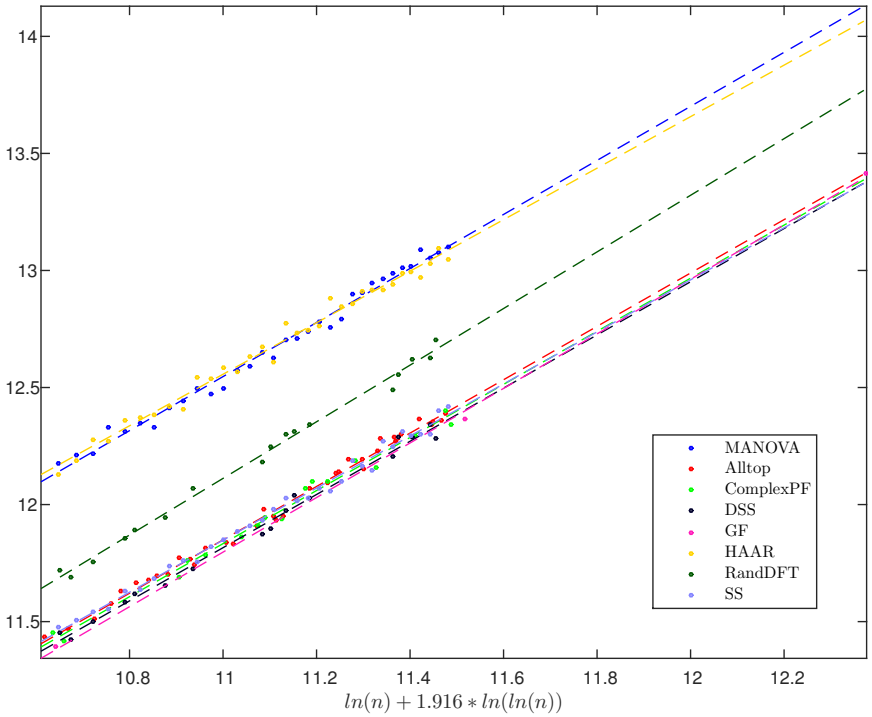

Figure 7: Test 2 for Ψ_{RIP}, complex frames $\gamma = 0.5$ and $\beta = 0.8$. Plot shows $-\ln \mathbb{E}_{K_n}(\Delta_\Psi(X^{(n)}_{K_n}; n, m_n, k_n)^2)$

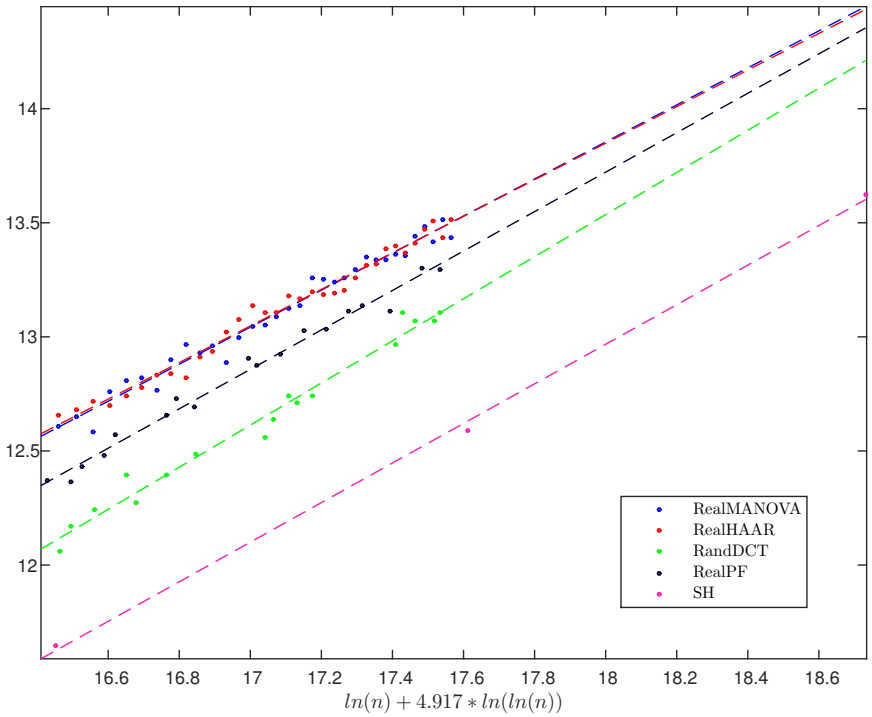

Figure 8: Test 2 for Ψ_{RIP}, real frames $\gamma = 0.5$ and $\beta = 0.8$. Plot shows $-\ln \mathbb{E}_{K_n}(\Delta_\Psi(X^{(n)}_{K_n}; n, m_n, k_n)^2)$

Frame	R^2	$\hat{b}$	$SE(\hat{b})$	p-value $b = b_{MANOVA}$
MANOVA	0.98923	1.15439	0.02164	1
DSS	0.99149	1.13602	0.02718	0.59944
GF	0.99930	1.16546	0.03085	0.77078
ComplexPF	0.98830	1.13383	0.03185	0.59592
Alltop	0.99222	1.13994	0.01706	0.60172
SS	0.99185	1.11181	0.01810	0.13628
HAAR	0.98580	1.10043	0.02372	0.09788
RandDFT	0.99341	1.20926	0.02543	0.10712
RealMANOVA	0.97531	0.81152	0.02319	1
RealPF	0.98636	0.86413	0.02540	0.13287
SH	0.99874	0.86734	0.03077	0.15720
RealHAAR	0.98185	0.80135	0.01957	0.73846
RandDCT	0.97830	0.92270	0.03549	0.01179

Table 5: Results of Test 2 for Ψ_{RIP}, $\gamma = 0.5$ and $\beta = 0.8$

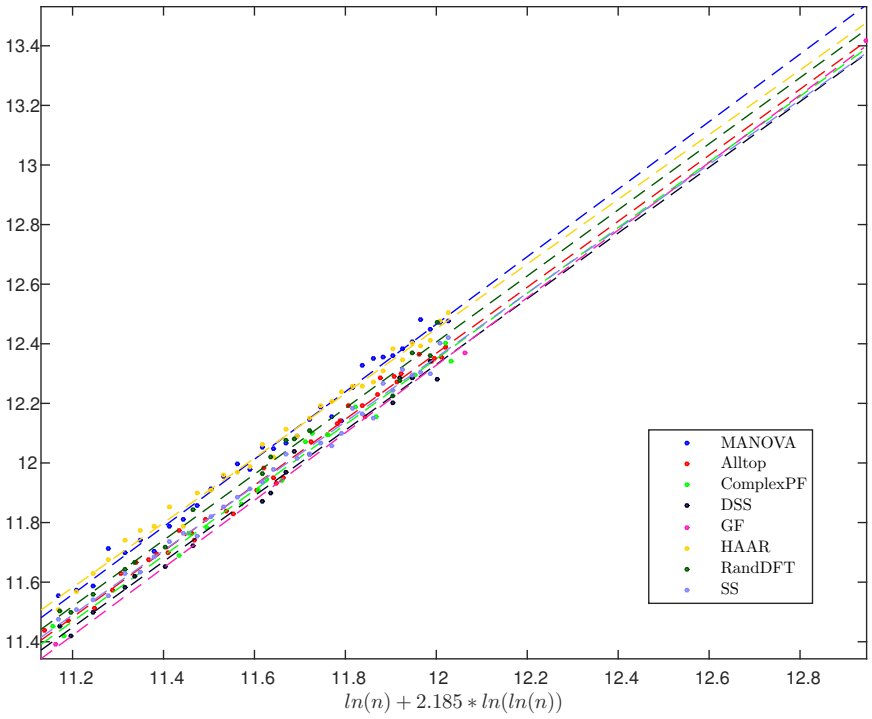

Figure 9: Test 2 for Ψ_{max}, complex frames $\gamma = 0.5$ and $\beta = 0.8$. Plot shows $-\ln \mathbb{E}_{K_n}(\Delta_\Psi(X^{(n)}_{K_n}; n, m_n, k_n)^2)$

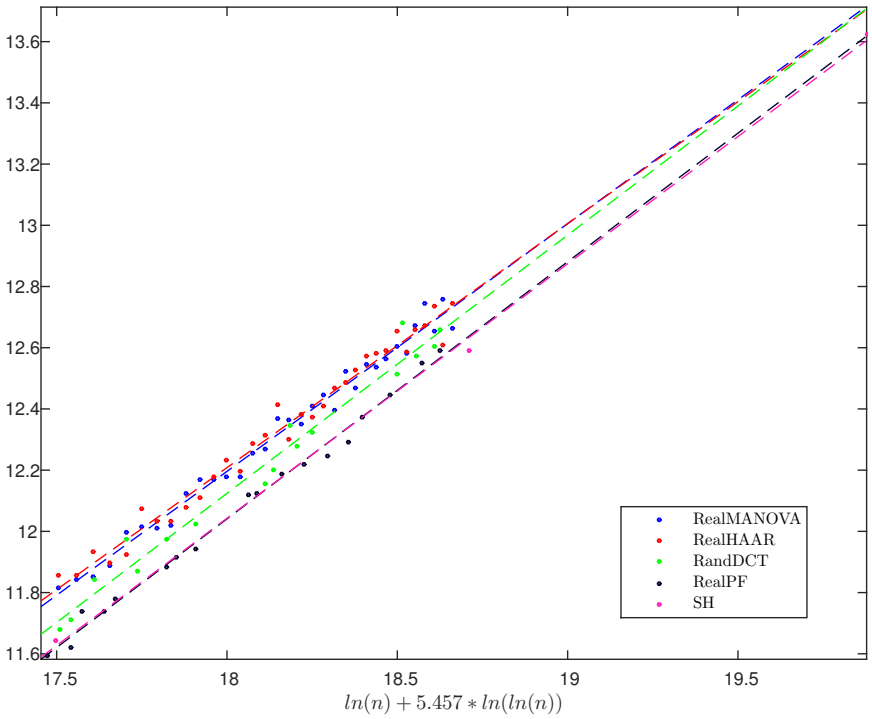

Figure 10: Test 2 for Ψ_{max}, real frames $\gamma = 0.5$ and $\beta = 0.8$. Plot shows $-\ln \mathbb{E}_{K_n}(\Delta_\Psi(X_{K_n}^{(n)}; n, m_n, k_n)^2)$

Frame	R^2	$\hat{b}$	$SE(\hat{b})$	p-value $b = b_{MANOVA}$
MANOVA	0.98814	1.13304	0.02230	1
DSS	0.99156	1.10269	0.02626	0.38298
GF	0.99927	1.13341	0.03066	0.99229
ComplexPF	0.98831	1.10156	0.03093	0.41339
Alltop	0.99221	1.10752	0.01659	0.36175
SS	0.99184	1.08018	0.01760	0.06754
HAAR	0.99201	1.08552	0.01750	0.09867
RandDFT	0.98924	1.10896	0.02986	0.52136
RealMANOVA	0.98467	0.80935	0.01814	1
RealPF	0.99328	0.84016	0.01727	0.22489
SH	0.99870	0.83147	0.03005	0.53311
RealHAAR	0.97961	0.79719	0.02066	0.65963
RandDCT	0.97613	0.84366	0.03406	0.37862

Table 6: Results of Test 2 for Ψ_{max}, $\gamma = 0.5$ and $\beta = 0.8$

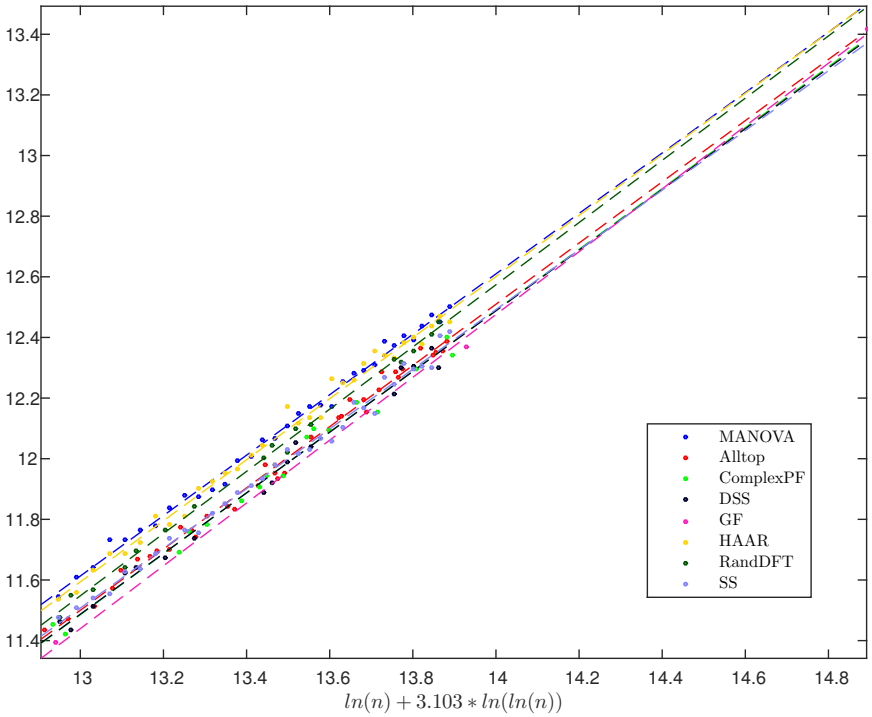

Figure 11: Test 2 for Ψ_{min}, complex frames $\gamma = 0.5$ and $\beta = 0.8$. Plot shows $-\ln \mathbb{E}_{K_n}(\Delta_\Psi(X_{K_n}^{(n)}; n, m_n, k_n)^2)$

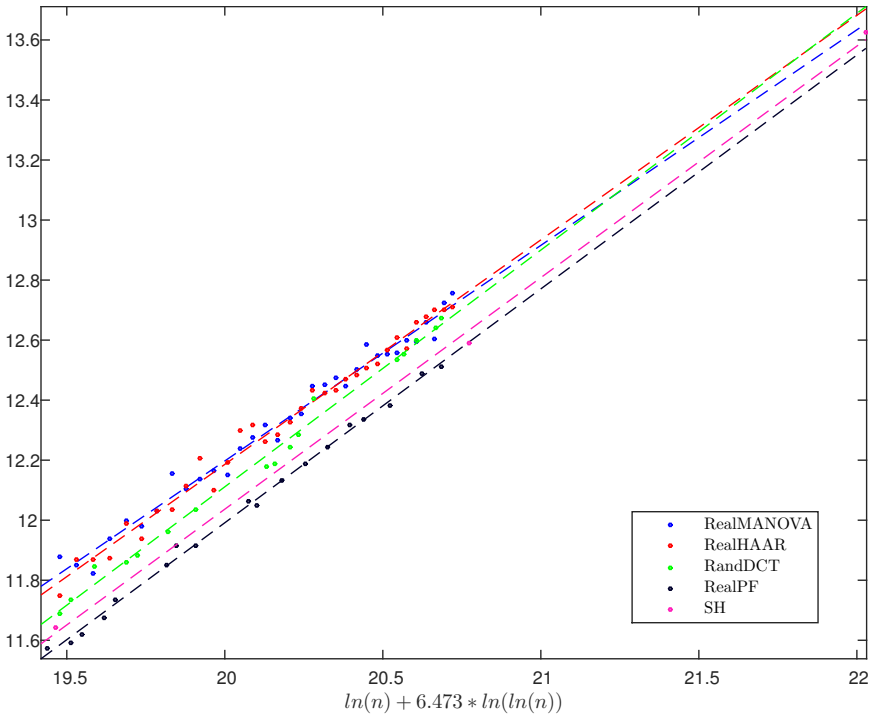

Figure 12: Test 2 for Ψ_{min}, real frames $\gamma = 0.5$ and $\beta = 0.8$. Plot shows $-\ln \mathbb{E}_{K_n}(\Delta_\Psi(X_{K_n}^{(n)}; n, m_n, k_n)^2)$

Frame	R^2	$\hat{b}$	$SE(\hat{b})$	p-value $b = b_{MANOVA}$
MANOVA	0.99436	0.99666	0.01349	1
DSS	0.99116	1.00093	0.02441	0.87915
GF	0.99917	1.03613	0.02984	0.23693
ComplexPF	0.98832	1.00403	0.02818	0.81466
Alltop	0.99218	1.00950	0.01515	0.52890
SS	0.99180	0.98459	0.01608	0.56697
HAAR	0.98749	1.00713	0.02036	0.66982
RandDFT	0.99683	1.02591	0.01494	0.15296
RealMANOVA	0.98138	0.71823	0.01777	1
RealPF	0.99691	0.77915	0.01084	0.00527
SH	0.99861	0.77139	0.02873	0.12540
RealHAAR	0.98525	0.74799	0.01644	0.22362
RandDCT	0.99177	0.78872	0.01855	0.00862

Table 7: Results of Test 2 for Ψ_{min}, $\gamma = 0.5$ and $\beta = 0.8$

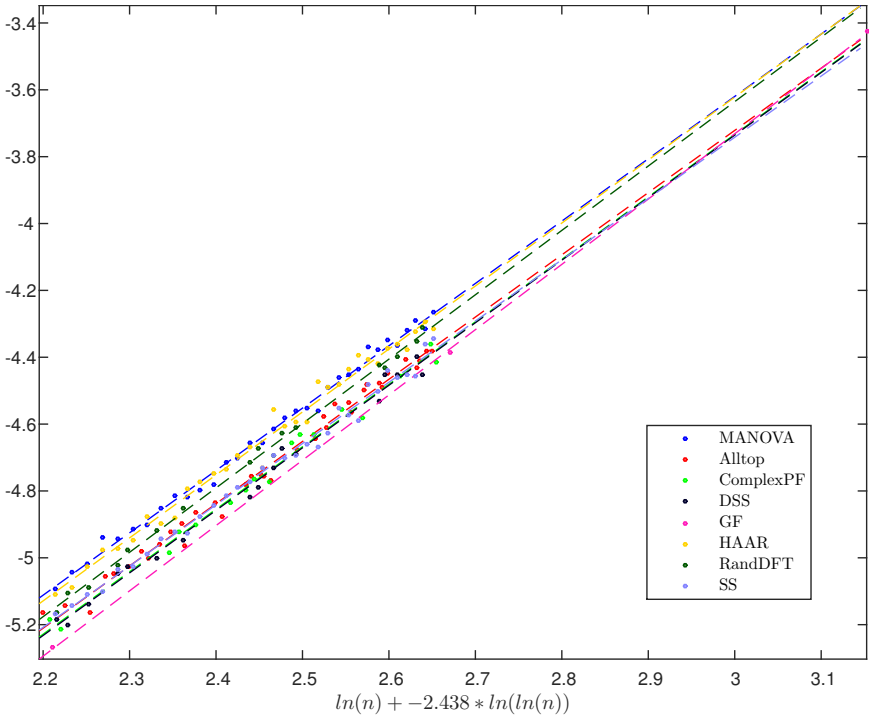

Figure 13: Test 2 for Ψ_{cond}, complex frames $\gamma = 0.5$ and $\beta = 0.8$. Plot shows $-\ln \mathbb{E}_{K_n}(\Delta_\Psi(X_{K_n}^{(n)}; n, m_n, k_n)^2)$

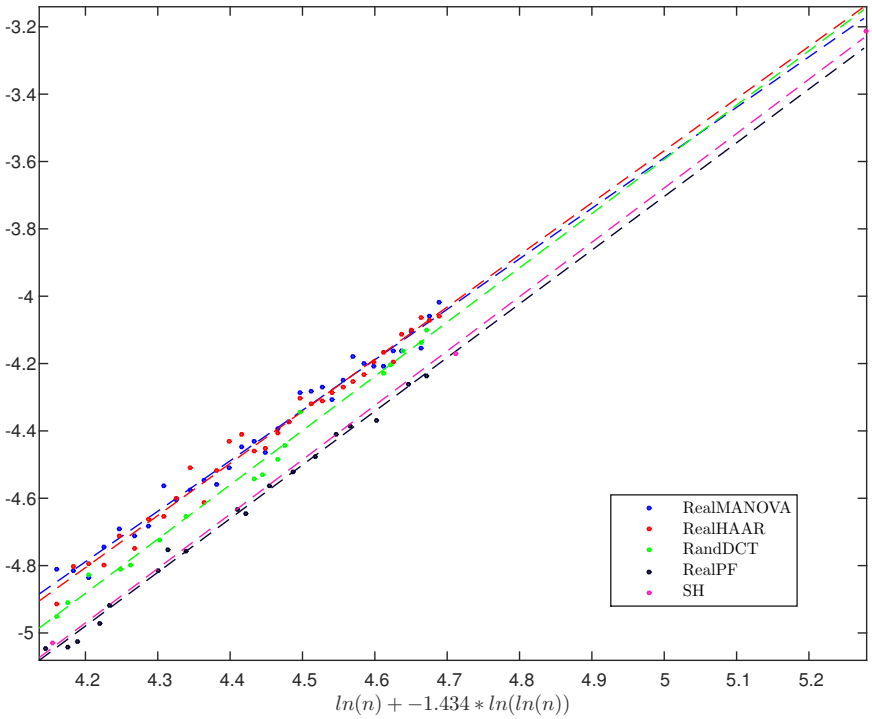

Figure 14: Test 2 for Ψ_{cond}, real frames $\gamma = 0.5$ and $\beta = 0.8$. Plot shows $-\ln \mathbb{E}_{K_n}(\Delta_\Psi(X_{K_n}^{(n)}; n, m_n, k_n)^2)$

Frame	R^2	$\hat{b}$	$SE(\hat{b})$	p-value $b = b_{MANOVA}$
MANOVA	0.99429	1.86502	0.02538	1
DSS	0.99123	1.87094	0.04544	0.91001
GF	0.99984	1.95342	0.02496	0.01845
ComplexPF	0.98754	1.86902	0.05420	0.94707
Alltop	0.98888	1.86134	0.03337	0.93033
SS	0.99138	1.83232	0.03068	0.41458
HAAR	0.98582	1.88372	0.04057	0.69736
RandDFT	0.99690	1.92584	0.02771	0.11237
RealMANOVA	0.98180	1.49940	0.03667	1
RealPF	0.99496	1.59459	0.02836	0.04560
SH	0.99946	1.61454	0.03762	0.03579
RealHAAR	0.98343	1.54766	0.03608	0.35181
RandDCT	0.99159	1.61102	0.03832	0.04079

Table 8: Results of Test 2 for Ψ_{cond}, $\gamma = 0.5$ and $\beta = 0.8$

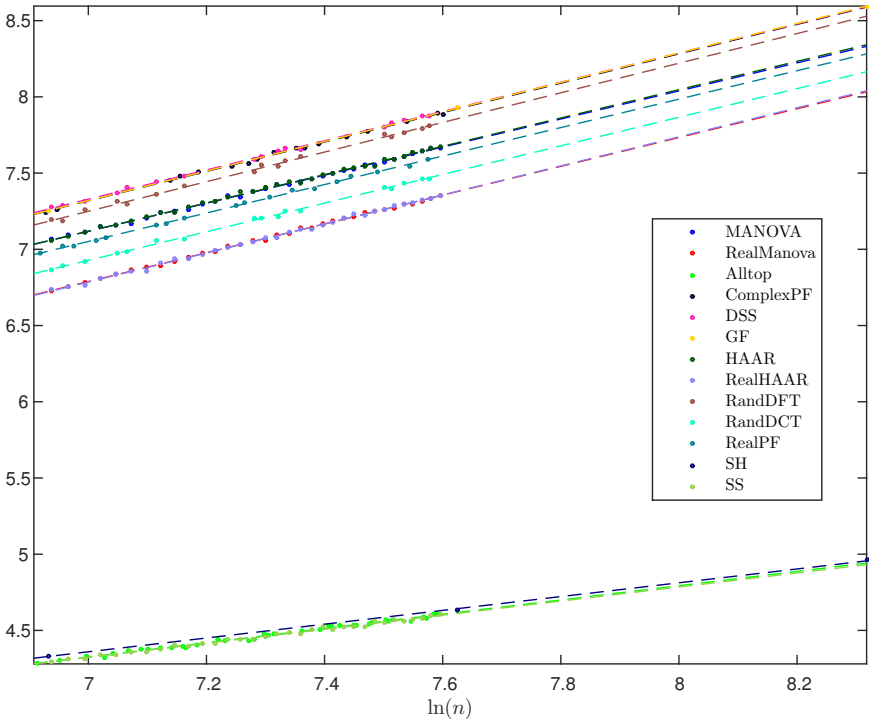

Figure 15: Test 1 for $\gamma = 0.5$ and $\beta = 0.6$. Plot shows $-\frac{1}{2}\ln Var_{K_n}(\Delta_{KS}(X_{K_n}^{(n)}; n, m_n, k_n))$ over $\ln(n)$.

Frame	R^2	$\hat{b}$	$SE(\hat{b})$	p-value $b = b_{MANOVA}$
MANOVA	0.99814	0.92084	0.00713	1
DSS	0.99860	0.95890	0.00926	0.00212
GF	0.99999	0.96831	0.00290	6.6980e-07
ComplexPF	0.99819	0.96451	0.01061	0.00134
Alltop	0.99015	0.46833	0.00790	1.0779e-49
SS	0.99240	0.46151	0.00725	3.7871e-49
HAAR	0.99770	0.92871	0.00801	0.46534
RandDFT	0.99569	0.97151	0.01651	0.00709
RealMANOVA	0.99857	0.94506	0.00642	1
RealPF	0.99858	0.93376	0.00879	0.30465
SH	0.99951	0.45280	0.01000	2.2473e-29
RealHAAR	0.99798	0.95281	0.00771	0.44290
RandDCT	0.99743	0.93887	0.01230	0.65766

Table 9: Results of Test 1 for $\gamma = 0.5$ and $\beta = 0.6$.

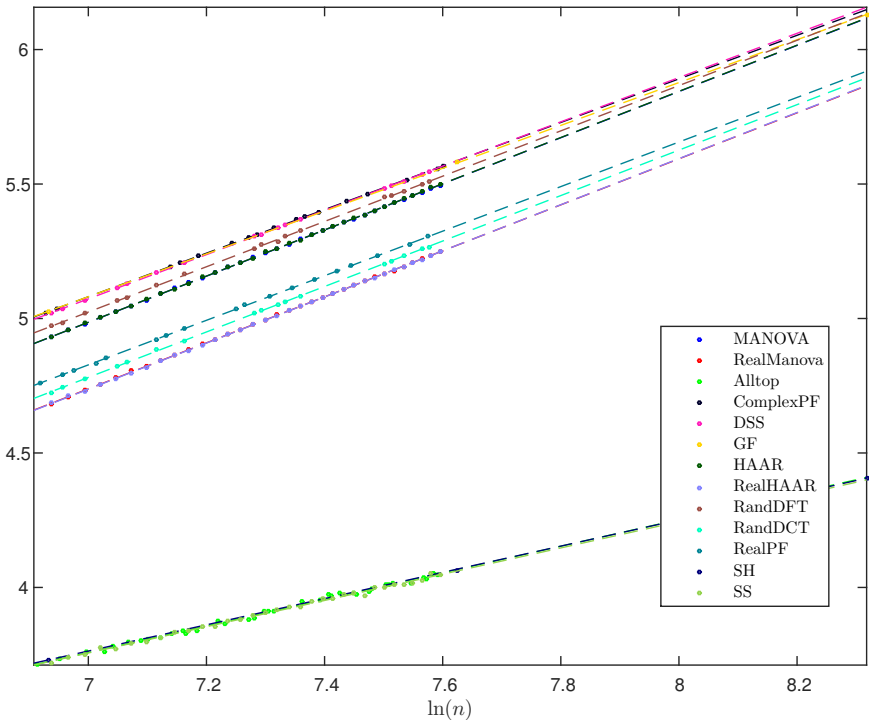

Figure 16: Test 1 for $\gamma = 0.5$ and $\beta = 0.6$. Plot shows $-\frac{1}{2}\ln \mathbb{E}_{K_n}(\Delta_{KS}(X_{K_n}^{(n)}; n, m_n, k_n)^2)$ over $\ln(n)$.

Frame	R^2	$\hat{b}$	$SE(\hat{b})$	p-value $b = b_{MANOVA}$
MANOVA	0.99996	0.85806	0.00092	1
DSS	0.99997	0.82286	0.00120	4.3933e-27
GF	0.99990	0.79630	0.00779	5.5243e-09
ComplexPF	0.99992	0.81016	0.00193	2.0014e-26
Alltop	0.99495	0.49409	0.00595	1.6481e-59
SS	0.99599	0.48823	0.00557	5.6720e-59
HAAR	0.99990	0.85853	0.00154	0.79203
RandDFT	0.99969	0.84205	0.00380	1.7174e-04
RealMANOVA	0.99992	0.85550	0.00134	1
RealPF	0.99994	0.82865	0.00164	8.3751e-17
SH	0.99994	0.48765	0.00380	2.9140e-40
RealHAAR	0.99983	0.85717	0.00204	0.49573
RandDCT	0.99990	0.84525	0.00216	2.0095e-04

Table 10: Results of Test 1 (MSE) for $\gamma = 0.5$ and $\beta = 0.6$.

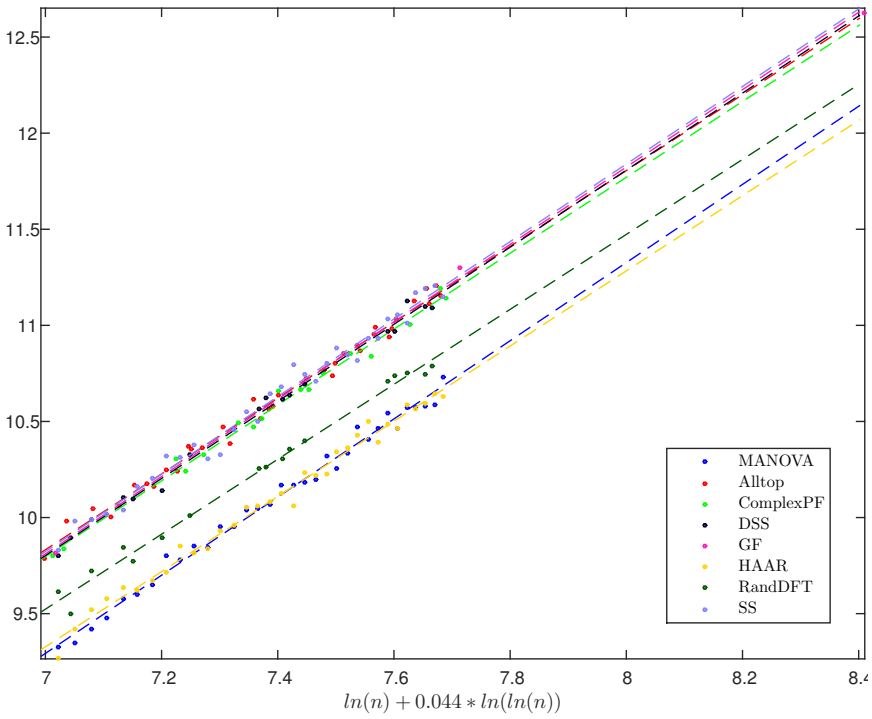

Figure 17: Test 2 for Ψ_{AC}, complex frames $\gamma = 0.5$ and $\beta = 0.6$. Plot shows $-\ln \mathbb{E}_{K_n}(\Delta_\Psi(X^{(n)}_{K_n}; n, m_n, k_n)^2)$

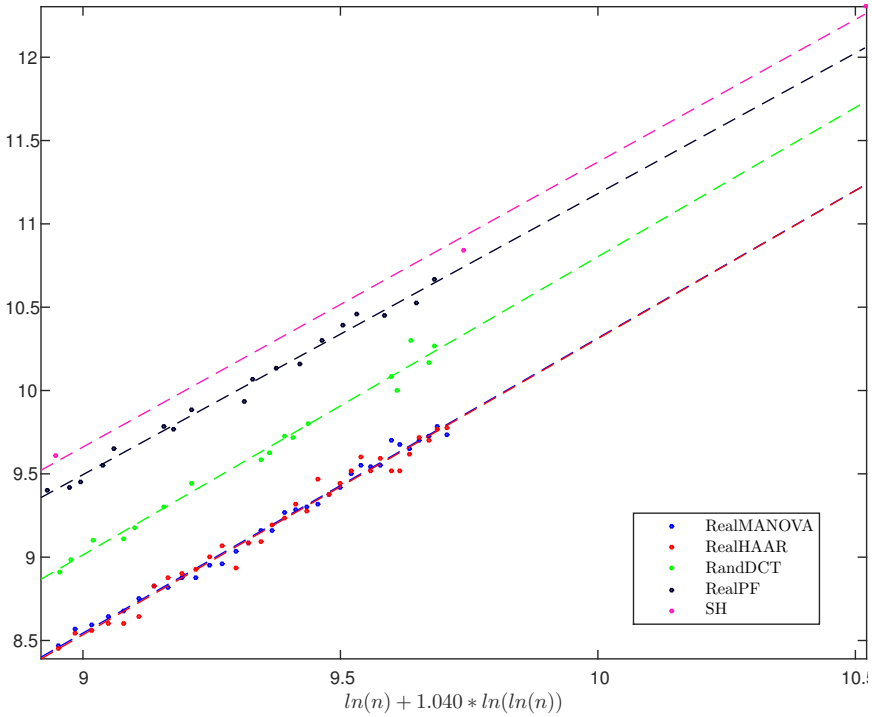

Figure 18: Test 2 for Ψ_{AC}, real frames $\gamma = 0.5$ and $\beta = 0.6$. Plot shows $-\ln \mathbb{E}_{K_n}(\Delta_\Psi(X^{(n)}_{K_n}; n, m_n, k_n)^2)$

Frame	R^2	$\hat{b}$	$SE(\hat{b})$	p-value $b = b_{MANOVA}$
MANOVA	0.99027	2.03344	0.03620	1
DSS	0.99321	2.00503	0.04279	0.61461
GF	0.99904	2.01301	0.06244	0.77891
ComplexPF	0.99038	1.97372	0.05022	0.33972
Alltop	0.99020	1.97327	0.03318	0.22480
SS	0.98367	2.01655	0.04667	0.77587
HAAR	0.98704	1.95623	0.04026	0.15887
RandDFT	0.99072	1.95007	0.04874	0.17636
RealMANOVA	0.99186	1.77068	0.02881	1
RealPF	0.98909	1.68647	0.04428	0.11761
SH	0.99745	1.71033	0.08648	0.51270
RealHAAR	0.98063	1.77667	0.04485	0.91097
RandDCT	0.98525	1.78997	0.05656	0.76255

Table 11: Results of Test 2 for Ψ_{AC}, $\gamma = 0.5$ and $\beta = 0.6$

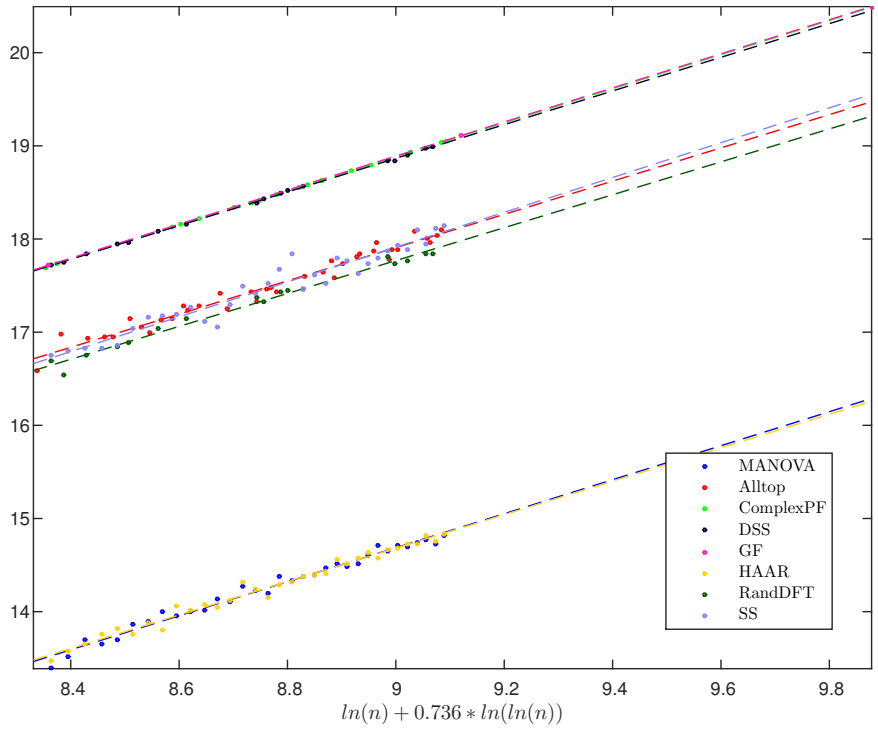

Figure 19: Test 2 for $\Psi_{Shannon}$, complex frames $\gamma = 0.5$ and $\beta = 0.6$. Plot shows $-\ln \mathbb{E}_{K_n}(\Delta_\Psi(X_{K_n}^{(n)}; n, m_n, k_n)^2)$

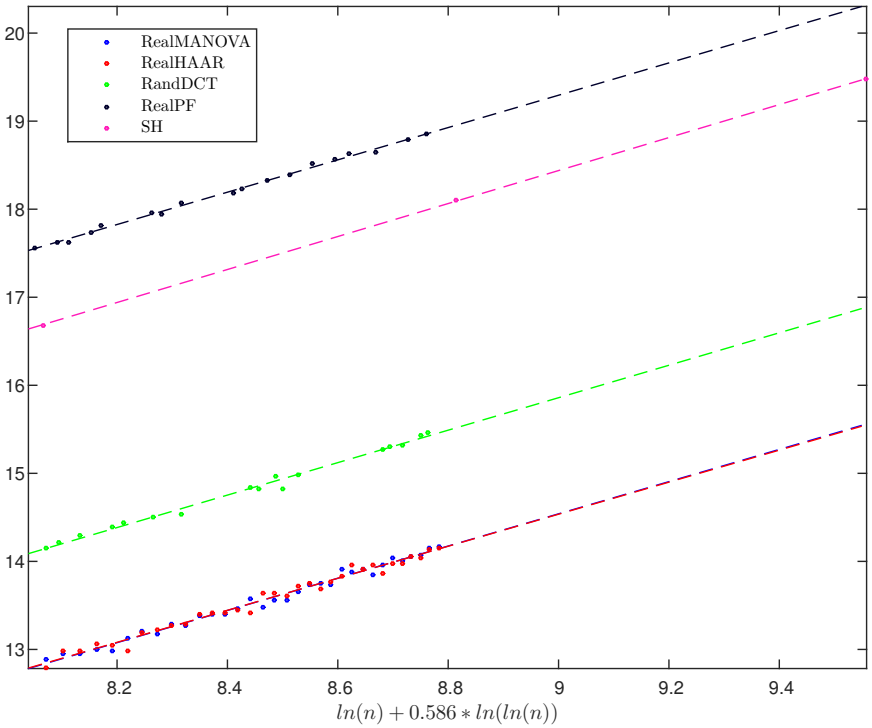

Figure 20: Test 2 for $\Psi_{Shannon}$, real frames $\gamma = 0.5$ and $\beta = 0.6$. Plot shows $-\ln \mathbb{E}_{K_n}(\Delta_\Psi(X^{(n)}_{K_n}; n, m_n, k_n)^2)$

Frame	R^2	$\hat{b}$	$SE(\hat{b})$	p-value $b = b_{MANOVA}$
MANOVA	0.98195	1.82538	0.04445	1
DSS	0.99945	1.80721	0.01098	0.69332
GF	1.00000	1.82884	0.00395	0.93869
ComplexPF	0.99992	1.82938	0.00435	0.92891
Alltop	0.96689	1.78431	0.05581	0.56685
SS	0.94035	1.86865	0.08453	0.65205
HAAR	0.98250	1.79577	0.04305	0.63396
RandDFT	0.98501	1.76630	0.05626	0.41425
RealMANOVA	0.98863	1.82907	0.03523	1
RealPF	0.99618	1.83544	0.02843	0.88885
SH	0.99996	1.87300	0.01129	0.24381
RealHAAR	0.98176	1.81917	0.04454	0.86218
RandDCT	0.99046	1.84329	0.04671	0.80910

Table 12: Results of Test 2 for $\Psi_{Shannon}$, $\gamma = 0.5$ and $\beta = 0.6$

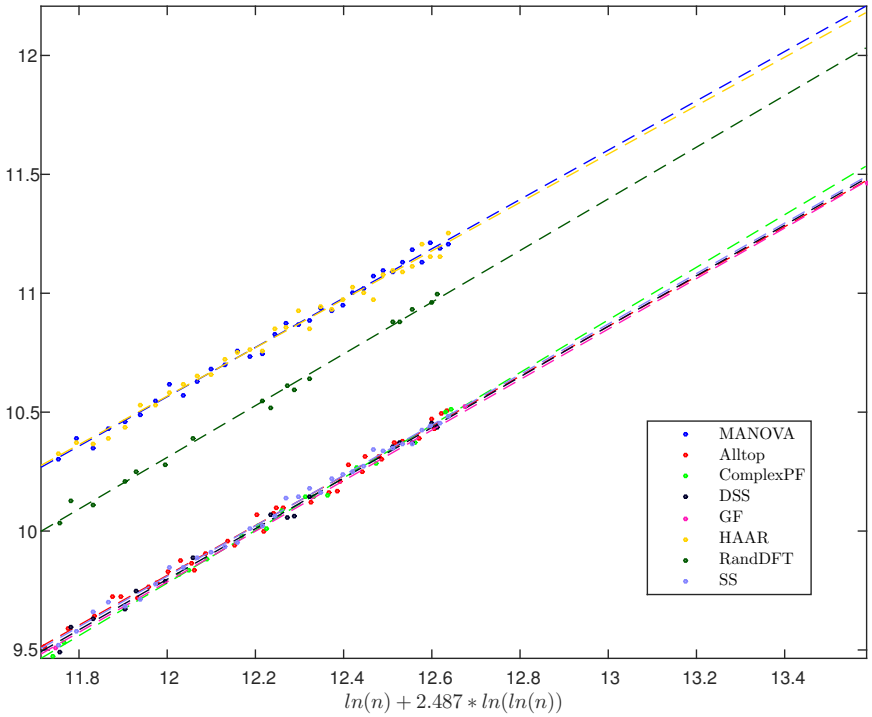

Figure 21: Test 2 for Ψ_{RIP}, complex frames $\gamma = 0.5$ and $\beta = 0.6$. Plot shows $-\ln \mathbb{E}_{K_n}(\Delta_\Psi(X_{K_n}^{(n)}; n, m_n, k_n)^2)$

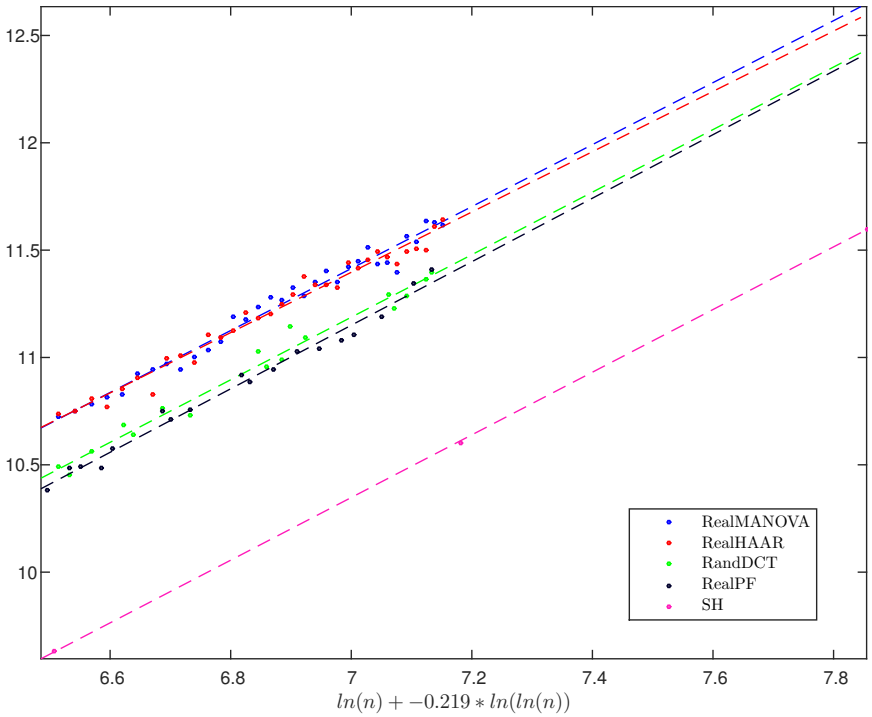

Figure 22: Test 2 for Ψ_{RIP}, real frames $\gamma = 0.5$ and $\beta = 0.6$. Plot shows $-\ln \mathbb{E}_{K_n}(\Delta_\Psi(X_{K_n}^{(n)}; n, m_n, k_n)^2)$

Frame	R^2	$\hat{b}$	$SE(\hat{b})$	p-value $b = b_{MANOVA}$
MANOVA	0.99243	1.03687	0.01627	1
DSS	0.99413	1.06366	0.02110	0.31982
GF	0.99979	1.06250	0.01522	0.25836
ComplexPF	0.99613	1.10638	0.01782	0.00600
Alltop	0.99175	1.04727	0.01614	0.65149
SS	0.99459	1.06078	0.01405	0.27016
HAAR	0.98830	1.01796	0.01989	0.46451
RandDFT	0.99482	1.08689	0.02024	0.06028
RealMANOVA	0.97822	1.44331	0.03868	1
RealPF	0.98593	1.47974	0.04419	0.53806
SH	0.99996	1.45956	0.00897	0.68503
RealHAAR	0.97735	1.40446	0.03840	0.47866
RandDCT	0.97878	1.45677	0.05538	0.84297

Table 13: Results of Test 2 for Ψ_{RIP}, $\gamma = 0.5$ and $\beta = 0.6$

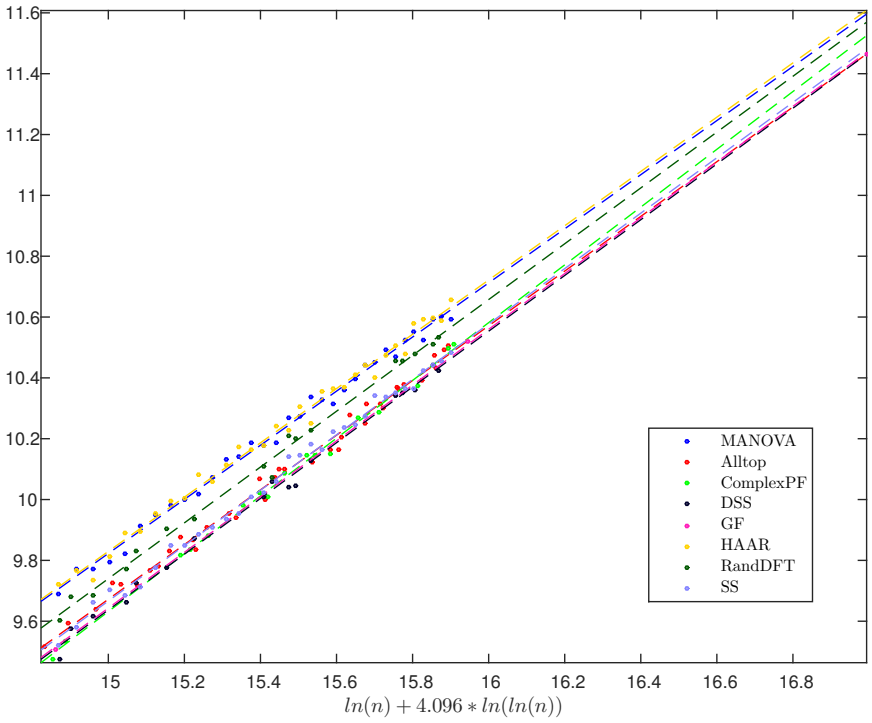

Figure 23: Test 2 for Ψ_{max}, complex frames $\gamma = 0.5$ and $\beta = 0.6$. Plot shows $-\ln \mathbb{E}_{K_n}(\Delta_\Psi(X_{K_n}^{(n)}; n, m_n, k_n)^2)$

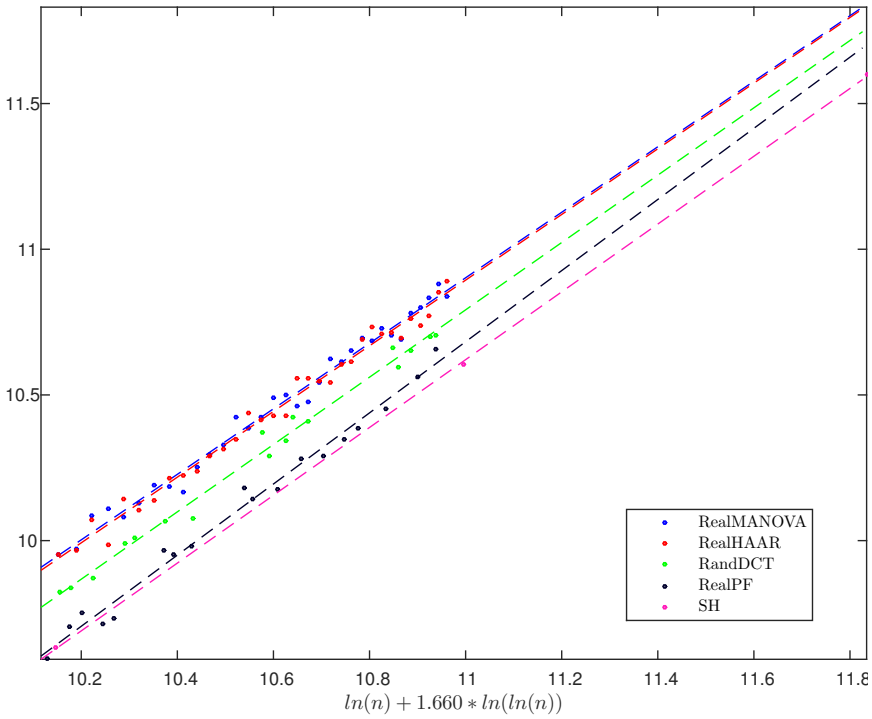

Figure 24: Test 2 for Ψ_{max}, real frames $\gamma = 0.5$ and $\beta = 0.6$. Plot shows $-\ln \mathbb{E}_{K_n}(\Delta_\Psi(X_{K_n}^{(n)}; n, m_n, k_n)^2)$

Frame	R^2	$\hat{b}$	$SE(\hat{b})$	p-value $b = b_{MANOVA}$
MANOVA	0.99377	0.88948	0.01265	1
DSS	0.99433	0.91641	0.01786	0.22480
GF	0.99987	0.91641	0.01063	0.11286
ComplexPF	0.99613	0.94975	0.01528	0.00391
Alltop	0.99170	0.89908	0.01391	0.61136
SS	0.99463	0.91071	0.01202	0.22818
HAAR	0.99114	0.89219	0.01515	0.89136
RandDFT	0.99454	0.91759	0.01756	0.20040
RealMANOVA	0.98572	1.12423	0.02431	1
RealPF	0.98712	1.22068	0.03485	0.02784
SH	0.99986	1.16349	0.01354	0.16777
RealHAAR	0.98431	1.12688	0.02555	0.94029
RandDCT	0.98969	1.15548	0.03045	0.42663

Table 14: Results of Test 2 for Ψ_{max}, $\gamma = 0.5$ and $\beta = 0.6$

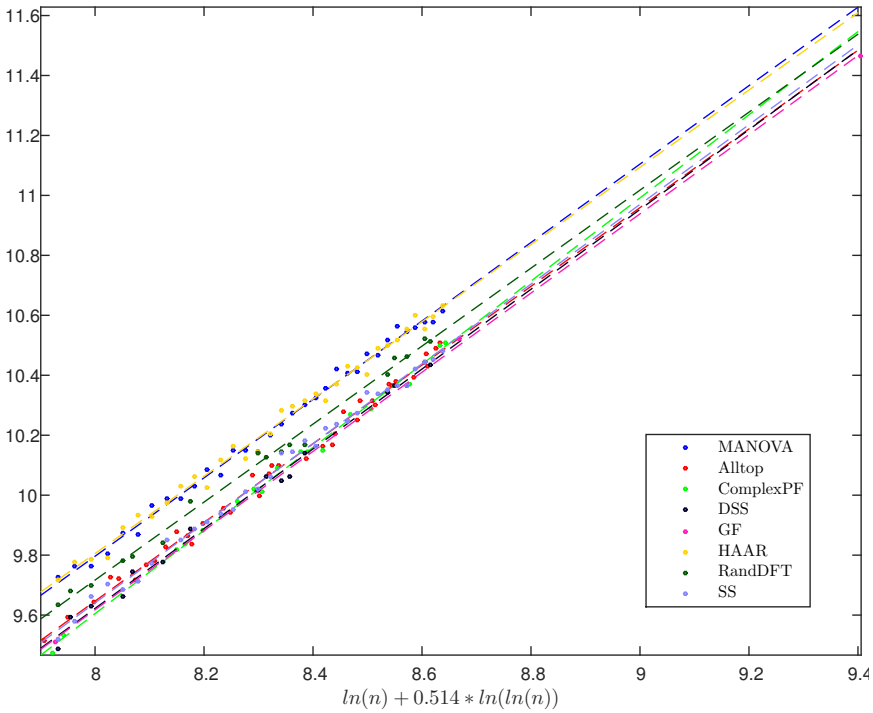

Figure 25: Test 2 for Ψ_{min}, complex frames $\gamma = 0.5$ and $\beta = 0.6$. Plot shows $-\ln \mathbb{E}_{K_n}(\Delta_\Psi(X^{(n)}_{K_n}; n, m_n, k_n)^2)$

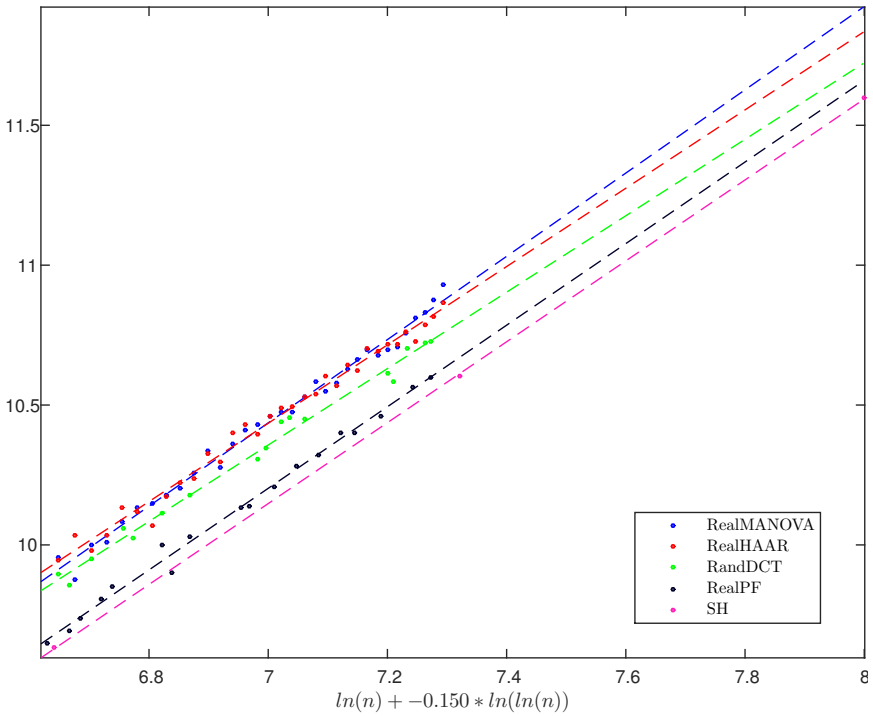

Figure 26: Test 2 for Ψ_{min}, real frames $\gamma = 0.5$ and $\beta = 0.6$. Plot shows $-\ln \mathbb{E}_{K_n}(\Delta_\Psi(X^{(n)}_{K_n}; n, m_n, k_n)^2)$

Frame	R^2	$\hat{b}$	$SE(\hat{b})$	p-value $b = b_{MANOVA}$
MANOVA	0.99411	1.30821	0.01808	1
DSS	0.99357	1.33096	0.02766	0.49466
GF	0.99963	1.32070	0.02528	0.69037
ComplexPF	0.99610	1.38691	0.02241	0.00888
Alltop	0.99185	1.31263	0.02011	0.87082
SS	0.99453	1.32947	0.01771	0.40430
HAAR	0.99080	1.28847	0.02230	0.49421
RandDFT	0.99424	1.30077	0.02556	0.81312
RealMANOVA	0.98906	1.48832	0.02812	1
RealPF	0.99292	1.45809	0.03077	0.47184
SH	0.99996	1.44606	0.00925	0.16305
RealHAAR	0.98646	1.40012	0.02947	0.03420
RandDCT	0.98944	1.36601	0.03643	0.01078

Table 15: Results of Test 2 for Ψ_{min}, $\gamma = 0.5$ and $\beta = 0.6$

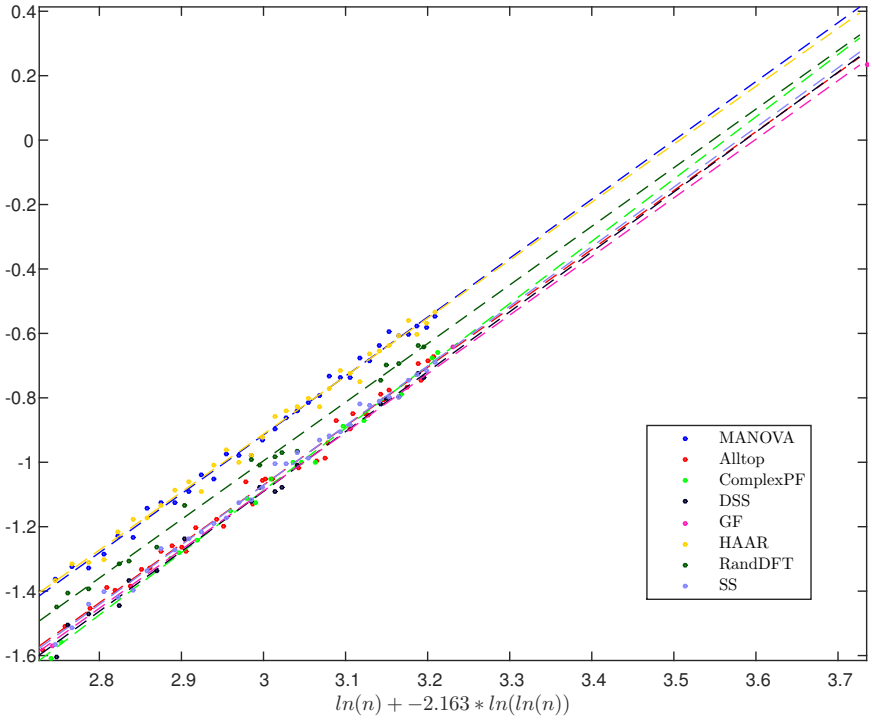

Figure 27: Test 2 for Ψ_{cond}, complex frames $\gamma = 0.5$ and $\beta = 0.6$. Plot shows $-\ln \mathbb{E}_{K_n}(\Delta_\Psi(X_{K_n}^{(n)}; n, m_n, k_n)^2)$

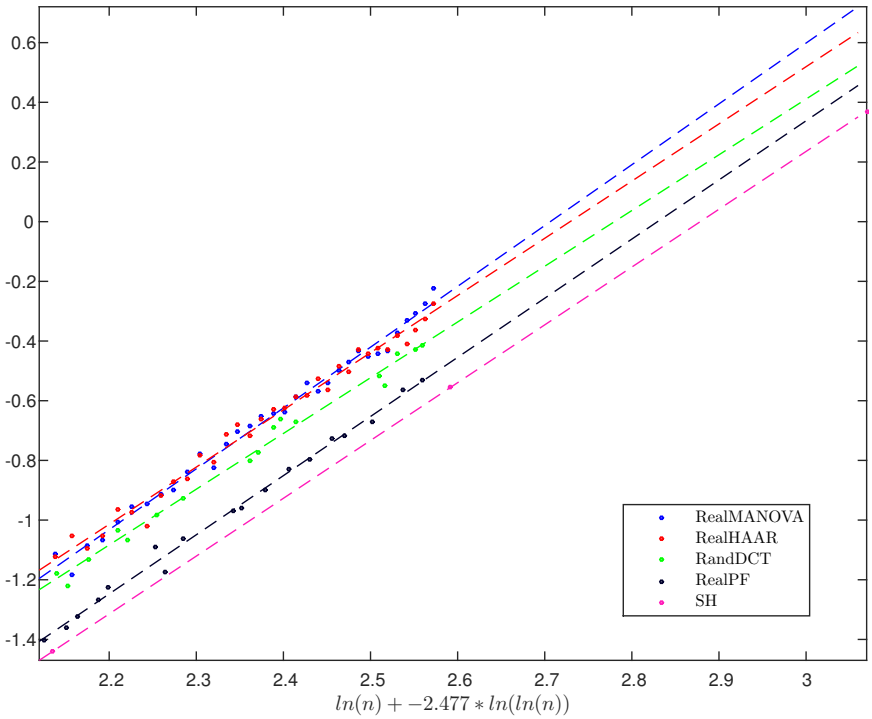

Figure 28: Test 2 for Ψ_{cond}, real frames $\gamma = 0.5$ and $\beta = 0.6$. Plot shows $-\ln \mathbb{E}_{K_n}(\Delta_\Psi(X^{(n)}_{K_n}; n, m_n, k_n)^2)$

Frame	R^2	$\hat{b}$	$SE(\hat{b})$	p-value $b = b_{MANOVA}$
MANOVA	0.99441	1.82815	0.02462	1
DSS	0.99352	1.85919	0.03875	0.50234
GF	0.99932	1.81990	0.04756	0.87861
ComplexPF	0.99606	1.93254	0.03138	0.01196
Alltop	0.99113	1.82833	0.02923	0.99618
SS	0.99447	1.85077	0.02478	0.51955
HAAR	0.99081	1.79953	0.03112	0.47360
RandDFT	0.99426	1.81952	0.03569	0.84323
RealMANOVA	0.98971	2.03829	0.03733	1
RealPF	0.99382	1.98193	0.03907	0.30225
SH	1.00000	1.93739	0.00213	0.01102
RealHAAR	0.98568	1.91682	0.04149	0.03334
RandDCT	0.98911	1.86786	0.05060	0.00941

Table 16: Results of Test 2 for Ψ_{cond}, $\gamma = 0.5$ and $\beta = 0.6$

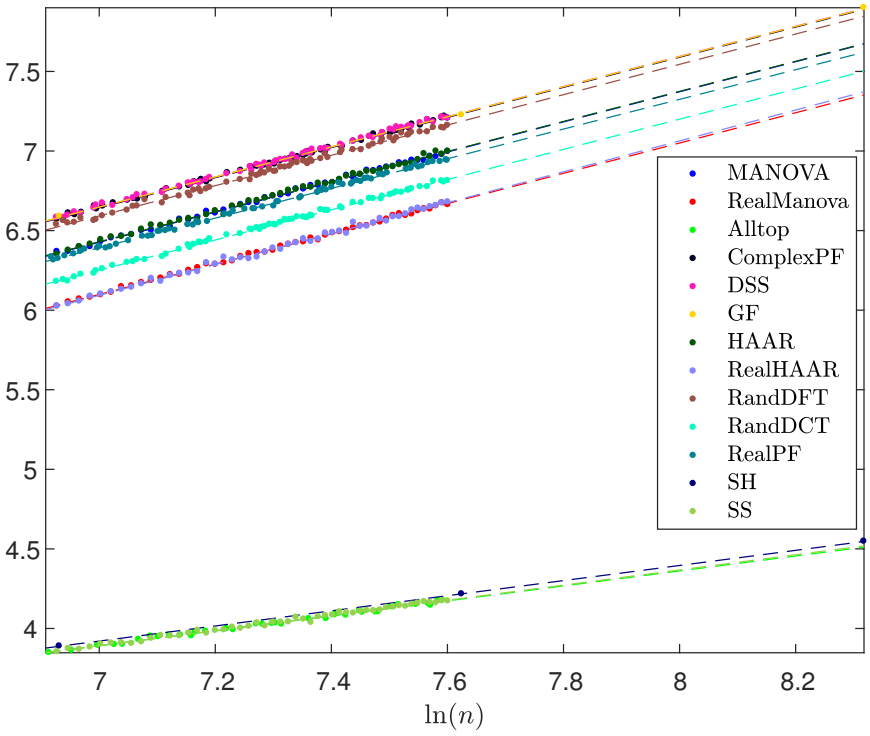

Figure 29: Test 1 for $\gamma = 0.5$ and $\beta = 0.3$. Plot shows $-\frac{1}{2}\ln Var_{K_n}(\Delta_{KS}(X^{(n)}_{K_n}; n, m_n, k_n))$ over $\ln(n)$.

Frame	R^2	$\hat{b}$	$SE(\hat{b})$	p-value $b = b_{MANOVA}$
MANOVA	0.99804	0.94562	0.00604	1
DSS	0.99751	0.94706	0.00583	0.86402
GF	0.99973	0.94566	0.01560	0.99790
ComplexPF	0.99808	0.94620	0.00511	0.94130
Alltop	0.99125	0.47008	0.00747	2.1545e-63
SS	0.99264	0.47654	0.00592	1.0558e-74
HAAR	0.99662	0.94502	0.00794	0.95233
RandDFT	0.99593	0.95281	0.00750	0.45698
RealMANOVA	0.99861	0.95142	0.00512	1
RealPF	0.99824	0.93244	0.00485	0.00822
SH	0.99999	0.47509	0.00123	3.4170e-56
RealHAAR	0.99574	0.97072	0.00917	0.06915
RandDCT	0.99807	0.94876	0.00513	0.71436

Table 17: Results of Test 1 for $\gamma = 0.5$ and $\beta = 0.3$.

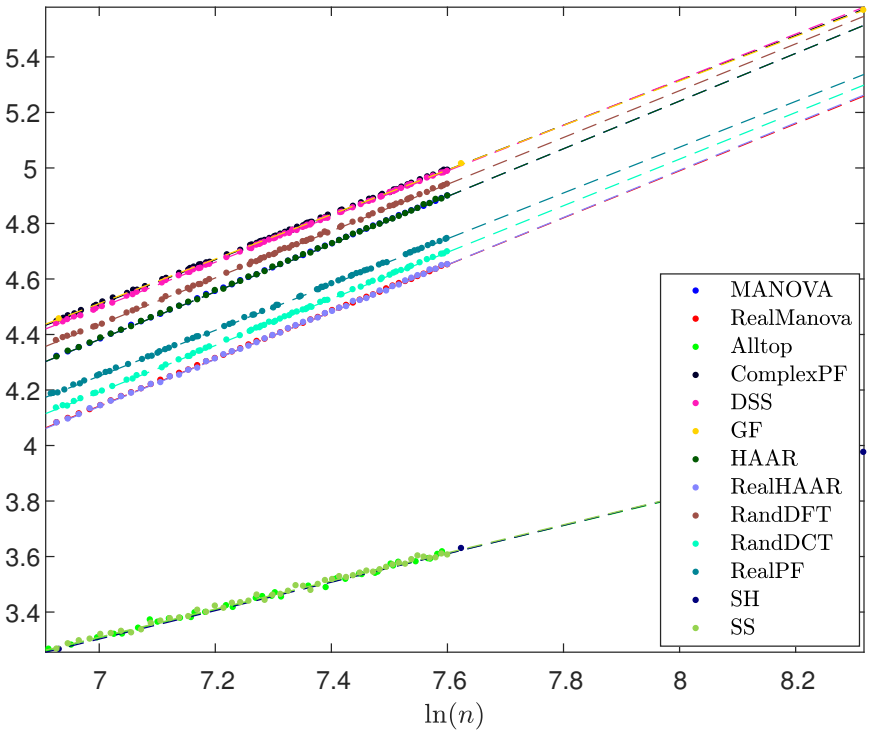

Figure 30: Test 1 for $\gamma = 0.5$ and $\beta = 0.3$. Plot shows $-\frac{1}{2}\ln \mathbb{E}_{K_n}(\Delta_{KS}(X^{(n)}_{K_n}; n, m_n, k_n)^2)$ over $\ln(n)$.

Frame	R^2	$\hat{b}$	$SE(\hat{b})$	p-value $b = b_{MANOVA}$
MANOVA	0.99996	0.85923	0.00078	1
DSS	0.99988	0.82205	0.00111	5.7008e-52
GF	0.99999	0.80192	0.00253	1.0432e-26
ComplexPF	0.99990	0.80801	0.00102	7.0584e-69
Alltop	0.99484	0.50500	0.00615	2.0456e-68
SS	0.99539	0.50645	0.00498	3.1506e-84
HAAR	0.99986	0.85892	0.00146	0.85431
RandDFT	0.99977	0.84332	0.00156	3.0710e-15
RealMANOVA	0.99995	0.84773	0.00086	1
RealPF	0.99989	0.82479	0.00108	4.7494e-32
SH	0.99980	0.51202	0.00718	3.6278e-42
RealHAAR	0.99968	0.85192	0.00221	0.08066
RandDCT	0.99983	0.83940	0.00133	7.4371e-07

Table 18: Results of Test 1 (MSE) for $\gamma = 0.5$ and $\beta = 0.3$.

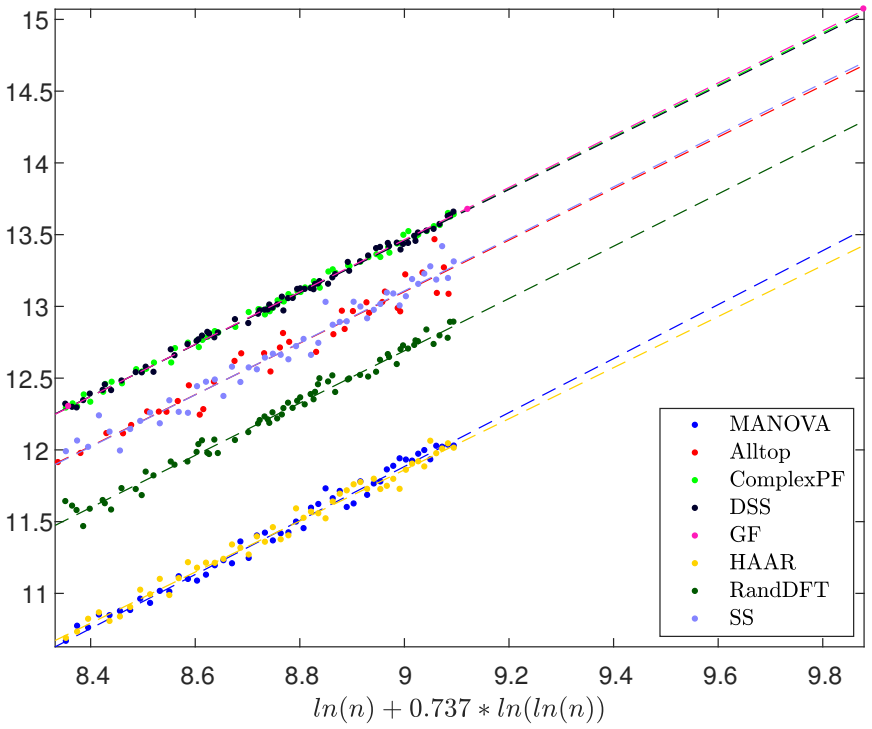

Figure 31: Test 2 for Ψ_{AC}, complex frames $\gamma = 0.5$ and $\beta = 0.3$. Plot shows $-\ln \mathbb{E}_{K_n}(\Delta_\Psi(X_{K_n}^{(n)}; n, m_n, k_n)^2)$

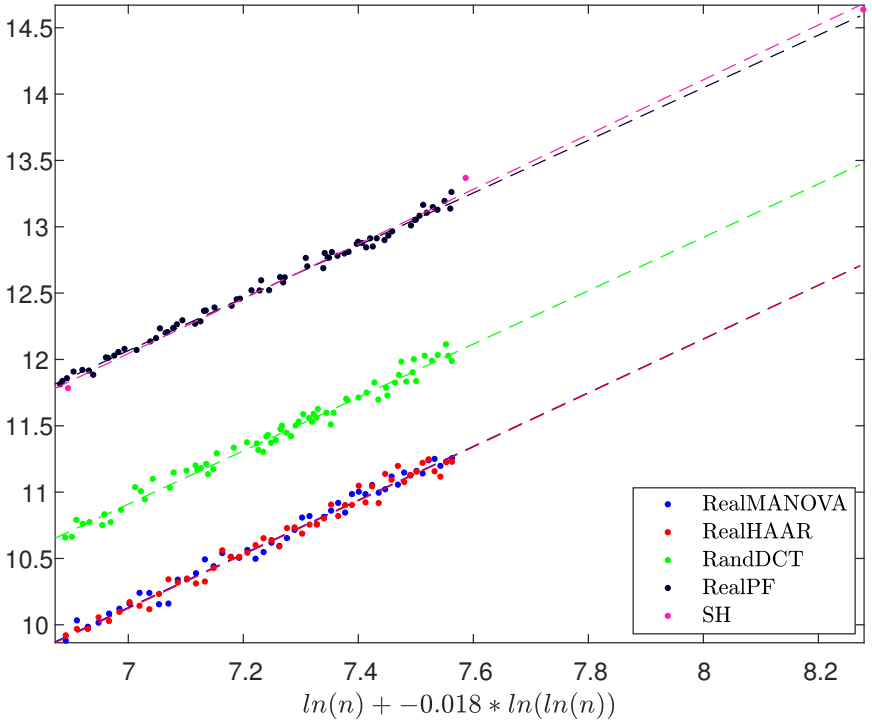

Figure 32: Test 2 for Ψ_{AC}, real frames $\gamma = 0.5$ and $\beta = 0.3$. Plot shows $-\ln \mathbb{E}_{K_n}(\Delta_\Psi(X_{K_n}^{(n)}; n, m_n, k_n)^2)$

Frame	R^2	$\hat{b}$	$SE(\hat{b})$	p-value $b = b_{MANOVA}$
MANOVA	0.98718	1.88076	0.03094	1
DSS	0.99544	1.80171	0.01500	0.02333
GF	0.99995	1.82112	0.01321	0.08250
ComplexPF	0.99635	1.80951	0.01349	0.03695
Alltop	0.94870	1.79549	0.07057	0.27168
SS	0.96730	1.81163	0.04808	0.22961
HAAR	0.98368	1.78037	0.03310	0.02907
RandDFT	0.98579	1.82179	0.02692	0.15326
RealMANOVA	0.98675	2.02493	0.03387	1
RealPF	0.99378	1.98183	0.01944	0.27211
SH	0.99595	2.06310	0.13161	0.78000
RealHAAR	0.98333	2.02932	0.03814	0.93170
RandDCT	0.98191	2.01123	0.03361	0.77441

Table 19: Results of Test 2 for Ψ_{AC}, $\gamma = 0.5$ and $\beta = 0.3$

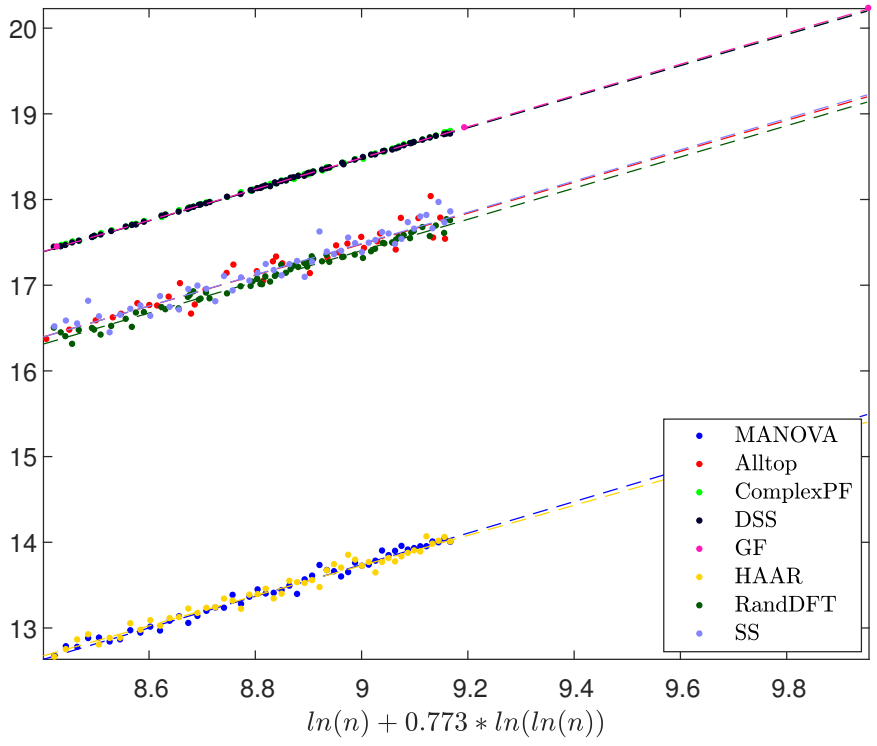

Figure 33: Test 2 for $\Psi_{Shannon}$, complex frames $\gamma = 0.5$ and $\beta = 0.3$. Plot shows $-\ln \mathbb{E}_{K_n}(\Delta_\Psi(X^{(n)}_{K_n}; n, m_n, k_n)^2)$

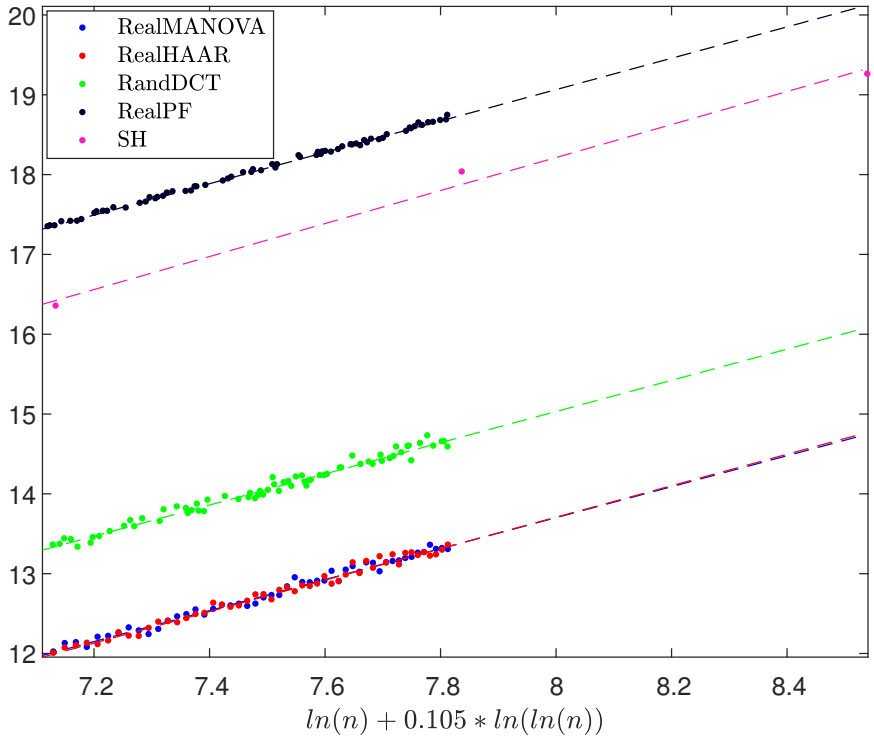

Figure 34: Test 2 for $\Psi_{Shannon}$, real frames $\gamma = 0.5$ and $\beta = 0.3$. Plot shows $-\ln \mathbb{E}_{K_n}(\Delta_\Psi(X_{K_n}^{(n)}; n, m_n, k_n)^2)$

Frame	R^2	$\hat{b}$	$SE(\hat{b})$	p-value $b = b_{MANOVA}$
MANOVA	0.98545	1.84293	0.03232	1
DSS	0.99970	1.81175	0.00387	0.34009
GF	0.99999	1.82300	0.00555	0.54620
ComplexPF	0.99961	1.81331	0.00441	0.36582
Alltop	0.91656	1.80667	0.09214	0.71129
SS	0.93825	1.82241	0.06748	0.78446
HAAR	0.97525	1.75883	0.04044	0.10755
RandDFT	0.98262	1.82136	0.02982	0.62471
RealMANOVA	0.98551	1.94022	0.03395	1
RealPF	0.99790	1.96483	0.01119	0.49266
SH	0.99193	2.06711	0.18642	0.50624
RealHAAR	0.98571	1.97104	0.03425	0.52432
RandDCT	0.97926	1.95288	0.03499	0.79562

Table 20: Results of Test 2 for $\Psi_{Shannon}$, $\gamma = 0.5$ and $\beta = 0.3$

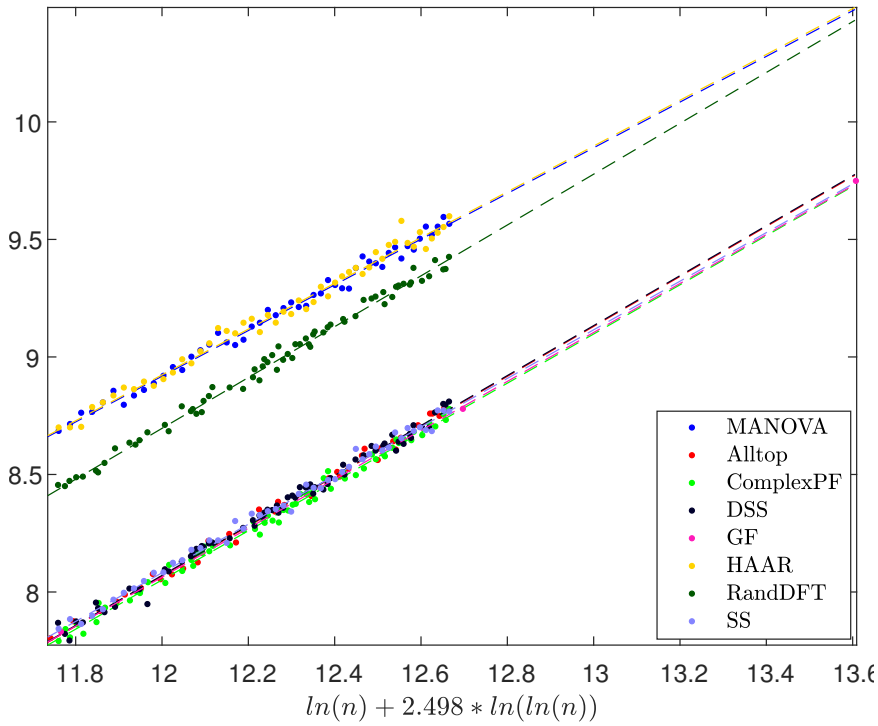

Figure 35: Test 2 for Ψ_{RIP}, complex frames $\gamma = 0.5$ and $\beta = 0.3$. Plot shows $-\ln \mathbb{E}_{K_n}(\Delta_\Psi(X_{K_n}^{(n)}; n, m_n, k_n)^2)$

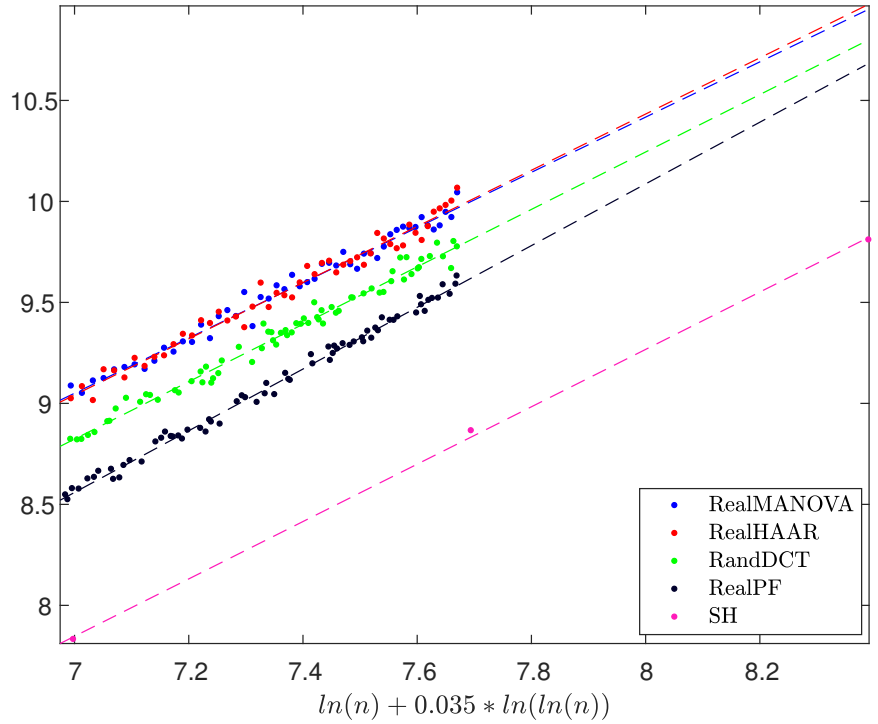

Figure 36: Test 2 for Ψ_{RIP}, real frames $\gamma = 0.5$ and $\beta = 0.3$. Plot shows $-\ln \mathbb{E}_{K_n}(\Delta_\Psi(X_{K_n}^{(n)}; n, m_n, k_n)^2)$

Frame	R^2	$\hat{b}$	$SE(\hat{b})$	p-value $b = b_{MANOVA}$
MANOVA	0.99022	0.97190	0.01394	1
DSS	0.99230	1.06289	0.01153	1.8462e-06
GF	0.99983	1.04116	0.01361	8.5024e-04
ComplexPF	0.99324	1.04645	0.01063	4.3545e-05
Alltop	0.99410	1.06272	0.01384	1.3734e-05
SS	0.99410	1.03385	0.01150	8.9722e-04
HAAR	0.98463	0.97387	0.01756	0.93002
RandDFT	0.99285	1.08149	0.01130	1.4463e-08
RealMANOVA	0.98044	1.36720	0.02787	1
RealPF	0.99275	1.52753	0.01619	2.3533e-06
SH	0.99933	1.42032	0.03666	0.25426
RealHAAR	0.97597	1.39123	0.03151	0.56908
RandDCT	0.98226	1.42152	0.02351	0.13904

Table 21: Results of Test 2 for Ψ_{RIP}, $\gamma = 0.5$ and $\beta = 0.3$

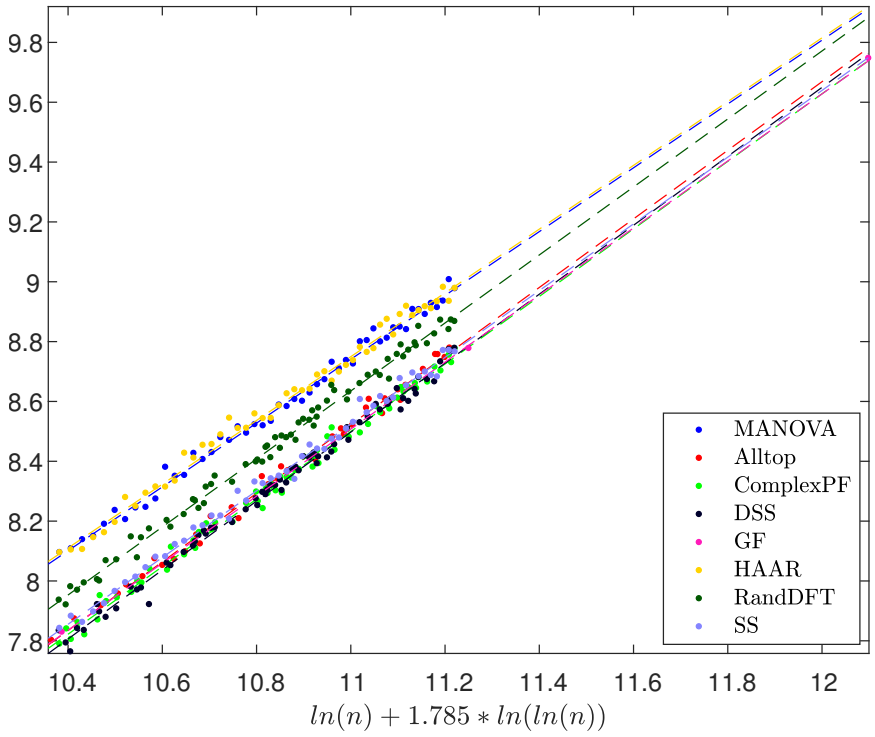

Figure 37: Test 2 for Ψ_{max}, complex frames $\gamma = 0.5$ and $\beta = 0.3$. Plot shows $-\ln \mathbb{E}_{K_n}(\Delta_\Psi(X_{K_n}^{(n)}; n, m_n, k_n)^2)$

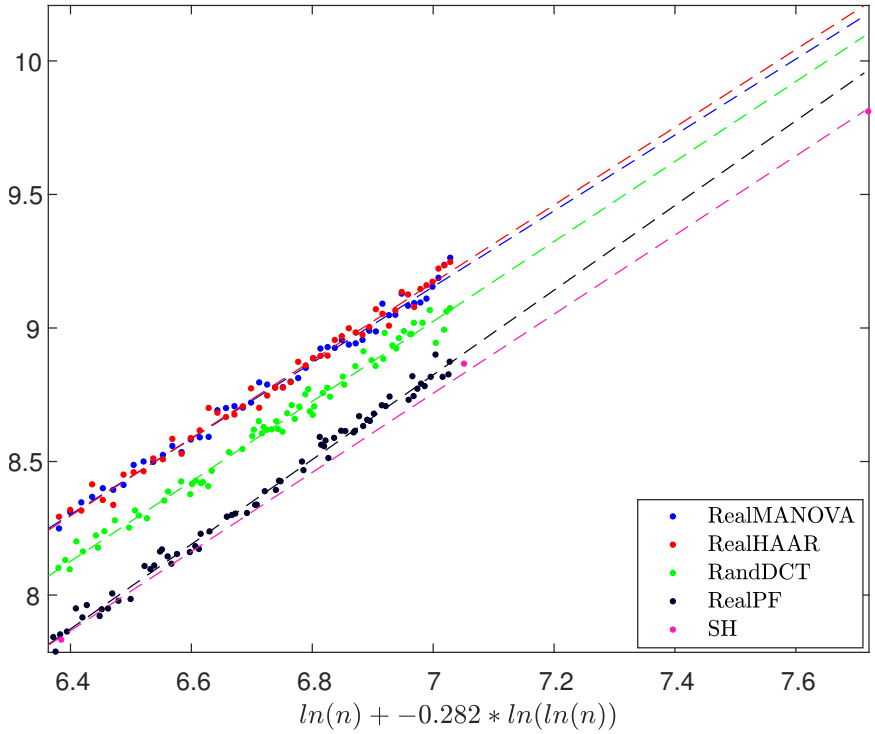

Figure 38: Test 2 for Ψ_{max}, real frames $\gamma = 0.5$ and $\beta = 0.3$. Plot shows $-\ln \mathbb{E}_{K_n}(\Delta_\Psi(X_{K_n}^{(n)}; n, m_n, k_n)^2)$

Frame	R^2	$\hat{b}$	$SE(\hat{b})$	p-value $b = b_{MANOVA}$
MANOVA	0.99275	1.06652	0.01316	1
DSS	0.99266	1.15219	0.01220	5.3891e-06
GF	0.99987	1.12022	0.01296	0.00547
ComplexPF	0.99324	1.12883	0.01146	5.2296e-04
Alltop	0.99412	1.14631	0.01490	1.3037e-04
SS	0.99409	1.11517	0.01241	0.00845
HAAR	0.99041	1.06568	0.01514	0.96659
RandDFT	0.99250	1.13637	0.01216	1.6393e-04
RealMANOVA	0.99017	1.42122	0.02044	1
RealPF	0.99221	1.58564	0.01743	1.3782e-08
SH	0.99927	1.48165	0.03992	0.18400
RealHAAR	0.98861	1.45533	0.02255	0.26515
RandDCT	0.98670	1.49715	0.02139	0.01158

Table 22: Results of Test 2 for Ψ_{max}, $\gamma = 0.5$ and $\beta = 0.3$

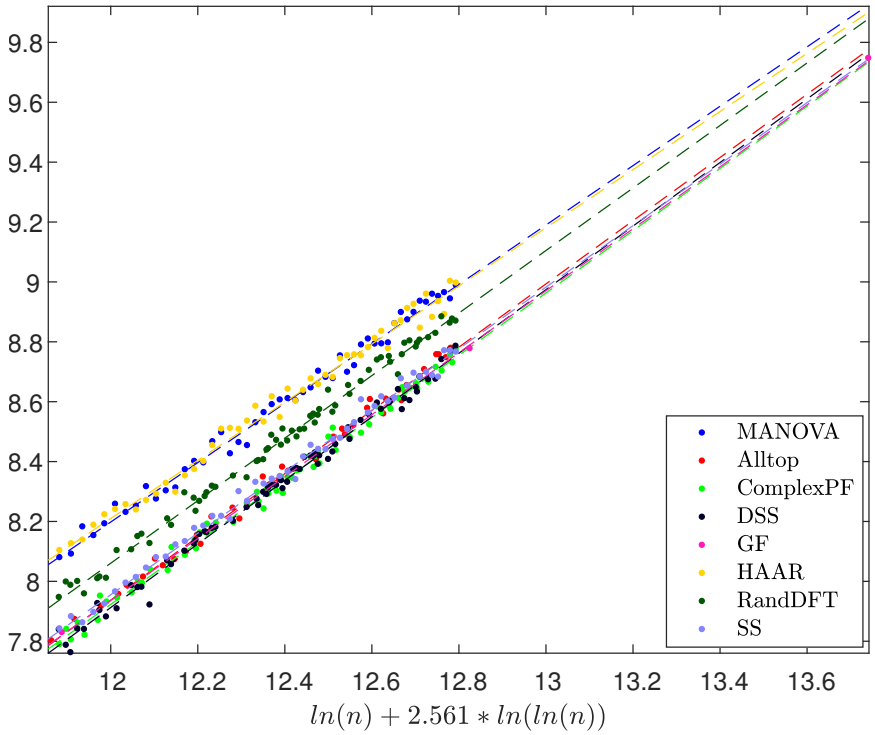

Figure 39: Test 2 for Ψ_{min}, complex frames $\gamma = 0.5$ and $\beta = 0.3$. Plot shows $-\ln \mathbb{E}_{K_n}(\Delta_\Psi(X_{K_n}^{(n)}; n, m_n, k_n)^2)$

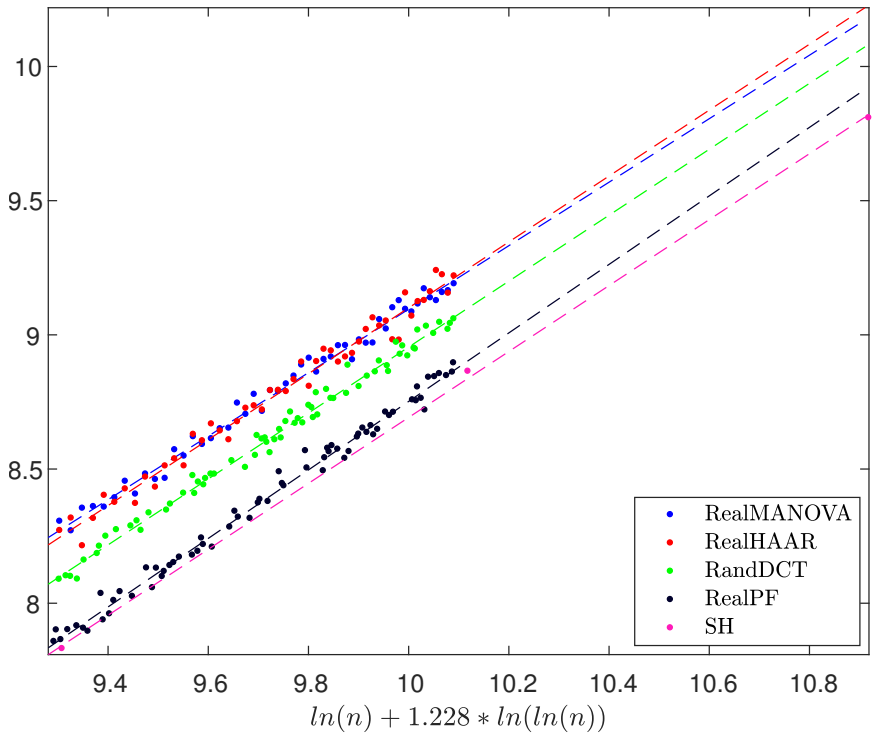

Figure 40: Test 2 for Ψ_{min}, real frames $\gamma = 0.5$ and $\beta = 0.3$. Plot shows $-\ln \mathbb{E}_{K_n}(\Delta_\Psi(X_{K_n}^{(n)}; n, m_n, k_n)^2)$

Frame	R^2	$\hat{b}$	$SE(\hat{b})$	p-value $b = b_{MANOVA}$
MANOVA	0.99056	0.99182	0.01397	1
DSS	0.99244	1.06161	0.01141	1.8239e-04
GF	0.99983	1.03473	0.01366	0.03283
ComplexPF	0.99324	1.03977	0.01056	0.00718
Alltop	0.99410	1.05594	0.01375	0.00157
SS	0.99410	1.02726	0.01142	0.05251
HAAR	0.98729	0.97082	0.01590	0.32367
RandDFT	0.99234	1.04425	0.01129	0.00424
RealMANOVA	0.98840	1.18289	0.01850	1
RealPF	0.99132	1.27638	0.01481	1.3915e-04
SH	0.99950	1.22853	0.02737	0.17335
RealHAAR	0.98073	1.22789	0.02484	0.14952
RandDCT	0.99002	1.22842	0.01518	0.05964

Table 23: Results of Test 2 for Ψ_{min}, $\gamma = 0.5$ and $\beta = 0.3$

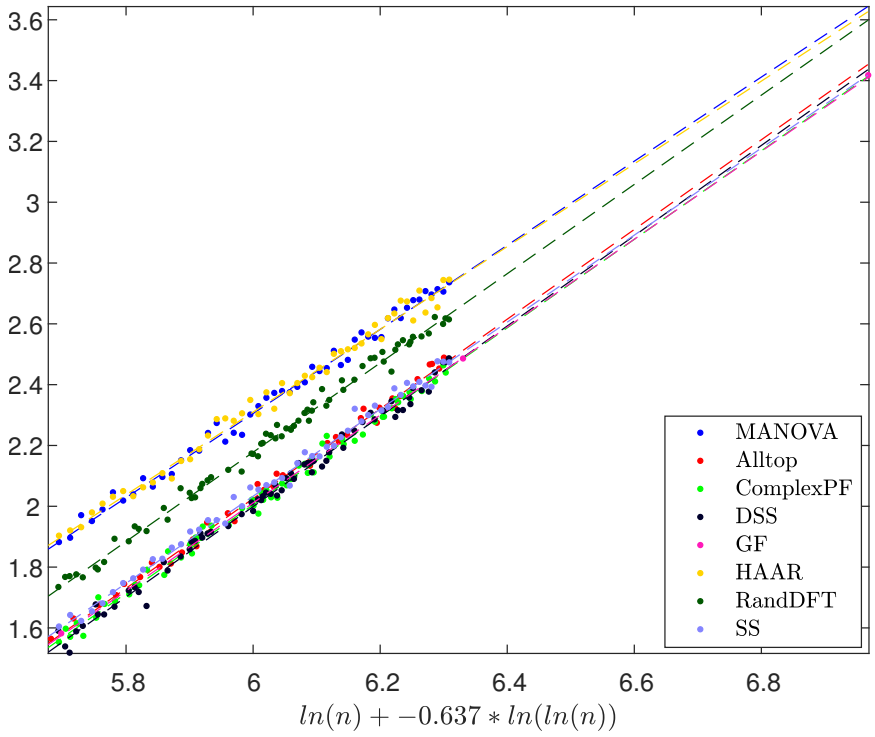

Figure 41: Test 2 for Ψ_{cond}, complex frames $\gamma = 0.5$ and $\beta = 0.3$. Plot shows $-\ln \mathbb{E}_{K_n}(\Delta_\Psi(X_{K_n}^{(n)}; n, m_n, k_n)^2)$

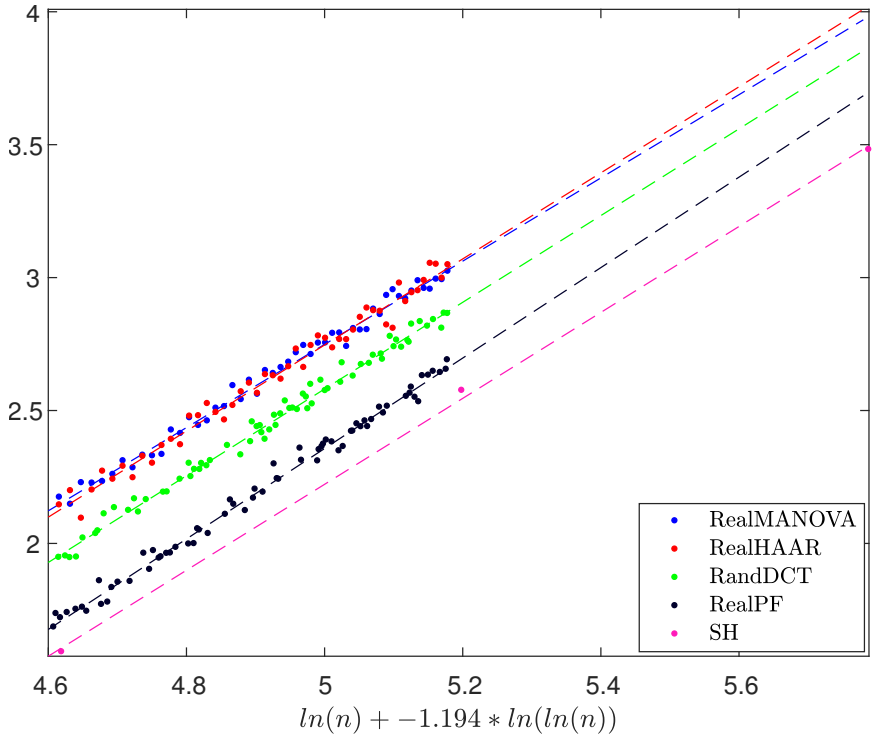

Figure 42: Test 2 for Ψ_{cond}, real frames $\gamma = 0.5$ and $\beta = 0.3$. Plot shows $-\ln \mathbb{E}_{K_n}(\Delta_\Psi(X_{K_n}^{(n)}; n, m_n, k_n)^2)$

Frame	R^2	$\hat{b}$	$SE(\hat{b})$	p-value $b = b_{MANOVA}$
MANOVA	0.99238	1.38324	0.01749	1
DSS	0.99216	1.48483	0.01625	4.3057e-05
GF	0.99996	1.44541	0.00911	0.00276
ComplexPF	0.99312	1.45565	0.01491	0.00208
Alltop	0.99463	1.47514	0.01832	4.9255e-04
SS	0.99399	1.43121	0.01607	0.04620
HAAR	0.98901	1.36048	0.02070	0.40310
RandDFT	0.99366	1.46787	0.01443	2.9738e-04
RealMANOVA	0.98972	1.56531	0.02303	1
RealPF	0.99237	1.70134	0.01851	1.0890e-05
SH	0.99918	1.61649	0.04624	0.32662
RealHAAR	0.98148	1.61870	0.03210	0.17972
RandDCT	0.99014	1.63103	0.02003	0.03340

Table 24: Results of Test 2 for Ψ_{cond}, $\gamma = 0.5$ and $\beta = 0.3$

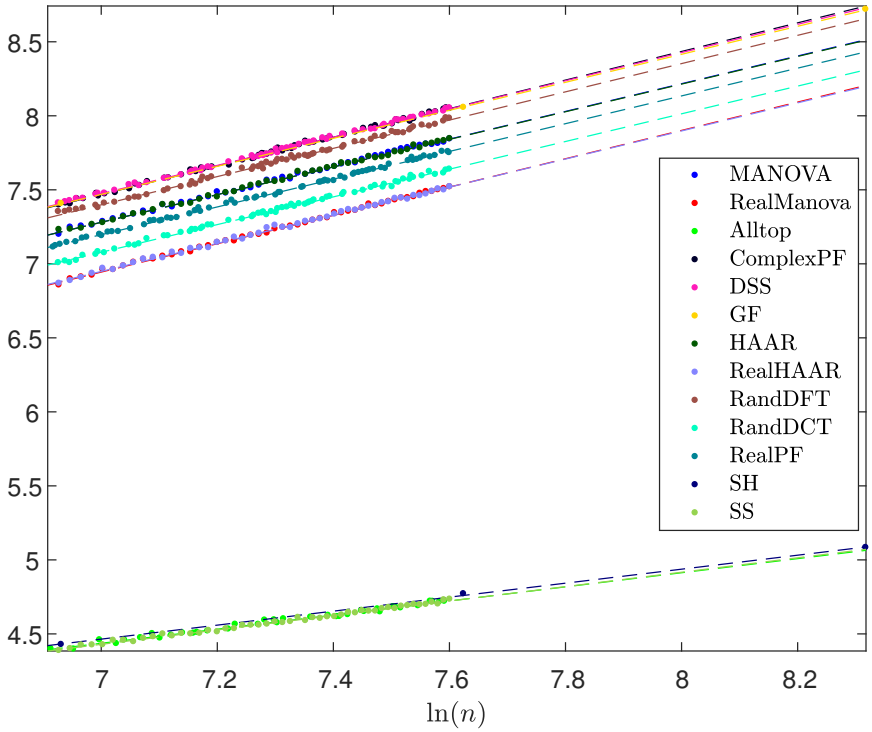

Figure 43: Test 1 for $\gamma = 0.5$ and $\beta = 0.7$. Plot shows $-\frac{1}{2}\ln Var_{K_n}(\Delta_{KS}(X^{(n)}_{K_n}; n, m_n, k_n))$ over $\ln(n)$.

Frame	R^2	$\hat{b}$	$SE(\hat{b})$	p-value $b = b_{MANOVA}$
MANOVA	0.99781	0.93614	0.00634	1
DSS	0.99862	0.95288	0.00436	0.03163
GF	0.99997	0.94619	0.00548	0.23647
ComplexPF	0.99812	0.96660	0.00516	3.0455e-04
Alltop	0.98575	0.47645	0.00968	8.9010e-56
SS	0.99349	0.48714	0.00569	1.1118e-72
HAAR	0.99755	0.93398	0.00667	0.81484
RandDFT	0.99692	0.95416	0.00653	0.05003
RealMANOVA	0.99854	0.95719	0.00528	1
RealPF	0.99847	0.93757	0.00455	0.00575
SH	0.99930	0.47252	0.01250	9.4783e-37
RealHAAR	0.99729	0.94907	0.00715	0.36285
RandDCT	0.99744	0.93559	0.00584	0.00702

Table 25: Results of Test 1 for $\gamma = 0.5$ and $\beta = 0.7$.

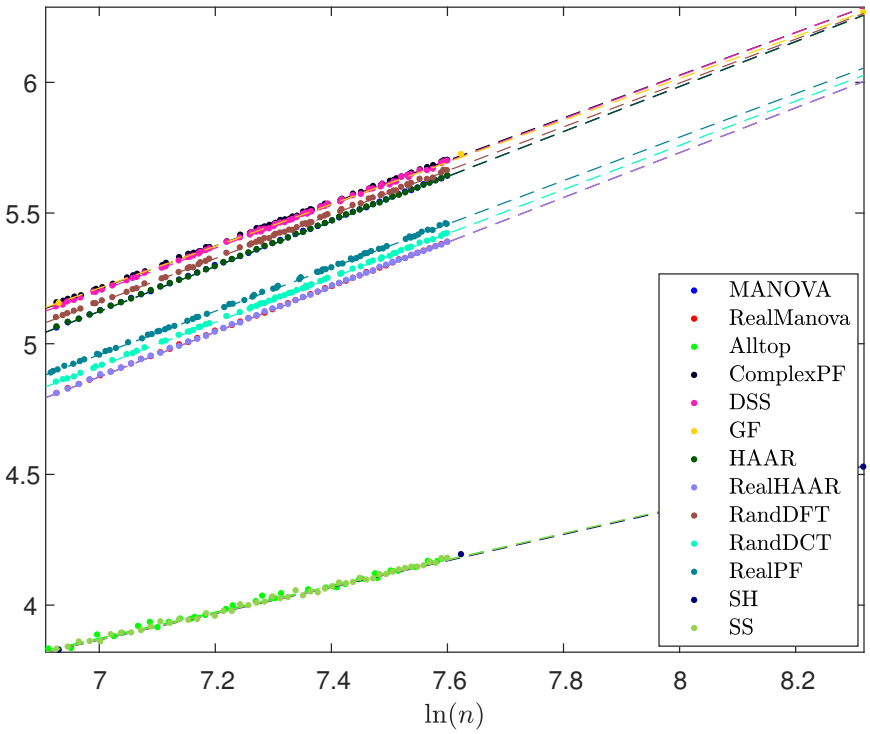

Figure 44: Test 1 for $\gamma = 0.5$ and $\beta = 0.7$. Plot shows $-\frac{1}{2}\ln \mathbb{E}_{K_n}(\Delta_{KS}(X^{(n)}_{K_n}; n, m_n, k_n)^2)$ over $\ln(n)$.

Frame	R^2	$\hat{b}$	$SE(\hat{b})$	p-value $b = b_{MANOVA}$
MANOVA	0.99995	0.86099	0.00089	1
DSS	0.99952	0.82437	0.00221	1.6297e-29
GF	0.99980	0.80241	0.01148	5.7020e-06
ComplexPF	0.99975	0.81672	0.00159	5.6500e-47
Alltop	0.99326	0.50123	0.00698	1.5720e-64
SS	0.99588	0.50803	0.00472	3.2682e-86
HAAR	0.99991	0.85964	0.00118	0.36383
RandDFT	0.99961	0.83909	0.00203	5.3952e-17
RealMANOVA	0.99994	0.85797	0.00098	1
RealPF	0.99982	0.83245	0.00137	5.8107e-29
SH	0.99937	0.50503	0.01265	1.1105e-31
RealHAAR	0.99983	0.85836	0.00160	0.83498
RandDCT	0.99986	0.84552	0.00125	2.3074e-12

Table 26: Results of Test 1 (MSE) for $\gamma = 0.5$ and $\beta = 0.7$.

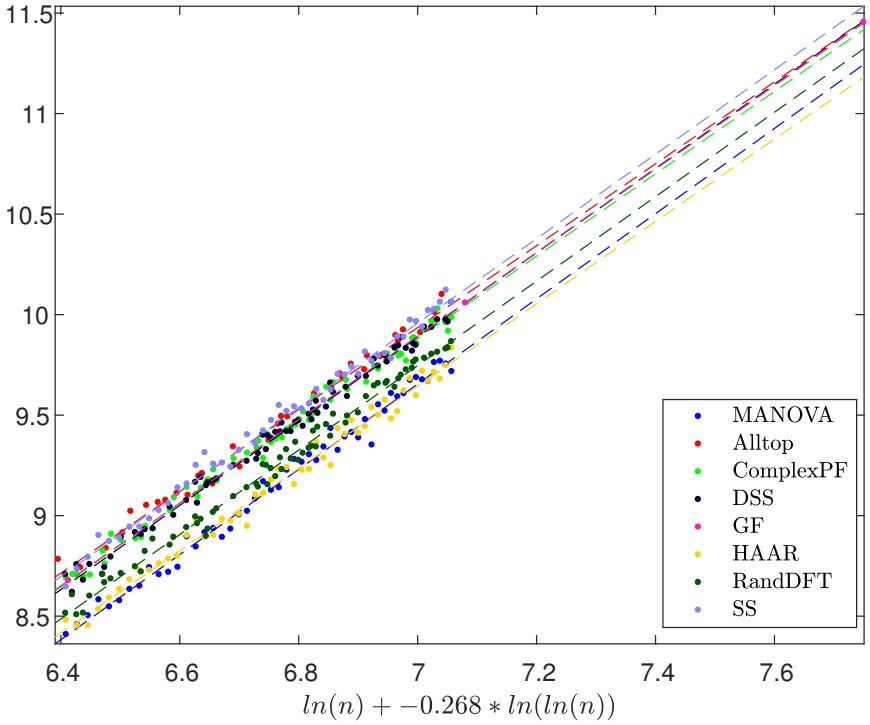

Figure 45: Test 2 for Ψ_{AC}, complex frames $\gamma = 0.5$ and $\beta = 0.7$. Plot shows $-\ln \mathbb{E}_{K_n}(\Delta_\Psi(X^{(n)}_{K_n}; n, m_n, k_n)^2)$

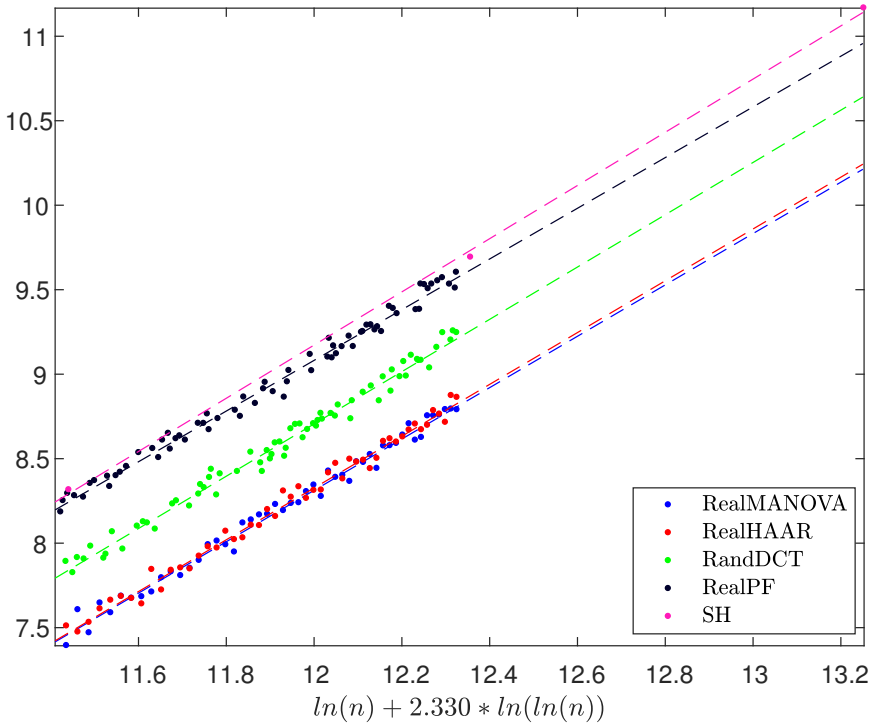

Figure 46: Test 2 for Ψ_{AC}, real frames $\gamma = 0.5$ and $\beta = 0.7$. Plot shows $-\ln \mathbb{E}_{K_n}(\Delta_\Psi(X^{(n)}_{K_n}; n, m_n, k_n)^2)$

Frame	R^2	$\hat{b}$	$SE(\hat{b})$	p-value $b = b_{MANOVA}$
MANOVA	0.98926	2.11954	0.03187	1
DSS	0.99236	2.09471	0.02262	0.52665
GF	1.00000	2.07672	0.00454	0.18970
ComplexPF	0.99162	2.04781	0.02317	0.07135
Alltop	0.98981	2.03636	0.03493	0.08224
SS	0.99064	2.10064	0.02946	0.66433
HAAR	0.98611	2.04757	0.03507	0.13217
RandDFT	0.99083	2.10030	0.02487	0.63509
RealMANOVA	0.98806	1.51990	0.02411	1
RealPF	0.98924	1.50015	0.01941	0.52485
SH	0.99932	1.57420	0.04097	0.25896
RealHAAR	0.98870	1.53283	0.02365	0.70259
RandDCT	0.98535	1.54744	0.02322	0.41238

Table 27: Results of Test 2 for Ψ_{AC}, $\gamma = 0.5$ and $\beta = 0.7$

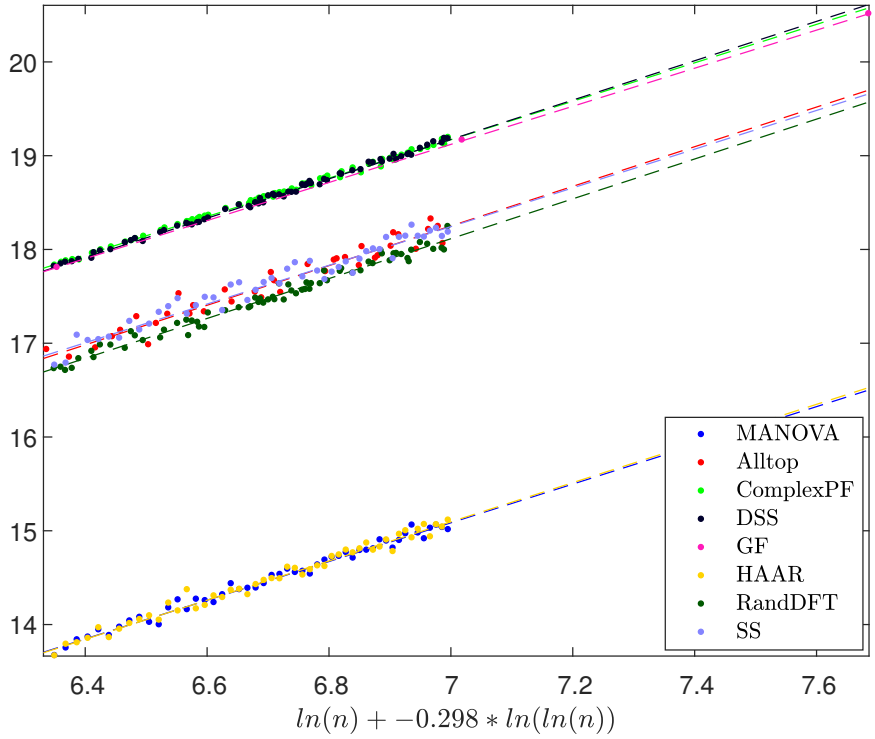

Figure 47: Test 2 for $\Psi_{Shannon}$, complex frames $\gamma = 0.5$ and $\beta = 0.7$. Plot shows $-\ln \mathbb{E}_{K_n}(\Delta_\Psi(X^{(n)}_{K_n}; n, m_n, k_n)^2)$

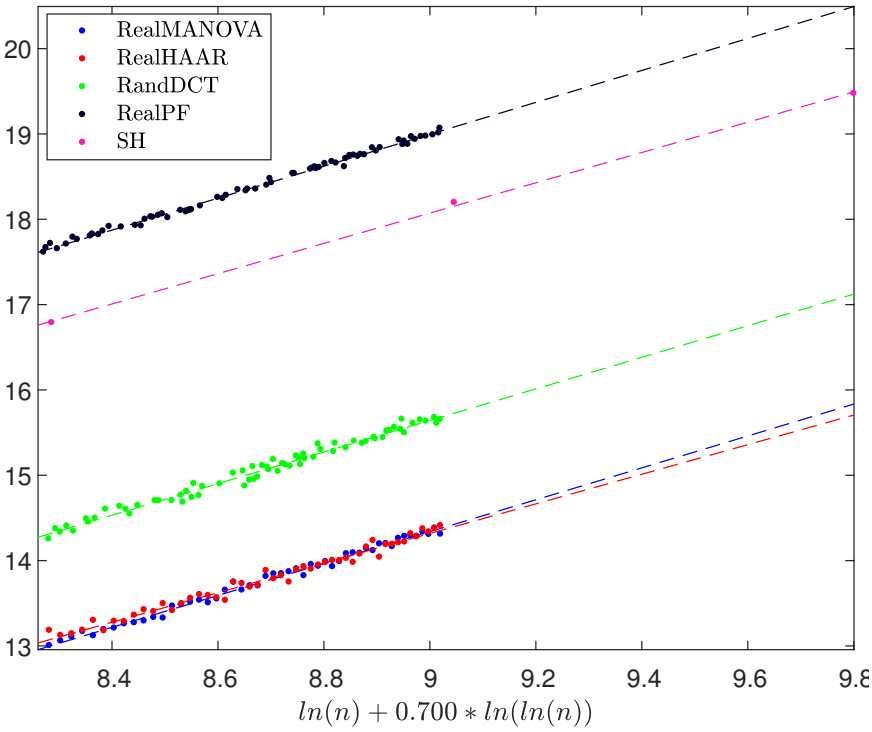

Figure 48: Test 2 for $\Psi_{Shannon}$, real frames $\gamma = 0.5$ and $\beta = 0.7$. Plot shows $-\ln \mathbb{E}_{K_n}(\Delta_\Psi(X^{(n)}_{K_n}; n, m_n, k_n)^2)$

Frame	R^2	$\hat{b}$	$SE(\hat{b})$	p-value $b = b_{MANOVA}$
MANOVA	0.98597	2.06467	0.03554	1
DSS	0.99697	2.09908	0.01424	0.37067
GF	0.99999	2.03088	0.00733	0.35636
ComplexPF	0.99759	2.04939	0.01241	0.68567
Alltop	0.94715	2.11342	0.08439	0.59588
SS	0.95593	2.06461	0.06399	0.99936
HAAR	0.98238	2.08832	0.04037	0.66114
RandDFT	0.97959	2.12566	0.03777	0.24205
RealMANOVA	0.99160	1.86924	0.02483	1
RealPF	0.99567	1.87123	0.01530	0.94592
SH	0.99933	1.77511	0.04585	0.07715
RealHAAR	0.98081	1.73457	0.03502	0.00227
RandDCT	0.98255	1.85061	0.03036	0.63561

Table 28: Results of Test 2 for $\Psi_{Shannon}$, $\gamma = 0.5$ and $\beta = 0.7$

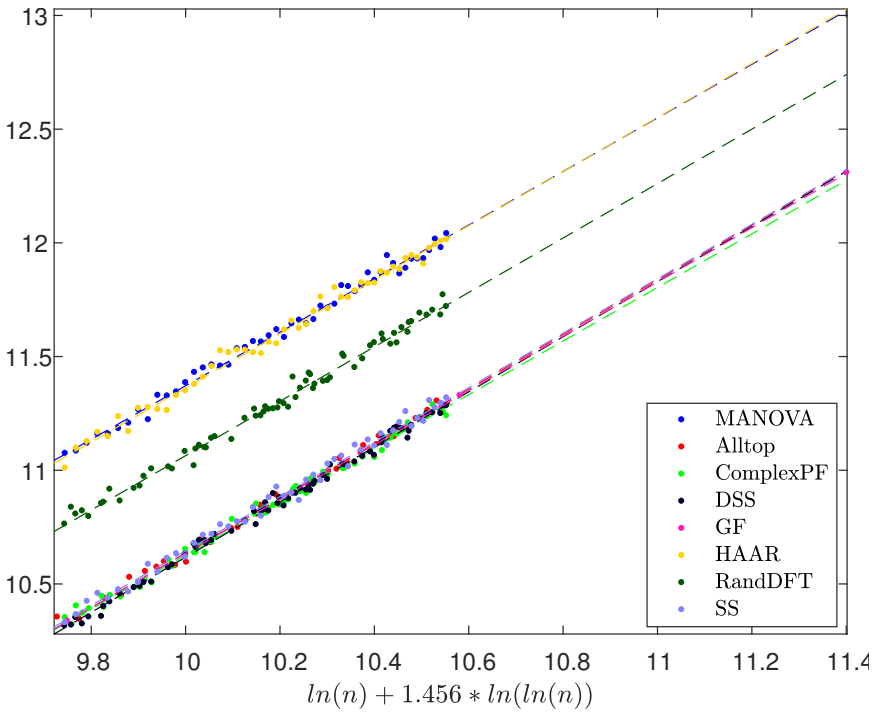

Figure 49: Test 2 for Ψ_{RIP}, complex frames $\gamma = 0.5$ and $\beta = 0.7$. Plot shows $-\ln \mathbb{E}_{K_n}(\Delta_\Psi(X_{K_n}^{(n)}; n, m_n, k_n)^2)$

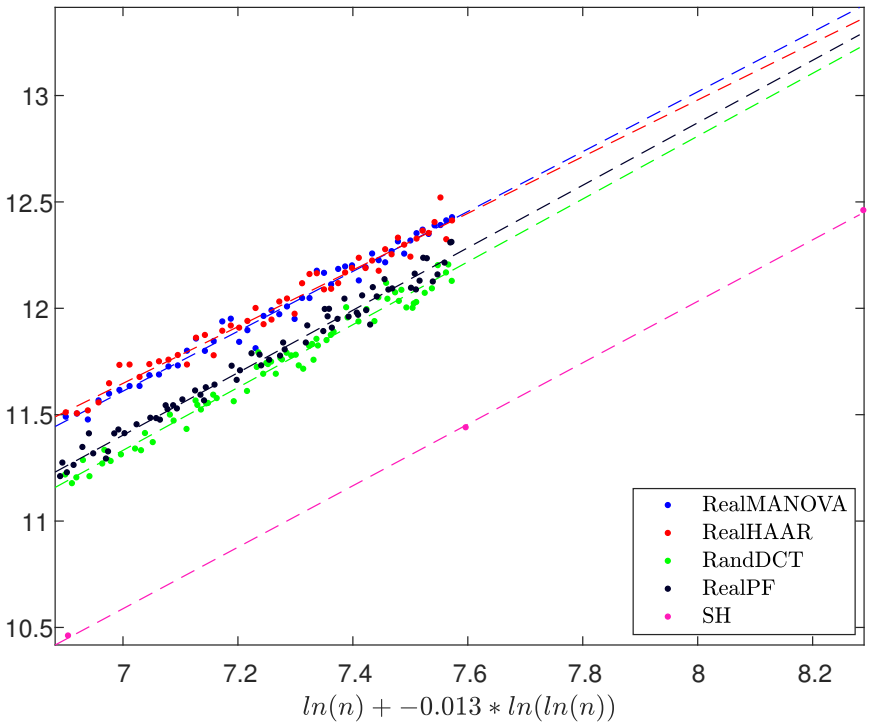

Figure 50: Test 2 for Ψ_{RIP}, real frames $\gamma = 0.5$ and $\beta = 0.7$. Plot shows $-\ln \mathbb{E}_{K_n}(\Delta_\Psi(X_{K_n}^{(n)}; n, m_n, k_n)^2)$

Frame	R^2	$\hat{b}$	$SE(\hat{b})$	p-value $b = b_{MANOVA}$
MANOVA	0.99163	1.17800	0.01562	1
DSS	0.99482	1.21202	0.01077	0.07552
GF	1.00000	1.19385	0.00000	0.31505
ComplexPF	0.99371	1.17836	0.01154	0.98495
Alltop	0.99525	1.20188	0.01403	0.25858
SS	0.99122	1.19728	0.01627	0.39463
HAAR	0.98964	1.18927	0.01756	0.63261
RandDFT	0.98963	1.19663	0.01508	0.39254
RealMANOVA	0.98031	1.40713	0.02878	1
RealPF	0.98171	1.46841	0.02486	0.10995
SH	0.99985	1.44473	0.01741	0.26908
RealHAAR	0.97038	1.33189	0.03359	0.09219
RandDCT	0.97728	1.47675	0.02772	0.08416

Table 29: Results of Test 2 for Ψ_{RIP}, $\gamma = 0.5$ and $\beta = 0.7$

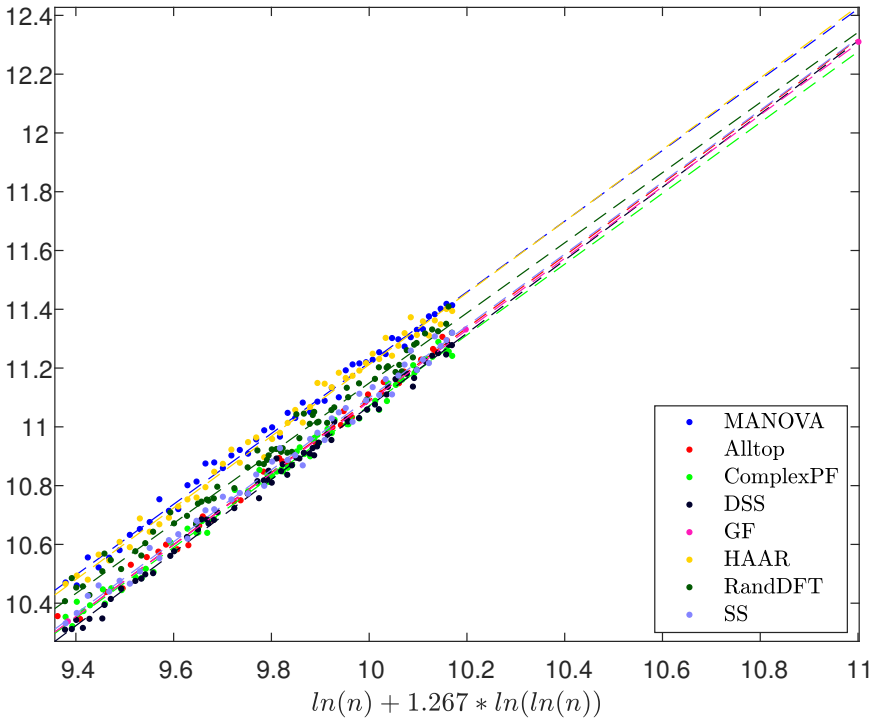

Figure 51: Test 2 for Ψ_{max}, complex frames $\gamma = 0.5$ and $\beta = 0.7$. Plot shows $-\ln \mathbb{E}_{K_n}(\Delta_\Psi(X_{K_n}^{(n)}; n, m_n, k_n)^2)$

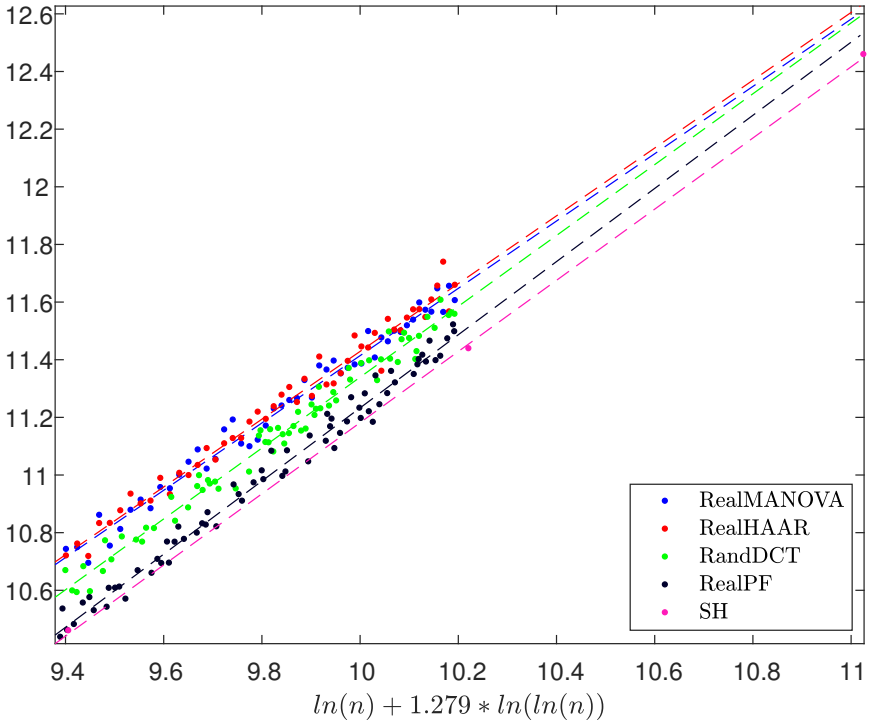

Figure 52: Test 2 for Ψ_{max}, real frames $\gamma = 0.5$ and $\beta = 0.7$. Plot shows $-\ln \mathbb{E}_{K_n}(\Delta_\Psi(X_{K_n}^{(n)}; n, m_n, k_n)^2)$

Frame	R^2	$\hat{b}$	$SE(\hat{b})$	p-value $b = b_{MANOVA}$
MANOVA	0.99281	1.20385	0.01479	1
DSS	0.99482	1.24351	0.01105	0.03381
GF	1.00000	1.21923	0.00057	0.30390
ComplexPF	0.99371	1.20440	0.01179	0.97686
Alltop	0.99526	1.22841	0.01433	0.23633
SS	0.99122	1.22371	0.01662	0.37430
HAAR	0.98968	1.21898	0.01797	0.51696
RandDFT	0.98896	1.19315	0.01552	0.61880
RealMANOVA	0.98140	1.16763	0.02320	1
RealPF	0.98604	1.26889	0.01873	9.4468e-04
SH	0.99975	1.23451	0.01960	0.03241
RealHAAR	0.97935	1.17595	0.02465	0.80640
RandDCT	0.98079	1.22919	0.02118	0.05250

Table 30: Results of Test 2 for Ψ_{max}, $\gamma = 0.5$ and $\beta = 0.7$

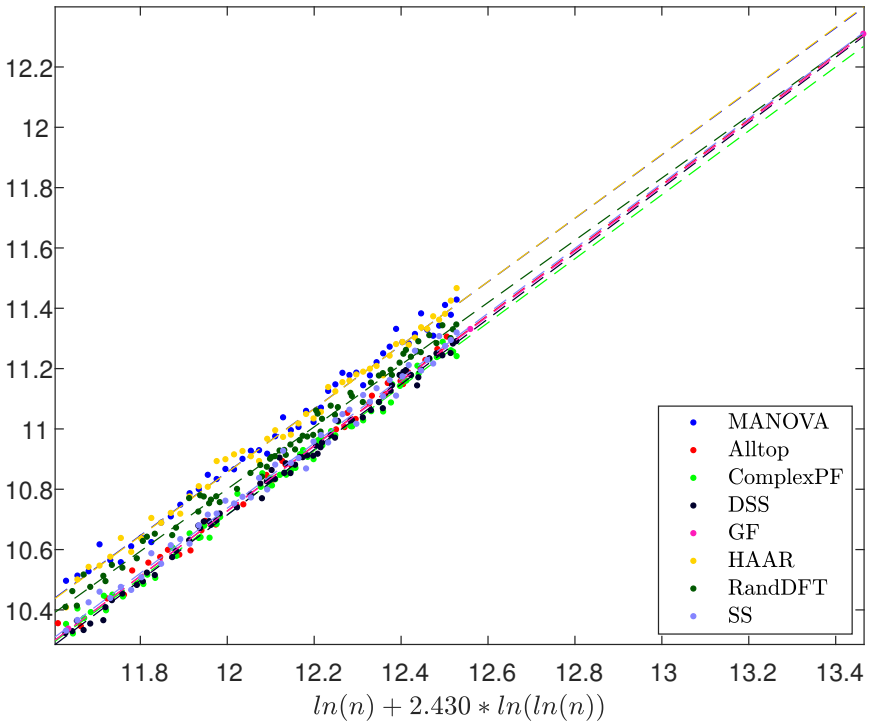

Figure 53: Test 2 for Ψ_{min}, complex frames $\gamma = 0.5$ and $\beta = 0.7$. Plot shows $-\ln \mathbb{E}_{K_n}(\Delta_\Psi(X_{K_n}^{(n)}; n, m_n, k_n)^2)$

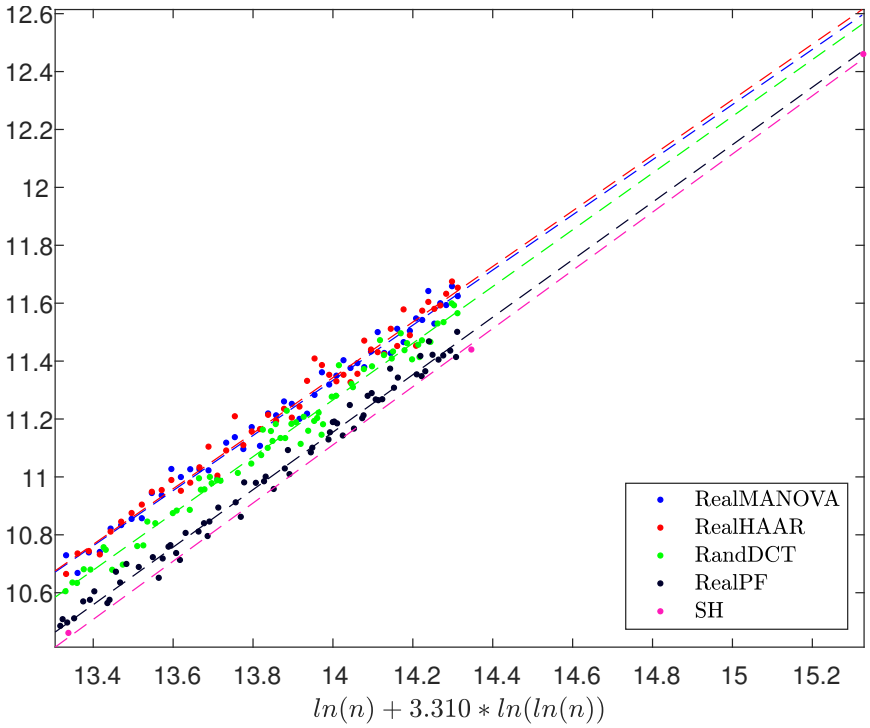

Figure 54: Test 2 for Ψ_{min}, real frames $\gamma = 0.5$ and $\beta = 0.7$. Plot shows $-\ln \mathbb{E}_{K_n}(\Delta_\Psi(X_{K_n}^{(n)}; n, m_n, k_n)^2)$

Frame	R^2	$\hat{b}$	$SE(\hat{b})$	p-value $b = b_{MANOVA}$
MANOVA	0.98978	1.05181	0.01542	1
DSS	0.99485	1.08386	0.00960	0.08035
GF	1.00000	1.07793	0.00231	0.10034
ComplexPF	0.99371	1.05999	0.01038	0.66086
Alltop	0.99521	1.08123	0.01268	0.14438
SS	0.99121	1.07709	0.01464	0.23750
HAAR	0.99139	1.05452	0.01419	0.89754
RandDFT	0.99236	1.03106	0.01114	0.27780
RealMANOVA	0.98343	0.95228	0.01784	1
RealPF	0.98827	0.99291	0.01342	0.07140
SH	0.99960	1.00464	0.02016	0.05755
RealHAAR	0.97875	0.95975	0.02041	0.78346
RandDCT	0.98148	0.97957	0.01656	0.26473

Table 31: Results of Test 2 for Ψ_{min}, $\gamma = 0.5$ and $\beta = 0.7$

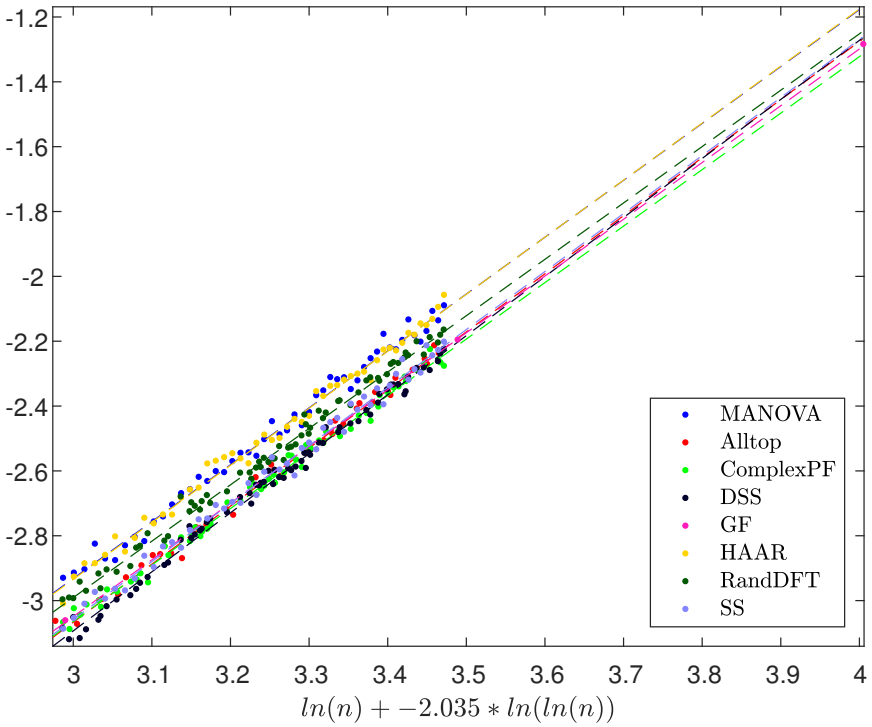

Figure 55: Test 2 for Ψ_{cond}, complex frames $\gamma = 0.5$ and $\beta = 0.7$. Plot shows $-\ln \mathbb{E}_{K_n}(\Delta_\Psi(X_{K_n}^{(n)}; n, m_n, k_n)^2)$

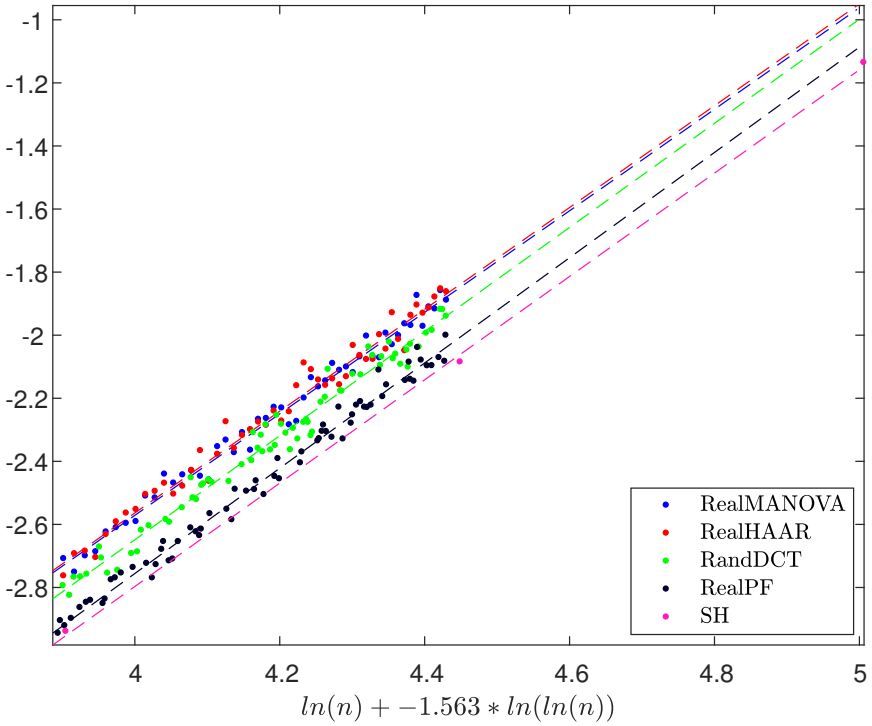

Figure 56: Test 2 for Ψ_{cond}, real frames $\gamma = 0.5$ and $\beta = 0.7$. Plot shows $-\ln \mathbb{E}_{K_n}(\Delta_\Psi(X_{K_n}^{(n)}; n, m_n, k_n)^2)$

Frame	R^2	$\hat{b}$	$SE(\hat{b})$	p-value $b = b_{MANOVA}$
MANOVA	0.98965	1.75454	0.02589	1
DSS	0.99336	1.82121	0.01833	0.03781
GF	0.99997	1.75070	0.00906	0.88906
ComplexPF	0.99371	1.74214	0.01706	0.68996
Alltop	0.99380	1.79103	0.02391	0.30355
SS	0.99076	1.78887	0.02494	0.34209
HAAR	0.99115	1.75885	0.02398	0.90316
RandDFT	0.99260	1.73868	0.01848	0.61896
RealMANOVA	0.98402	1.60942	0.02960	1
RealPF	0.98886	1.66891	0.02197	0.10931
SH	0.99944	1.63824	0.03888	0.55800
RealHAAR	0.97847	1.61412	0.03456	0.91781
RandDCT	0.97841	1.65074	0.03019	0.33042

Table 32: Results of Test 2 for Ψ_{cond}, $\gamma = 0.5$ and $\beta = 0.7$

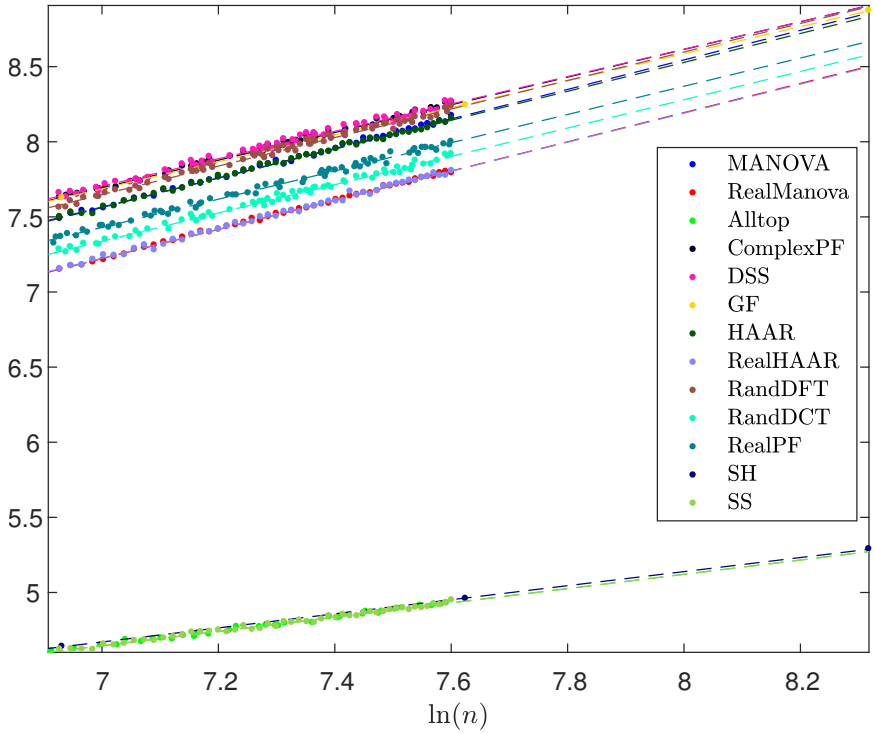

Figure 57: Test 1 for $\gamma = 0.5$ and $\beta = 0.9$. Plot shows $-\frac{1}{2}\ln Var_{K_n}(\Delta_{KS}(X^{(n)}_{K_n}; n, m_n, k_n))$ over $\ln(n)$.

Frame	R^2	$\hat{b}$	$SE(\hat{b})$	p-value $b = b_{MANOVA}$
MANOVA	0.99732	0.98259	0.00735	1
DSS	0.98932	0.91180	0.01166	1.1690e-06
GF	0.99998	0.89936	0.00381	1.6760e-13
ComplexPF	0.99399	0.92132	0.00882	4.8588e-07
Alltop	0.99177	0.47542	0.00732	5.7451e-63
SS	0.98941	0.47522	0.00710	2.7937e-70
HAAR	0.99660	0.96236	0.00811	0.06766
RandDFT	0.99163	0.94924	0.01074	0.01169
RealMANOVA	0.99857	0.97216	0.00531	1
RealPF	0.99335	0.93988	0.00954	0.00380
SH	0.99991	0.46842	0.00455	2.2473e-51
RealHAAR	0.99590	0.96622	0.00895	0.56919
RandDCT	0.99255	0.94213	0.01005	0.00939

Table 33: Results of Test 1 for $\gamma = 0.5$ and $\beta = 0.9$.

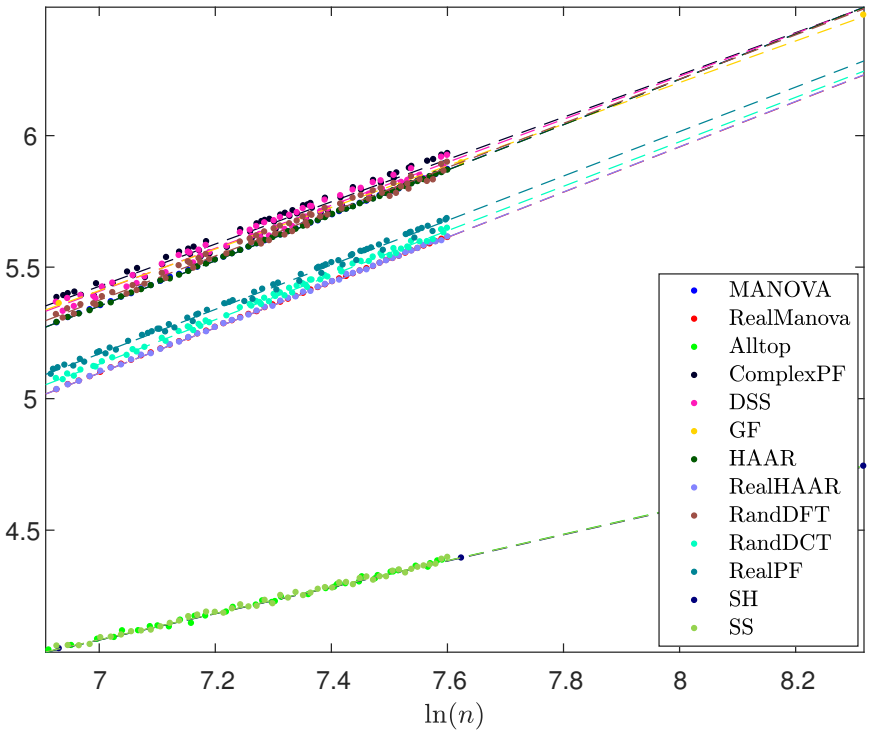

Figure 58: Test 1 for $\gamma = 0.5$ and $\beta = 0.9$. Plot shows $-\frac{1}{2}\ln \mathbb{E}_{K_n}(\Delta_{KS}(X_{K_n}^{(n)}; n, m_n, k_n)^2)$ over $\ln(n)$.

Frame	R^2	$\hat{b}$	$SE(\hat{b})$	p-value $b = b_{MANOVA}$
MANOVA	0.99994	0.86237	0.00092	1
DSS	0.98138	0.81763	0.01386	0.00167
GF	0.99980	0.79101	0.01117	6.3477e-08
ComplexPF	0.98209	0.80361	0.01336	2.5626e-05
Alltop	0.99553	0.50248	0.00569	1.6203e-71
SS	0.99450	0.50029	0.00537	4.3414e-82
HAAR	0.99986	0.86226	0.00147	0.94967
RandDFT	0.99072	0.84053	0.01001	0.03190
RealMANOVA	0.99996	0.86012	0.00076	1
RealPF	0.99681	0.84517	0.00593	0.01375
SH	0.99998	0.50030	0.00195	7.5424e-70
RealHAAR	0.99972	0.86079	0.00209	0.76526
RandDCT	0.99755	0.84547	0.00516	0.00584

Table 34: Results of Test 1 (MSE) for $\gamma = 0.5$ and $\beta = 0.9$.

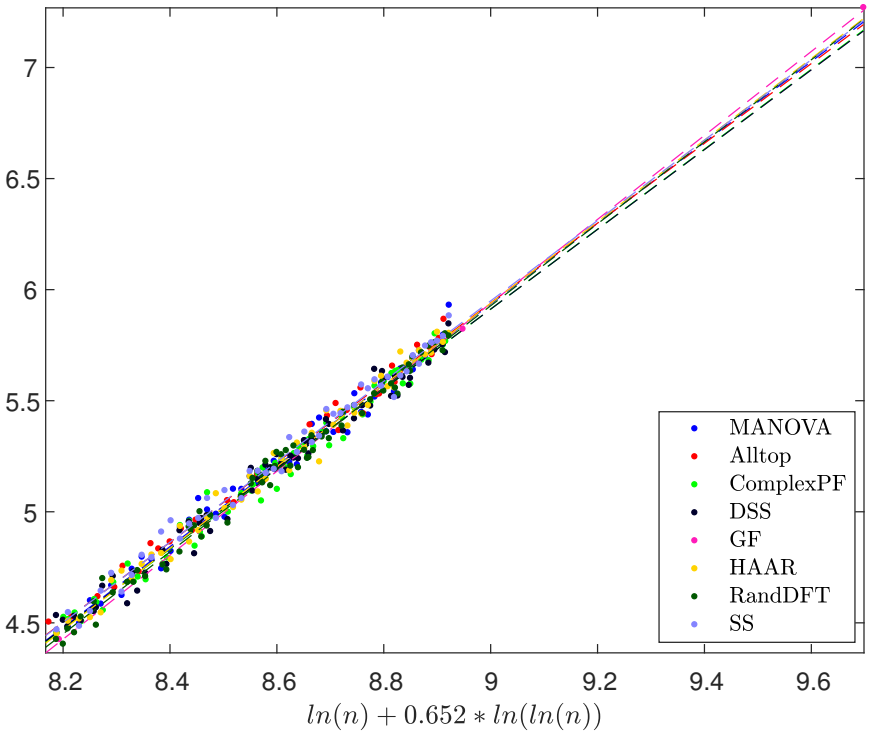

Figure 59: Test 2 for Ψ_{AC}, complex frames $\gamma = 0.5$ and $\beta = 0.9$. Plot shows $-\ln \mathbb{E}_{K_n}(\Delta_\Psi(X_{K_n}^{(n)}; n, m_n, k_n)^2)$

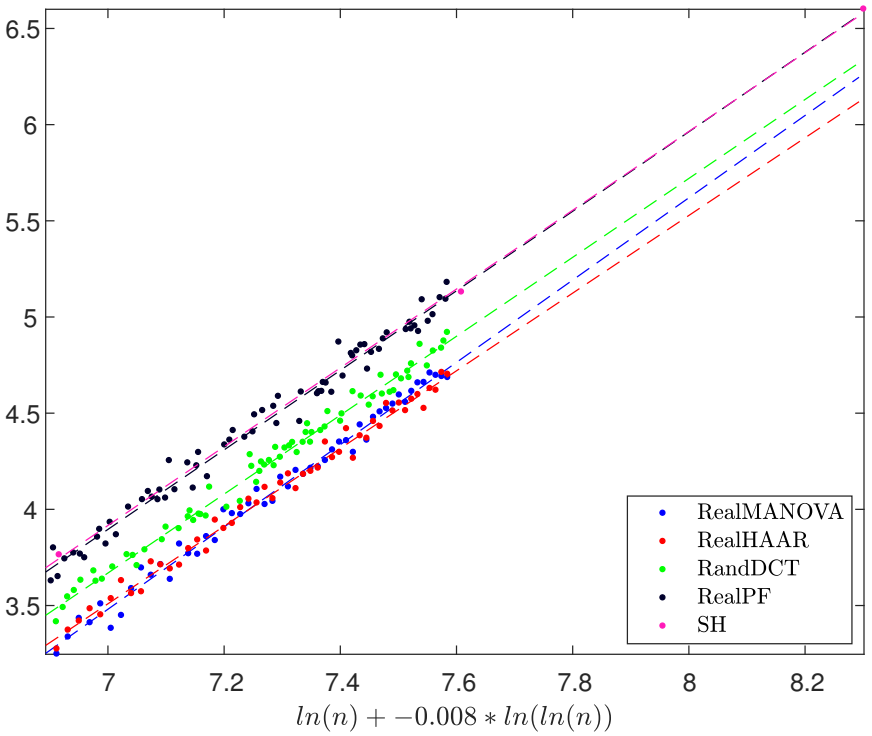

Figure 60: Test 2 for Ψ_{AC}, real frames $\gamma = 0.5$ and $\beta = 0.9$. Plot shows $-\ln \mathbb{E}_{K_n}(\Delta_\Psi(X_{K_n}^{(n)}; n, m_n, k_n)^2)$

Frame	R^2	$\hat{b}$	$SE(\hat{b})$	p-value $b = b_{MANOVA}$
MANOVA	0.98519	1.81997	0.03221	1
DSS	0.98443	1.79553	0.02779	0.56672
GF	0.99985	1.88996	0.02309	0.08366
ComplexPF	0.98608	1.80019	0.02633	0.63532
Alltop	0.98992	1.79620	0.03064	0.59418
SS	0.98759	1.80978	0.02929	0.81535
HAAR	0.98712	1.83770	0.03030	0.68949
RandDFT	0.98865	1.84632	0.02435	0.51546
RealMANOVA	0.98846	2.13921	0.03336	1
RealPF	0.98279	2.06724	0.03393	0.13322
SH	0.99955	2.04870	0.04346	0.10490
RealHAAR	0.98836	2.01886	0.03163	0.01028
RandDCT	0.98791	2.05145	0.02794	0.04606

Table 35: Results of Test 2 for Ψ_{AC}, $\gamma = 0.5$ and $\beta = 0.9$

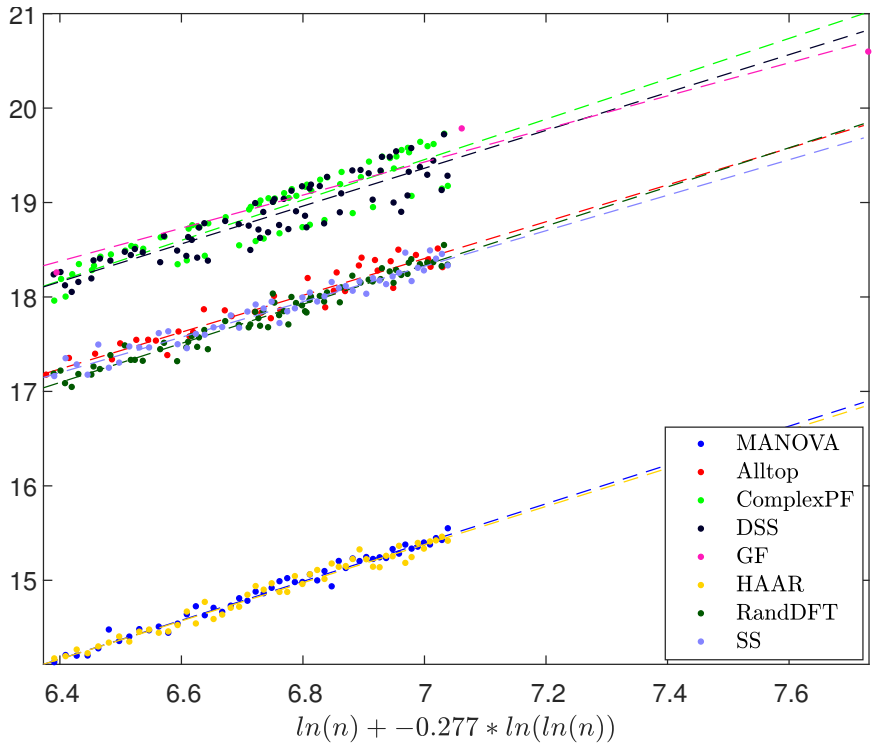

Figure 61: Test 2 for $\Psi_{Shannon}$, complex frames $\gamma = 0.5$ and $\beta = 0.9$. Plot shows $-\ln \mathbb{E}_{K_n}(\Delta_\Psi(X^{(n)}_{K_n}; n, m_n, k_n)^2)$

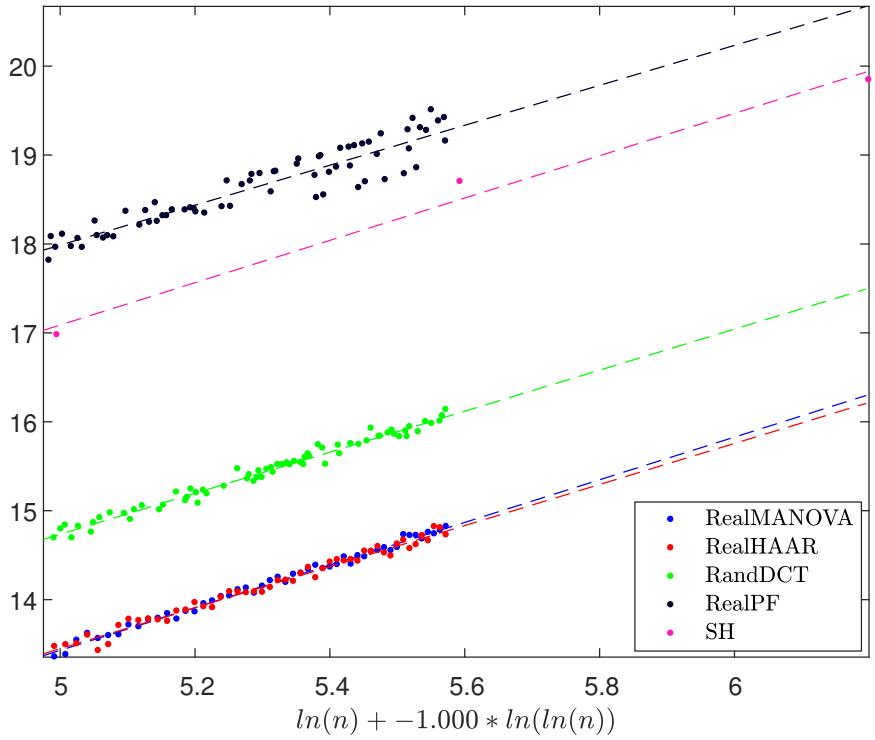

Figure 62: Test 2 for $\Psi_{Shannon}$, real frames $\gamma = 0.5$ and $\beta = 0.9$. Plot shows $-\ln \mathbb{E}_{K_n}(\Delta_\Psi(X^{(n)}_{K_n}; n, m_n, k_n)^2)$

Frame	R^2	$\hat{b}$	$SE(\hat{b})$	p-value $b = b_{MANOVA}$
MANOVA	0.98341	2.05508	0.03853	1
DSS	0.82831	2.00371	0.11229	0.66607
GF	0.96971	1.75044	0.30938	0.33329
ComplexPF	0.83591	2.13794	0.11660	0.50122
Alltop	0.91820	1.94898	0.09833	0.31796
SS	0.94928	1.87912	0.06270	0.01875
HAAR	0.97204	2.01977	0.04945	0.57450
RandDFT	0.95750	2.07089	0.05370	0.81142
RealMANOVA	0.99145	2.39788	0.03214	1
RealPF	0.87309	2.24624	0.10622	0.17453
SH	0.98556	2.38035	0.28810	0.95201
RealHAAR	0.98151	2.30834	0.04573	0.11241
RandDCT	0.97992	2.30731	0.04066	0.08321

Table 36: Results of Test 2 for $\Psi_{Shannon}$, $\gamma = 0.5$ and $\beta = 0.9$

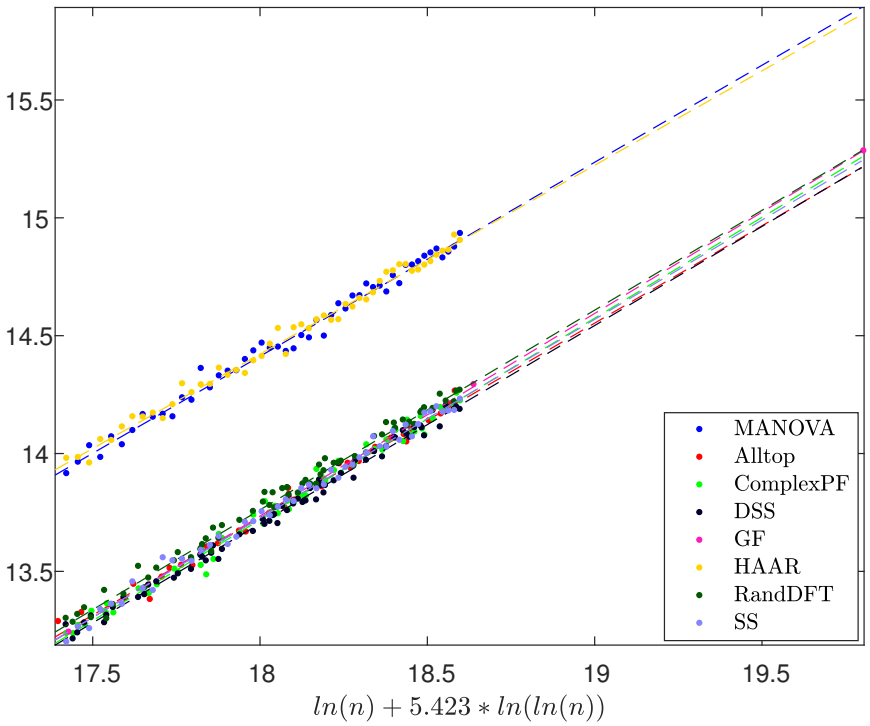

Figure 63: Test 2 for Ψ_{RIP}, complex frames $\gamma = 0.5$ and $\beta = 0.9$. Plot shows $-\ln \mathbb{E}_{K_n}(\Delta_\Psi(X_{K_n}^{(n)}; n, m_n, k_n)^2)$

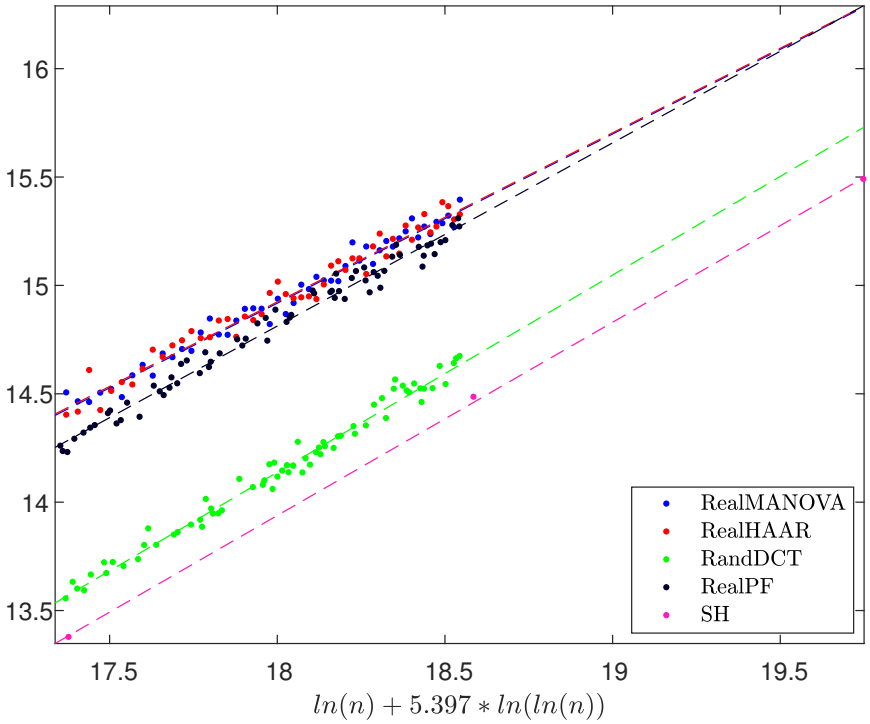

Figure 64: Test 2 for Ψ_{RIP}, real frames $\gamma = 0.5$ and $\beta = 0.9$. Plot shows $-\ln \mathbb{E}_{K_n}(\Delta_\Psi(X_{K_n}^{(n)}; n, m_n, k_n)^2)$

Frame	R^2	$\hat{b}$	$SE(\hat{b})$	p-value $b = b_{MANOVA}$
MANOVA	0.98831	0.82317	0.01292	1
DSS	0.99260	0.84095	0.00894	0.26042
GF	0.99997	0.85981	0.00484	0.01069
ComplexPF	0.98990	0.85543	0.01064	0.05647
Alltop	0.99162	0.82576	0.01283	0.88732
SS	0.99209	0.84278	0.01086	0.24837
HAAR	0.98958	0.80122	0.01187	0.21385
RandDFT	0.98969	0.84711	0.01064	0.15548
RealMANOVA	0.97813	0.78081	0.01685	1
RealPF	0.98156	0.84519	0.01437	0.00440
SH	0.99970	0.89155	0.01539	1.2847e-05
RealHAAR	0.96869	0.78013	0.02024	0.97956
RandDCT	0.98305	0.90978	0.01470	7.0613e-08

Table 37: Results of Test 2 for Ψ_{RIP}, $\gamma = 0.5$ and $\beta = 0.9$

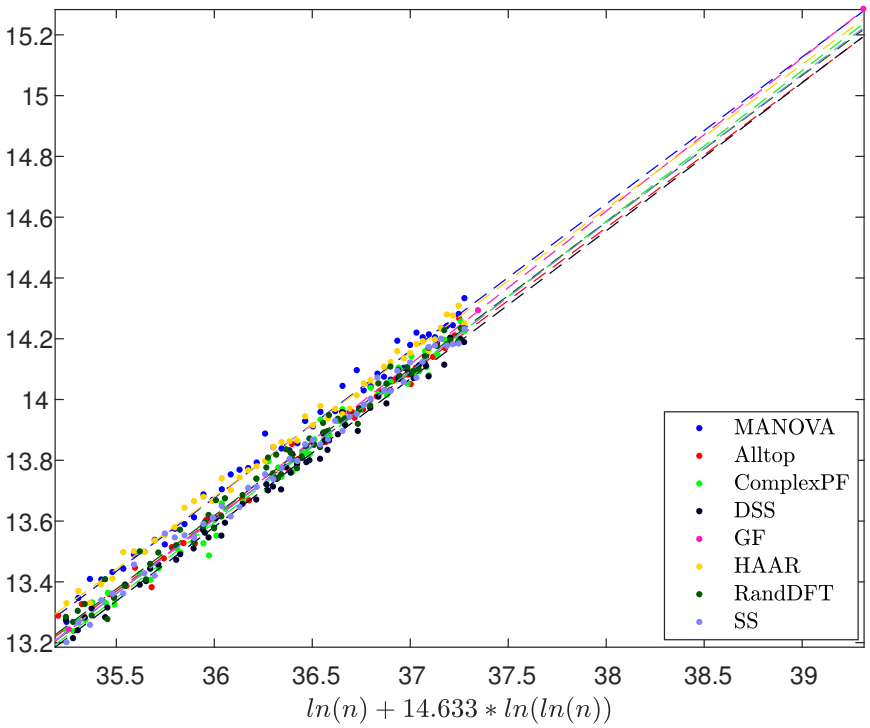

Figure 65: Test 2 for Ψ_{max}, complex frames $\gamma = 0.5$ and $\beta = 0.9$. Plot shows $-\ln \mathbb{E}_{K_n}(\Delta_\Psi(X_{K_n}^{(n)}; n, m_n, k_n)^2)$

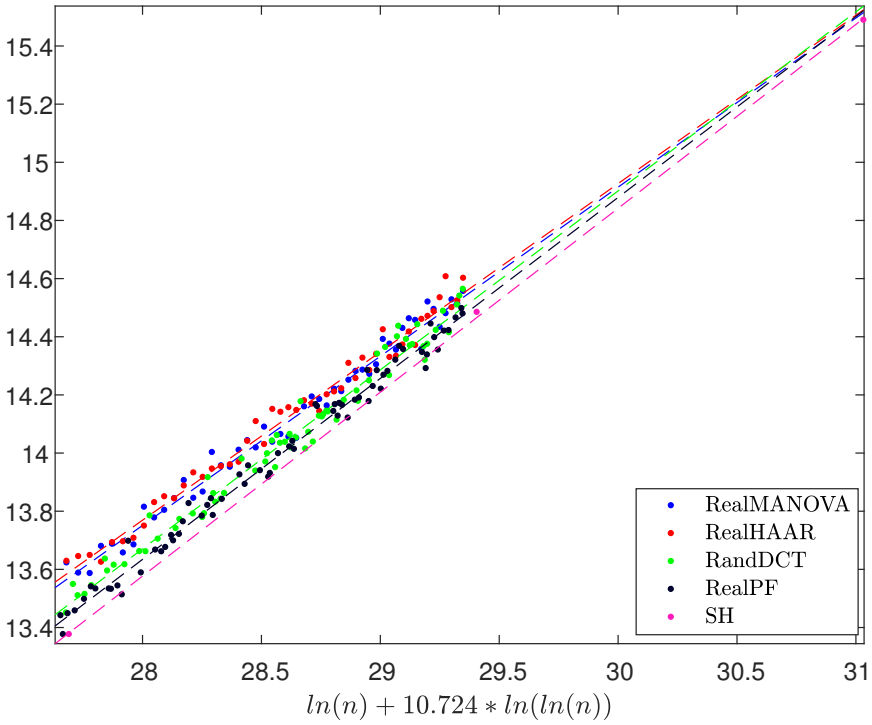

Figure 66: Test 2 for Ψ_{max}, real frames $\gamma = 0.5$ and $\beta = 0.9$. Plot shows $-\ln \mathbb{E}_{K_n}(\Delta_\Psi(X_{K_n}^{(n)}; n, m_n, k_n)^2)$

Frame	R^2	$\hat{b}$	$SE(\hat{b})$	p-value $b = b_{MANOVA}$
MANOVA	0.98860	0.48357	0.00750	1
DSS	0.99251	0.48723	0.00521	0.68865
GF	1.00000	0.50364	0.00036	0.01013
ComplexPF	0.98987	0.49566	0.00617	0.21561
Alltop	0.99142	0.47856	0.00752	0.63875
SS	0.99217	0.48847	0.00626	0.61688
HAAR	0.99308	0.47461	0.00572	0.34463
RandDFT	0.98890	0.48284	0.00630	0.94092
RealMANOVA	0.98303	0.58172	0.01103	1
RealPF	0.98749	0.62242	0.00869	0.00451
SH	0.99984	0.63242	0.00809	5.3680e-04
RealHAAR	0.98397	0.57885	0.01066	0.85218
RandDCT	0.97938	0.61567	0.01100	0.03136

Table 38: Results of Test 2 for Ψ_{max}, $\gamma = 0.5$ and $\beta = 0.9$

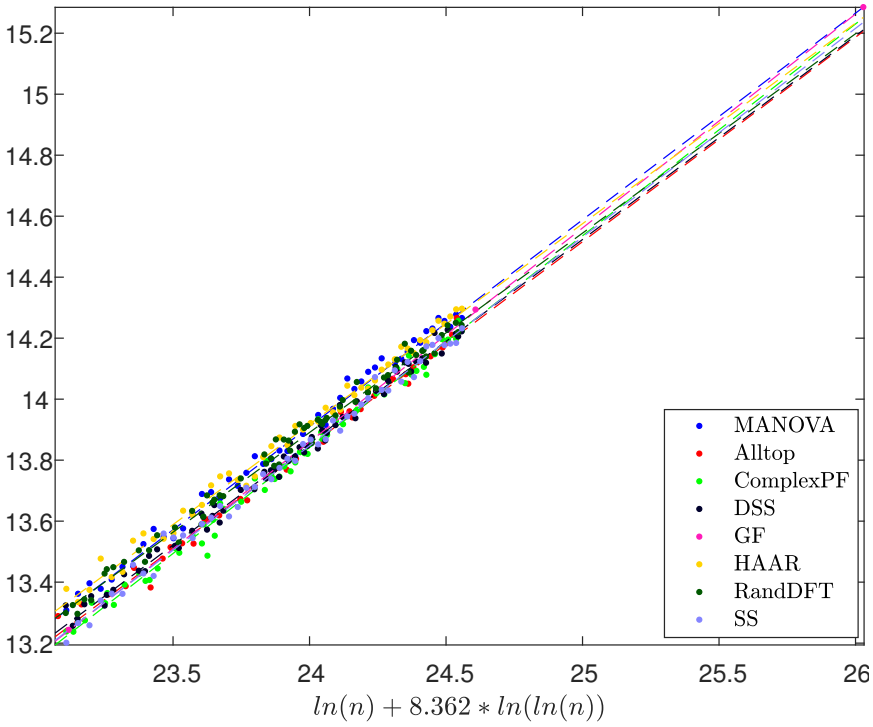

Figure 67: Test 2 for Ψ_{min}, complex frames $\gamma = 0.5$ and $\beta = 0.9$. Plot shows $-\ln \mathbb{E}_{K_n}(\Delta_\Psi(X_{K_n}^{(n)}; n, m_n, k_n)^2)$

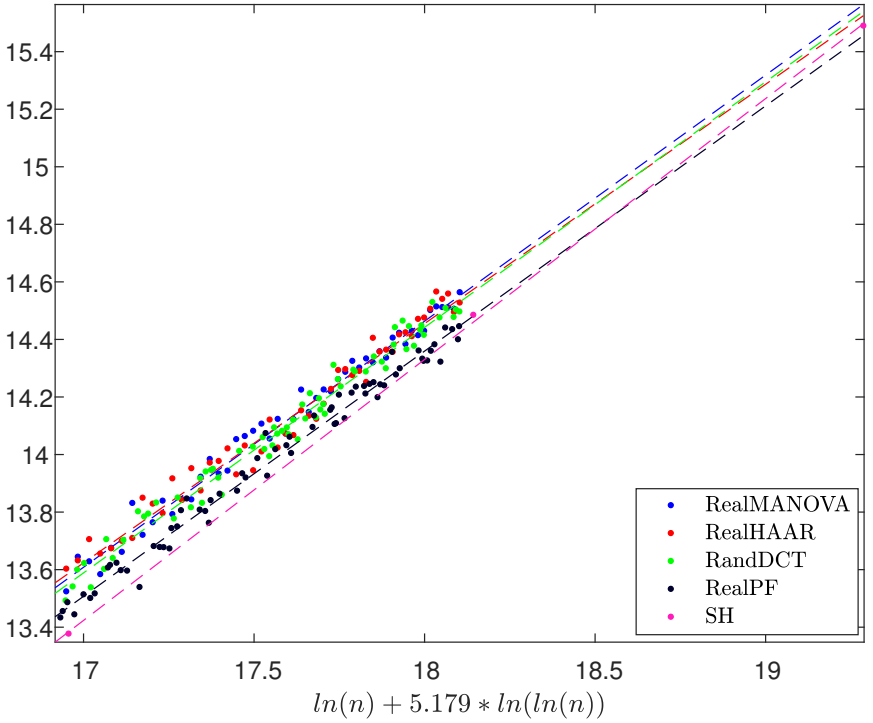

Figure 68: Test 2 for Ψ_{min}, real frames $\gamma = 0.5$ and $\beta = 0.9$. Plot shows $-\ln \mathbb{E}_{K_n}(\Delta_\Psi(X_{K_n}^{(n)}; n, m_n, k_n)^2)$

Frame	R^2	$\hat{b}$	$SE(\hat{b})$	p-value $b = b_{MANOVA}$
MANOVA	0.99144	0.67766	0.00909	1
DSS	0.99275	0.66805	0.00703	0.40499
GF	0.99999	0.70150	0.00197	0.01346
ComplexPF	0.98989	0.69455	0.00864	0.18061
Alltop	0.99153	0.67052	0.01047	0.60836
SS	0.99213	0.68437	0.00880	0.59690
HAAR	0.99182	0.65770	0.00862	0.11445
RandDFT	0.99047	0.65376	0.00789	0.04952
RealMANOVA	0.98532	0.85518	0.01507	1
RealPF	0.98463	0.85215	0.01321	0.88004
SH	0.99969	0.90673	0.01589	0.02263
RealHAAR	0.97575	0.83153	0.01892	0.33067
RandDCT	0.97957	0.85324	0.01517	0.92762

Table 39: Results of Test 2 for Ψ_{min}, $\gamma = 0.5$ and $\beta = 0.9$

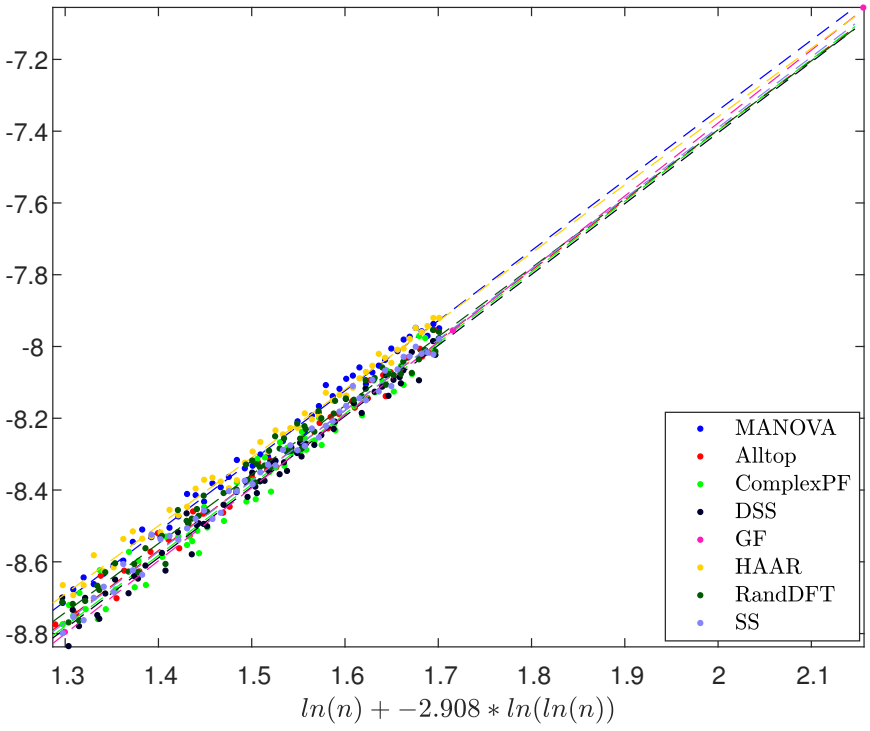

Figure 69: Test 2 for Ψ_{cond}, complex frames $\gamma = 0.5$ and $\beta = 0.9$. Plot shows $-\ln \mathbb{E}_{K_n}(\Delta_\Psi(X_{K_n}^{(n)}; n, m_n, k_n)^2)$

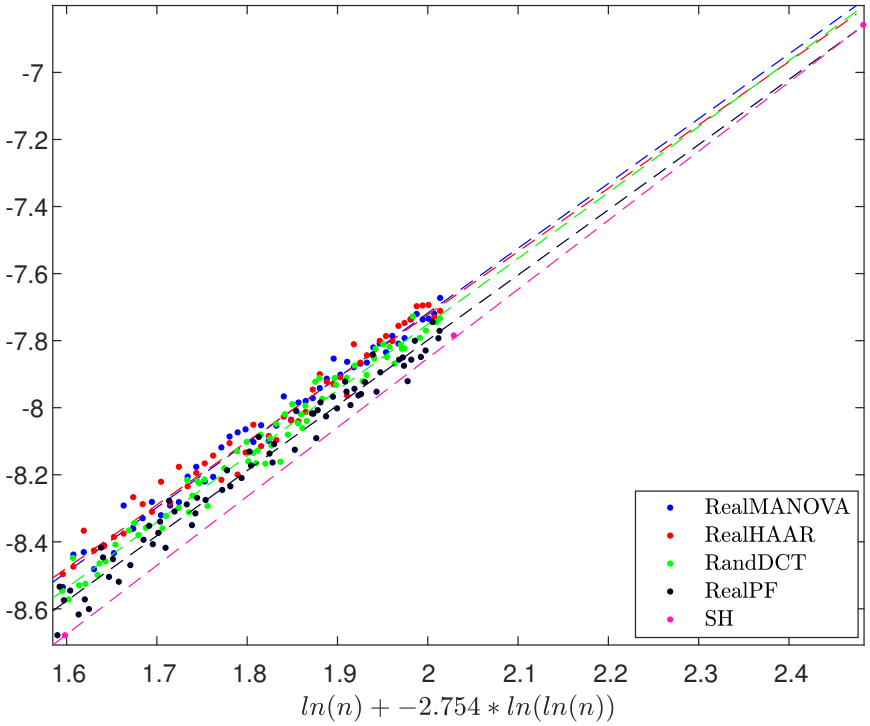

Figure 70: Test 2 for Ψ_{cond}, real frames $\gamma = 0.5$ and $\beta = 0.9$. Plot shows $-\ln \mathbb{E}_{K_n}(\Delta_\Psi(X_{K_n}^{(n)}; n, m_n, k_n)^2)$

Frame	R^2	$\hat{b}$	$SE(\hat{b})$	p-value $b = b_{MANOVA}$
MANOVA	0.99113	1.95395	0.02668	1
DSS	0.98283	1.97382	0.03212	0.63499
GF	0.99999	2.03289	0.00687	0.00612
ComplexPF	0.97497	1.97360	0.03892	0.67791
Alltop	0.98906	1.95346	0.03472	0.99102
SS	0.99170	1.96955	0.02601	0.67635
HAAR	0.99186	1.90046	0.02485	0.14566
RandDFT	0.98624	1.92154	0.02794	0.40323
RealMANOVA	0.98364	1.93223	0.03597	1
RealPF	0.97535	1.94418	0.03834	0.82068
SH	0.99998	2.05891	0.00950	0.00133
RealHAAR	0.97542	1.88870	0.04328	0.44108
RandDCT	0.97893	1.96572	0.03550	0.50885

Table 40: Results of Test 2 for Ψ_{cond}, $\gamma = 0.5$ and $\beta = 0.9$

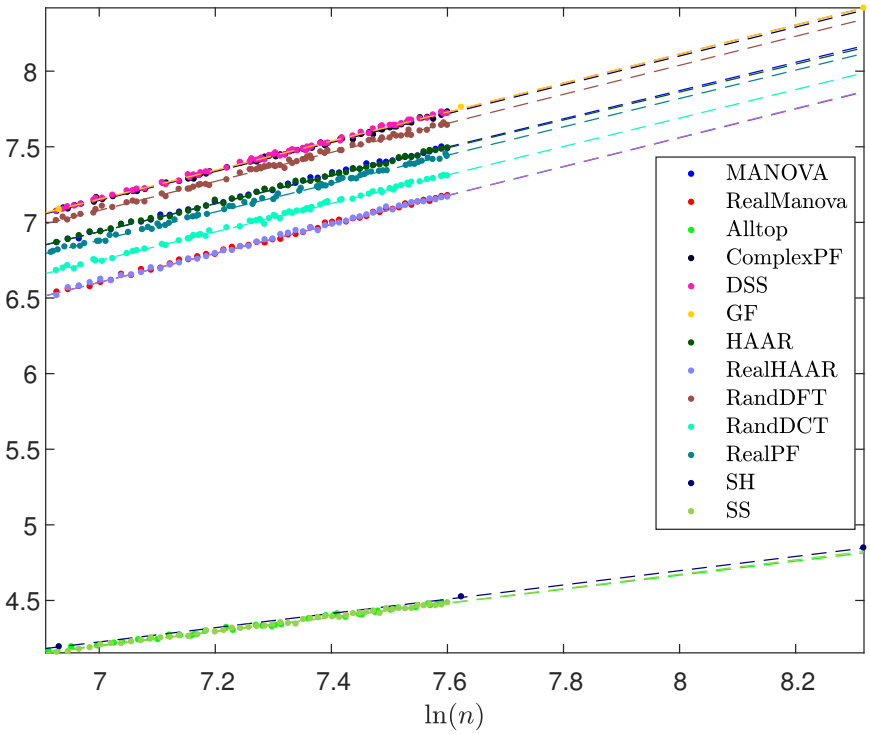

Figure 71: Test 1 for $\gamma = 0.5$ and $\beta = 0.5$. Plot shows $-\frac{1}{2}\ln Var_{K_n}(\Delta_{KS}(X^{(n)}_{K_n}; n, m_n, k_n))$ over $\ln(n)$.

Frame	R^2	$\hat{b}$	$SE(\hat{b})$	p-value $b = b_{MANOVA}$
MANOVA	0.99815	0.93372	0.00581	1
DSS	0.99783	0.96204	0.00552	5.9380e-04
GF	0.99992	0.96006	0.00868	0.01495
ComplexPF	0.99816	0.95481	0.00504	0.00710
Alltop	0.99175	0.46436	0.00716	2.2425e-64
SS	0.99472	0.47605	0.00500	1.0496e-77
HAAR	0.99784	0.92333	0.00620	0.22425
RandDFT	0.99614	0.95936	0.00735	0.00721
RealMANOVA	0.99789	0.95624	0.00634	1
RealPF	0.99818	0.93809	0.00497	0.02620
SH	0.99995	0.47116	0.00332	4.2284e-50
RealHAAR	0.99734	0.95888	0.00715	0.78370
RandDCT	0.99763	0.94122	0.00564	0.07938

Table 41: Results of Test 1 for $\gamma = 0.5$ and $\beta = 0.5$.

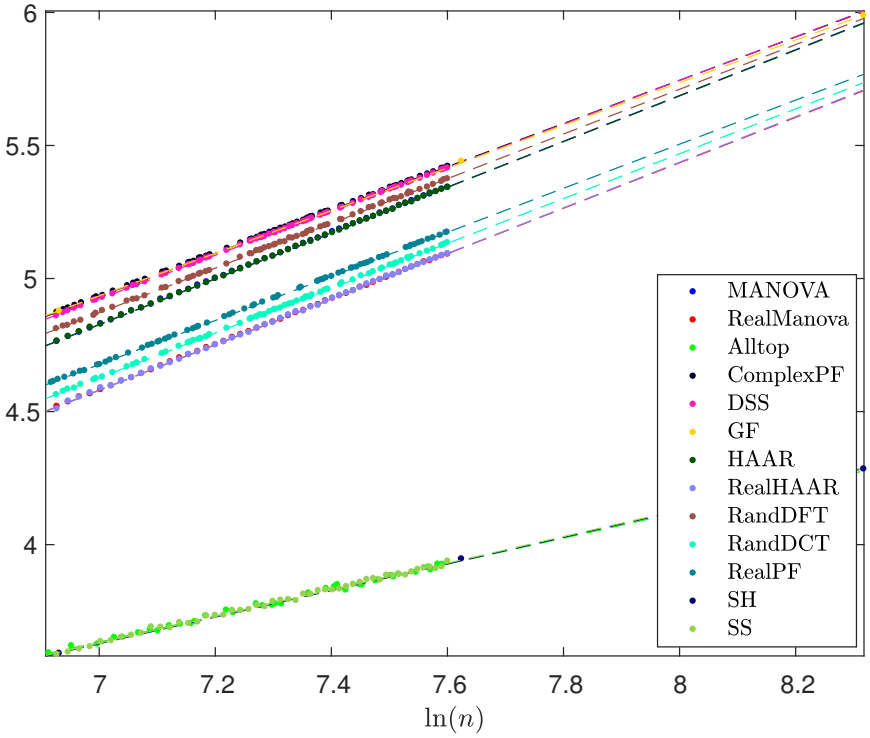

Figure 72: Test 1 for $\gamma = 0.5$ and $\beta = 0.5$. Plot shows $-\frac{1}{2}\ln \mathbb{E}_{K_n}(\Delta_{KS}(X_{K_n}^{(n)}; n, m_n, k_n)^2)$ over $\ln(n)$.

Frame	R^2	$\hat{b}$	$SE(\hat{b})$	p-value $b = b_{MANOVA}$
MANOVA	0.99993	0.86072	0.00103	1
DSS	0.99994	0.82123	0.00078	8.4214e-57
GF	0.99994	0.80128	0.00645	4.2150e-12
ComplexPF	0.99995	0.81250	0.00071	2.5915e-67
Alltop	0.99486	0.48805	0.00593	3.0106e-71
SS	0.99648	0.50058	0.00430	1.9215e-90
HAAR	0.99990	0.85941	0.00125	0.42153
RandDFT	0.99982	0.83974	0.00139	2.7976e-22
RealMANOVA	0.99993	0.85472	0.00104	1
RealPF	0.99997	0.82798	0.00060	4.7676e-43
SH	0.99980	0.49985	0.00714	2.3203e-43
RealHAAR	0.99970	0.85719	0.00213	0.29928
RandDCT	0.99990	0.84206	0.00105	6.5828e-14

Table 42: Results of Test 1 (MSE) for $\gamma = 0.5$ and $\beta = 0.5$.

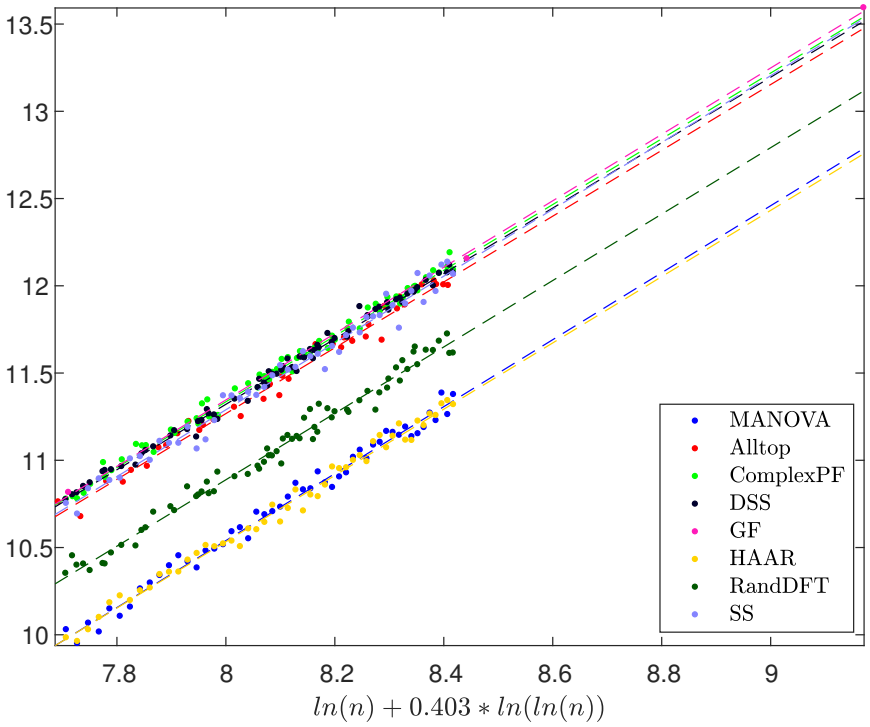

Figure 73: Test 2 for Ψ_{AC}, complex frames $\gamma = 0.5$ and $\beta = 0.5$. Plot shows $-\ln \mathbb{E}_{K_n}(\Delta_\Psi(X^{(n)}_{K_n}; n, m_n, k_n)^2)$

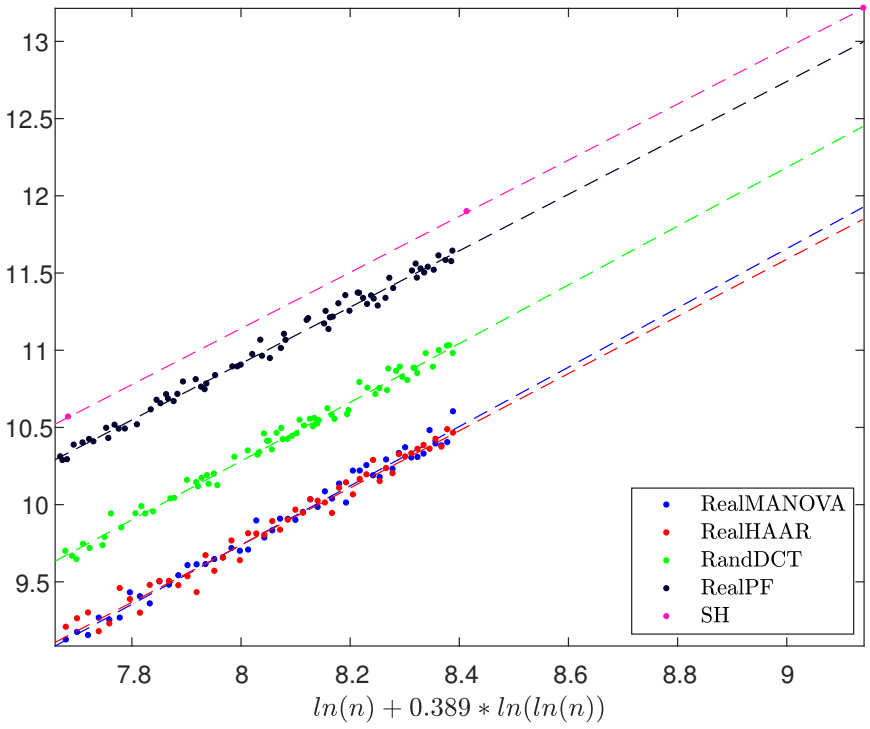

Figure 74: Test 2 for Ψ_{AC}, real frames $\gamma = 0.5$ and $\beta = 0.5$. Plot shows $-\ln \mathbb{E}_{K_n}(\Delta_\Psi(X^{(n)}_{K_n}; n, m_n, k_n)^2)$

Frame	R^2	$\hat{b}$	$SE(\hat{b})$	p-value $b = b_{MANOVA}$
MANOVA	0.98768	1.91916	0.03094	1
DSS	0.99415	1.87450	0.01770	0.21274
GF	0.99951	1.90258	0.04203	0.75204
ComplexPF	0.99217	1.88385	0.02060	0.34409
Alltop	0.98534	1.88572	0.03888	0.50280
SS	0.98094	1.91456	0.03852	0.92601
HAAR	0.98947	1.89891	0.02827	0.62998
RandDFT	0.98291	1.90320	0.03089	0.71563
RealMANOVA	0.98476	1.91927	0.03447	1
RealPF	0.98984	1.82658	0.02295	0.02716
SH	1.00000	1.81680	0.00241	0.00465
RealHAAR	0.97811	1.85068	0.03996	0.19682
RandDCT	0.98731	1.90189	0.02654	0.69022

Table 43: Results of Test 2 for Ψ_{AC}, $\gamma = 0.5$ and $\beta = 0.5$

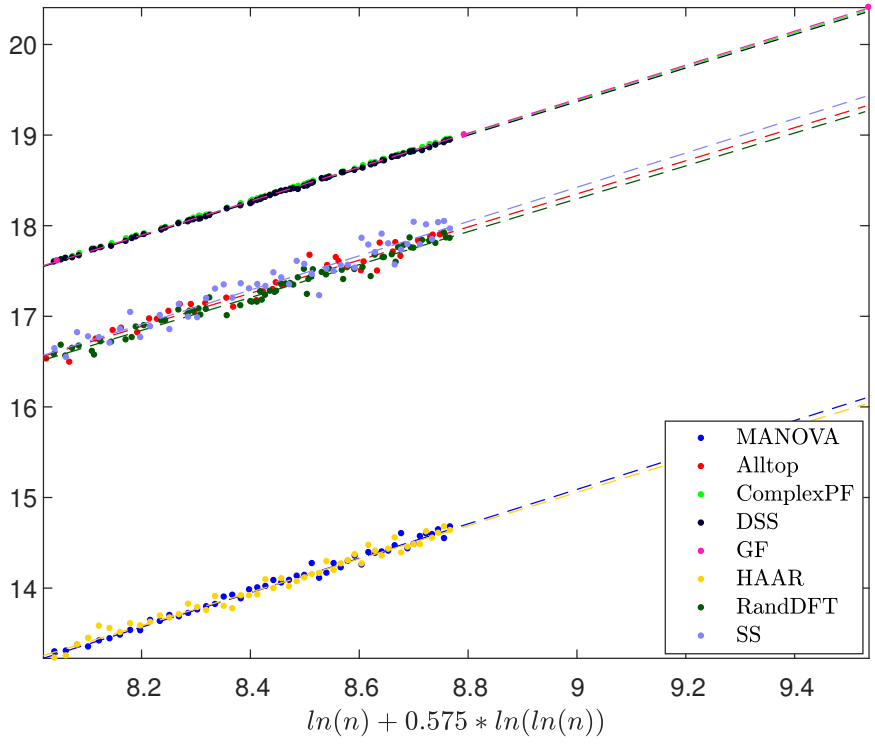

Figure 75: Test 2 for $\Psi_{Shannon}$, complex frames $\gamma = 0.5$ and $\beta = 0.5$. Plot shows $-\ln \mathbb{E}_{K_n}(\Delta_\Psi(X_{K_n}^{(n)}; n, m_n, k_n)^2)$

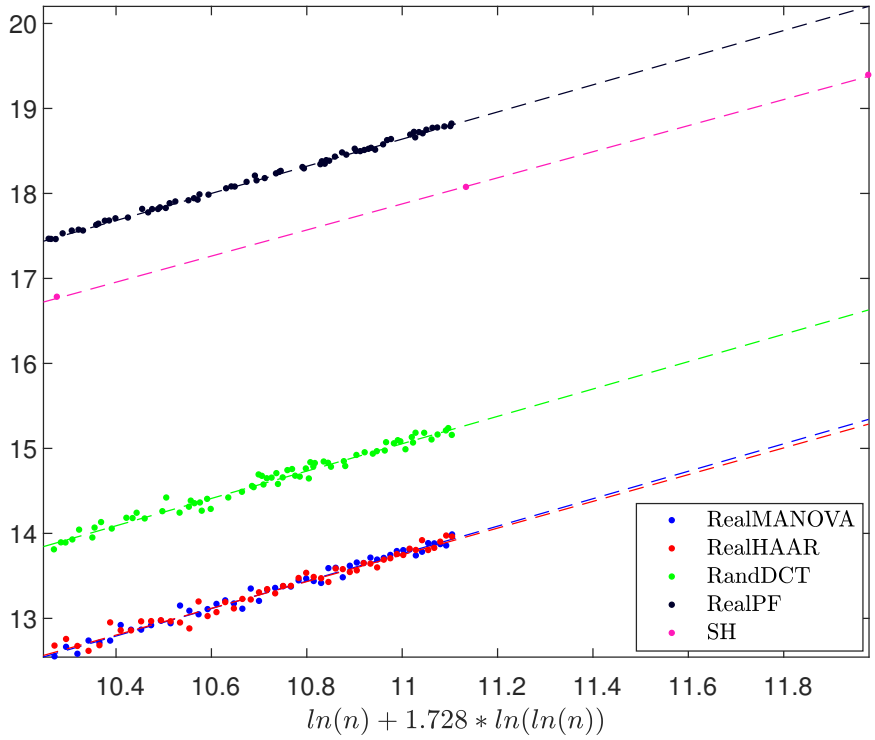

Figure 76: Test 2 for $\Psi_{Shannon}$, real frames $\gamma = 0.5$ and $\beta = 0.5$. Plot shows $-\ln \mathbb{E}_{K_n}(\Delta_\Psi(X^{(n)}_{K_n}; n, m_n, k_n)^2)$

Frame	R^2	$\hat{b}$	$SE(\hat{b})$	p-value $b = b_{MANOVA}$
MANOVA	0.98997	1.90079	0.02761	1
DSS	0.99950	1.85589	0.00513	0.11268
GF	0.99998	1.87611	0.00907	0.39999
ComplexPF	0.99988	1.86216	0.00250	0.16629
Alltop	0.95969	1.82753	0.06331	0.29190
SS	0.93263	1.89080	0.07335	0.89882
HAAR	0.97883	1.83752	0.03900	0.18867
RandDFT	0.97247	1.81594	0.03761	0.07161
RealMANOVA	0.98363	1.61553	0.03008	1
RealPF	0.99750	1.59706	0.00991	0.56099
SH	0.99988	1.53491	0.01669	0.02322
RealHAAR	0.97400	1.57295	0.03709	0.37490
RandDCT	0.97852	1.60953	0.02935	0.88673

Table 44: Results of Test 2 for $\Psi_{Shannon}$, $\gamma = 0.5$ and $\beta = 0.5$

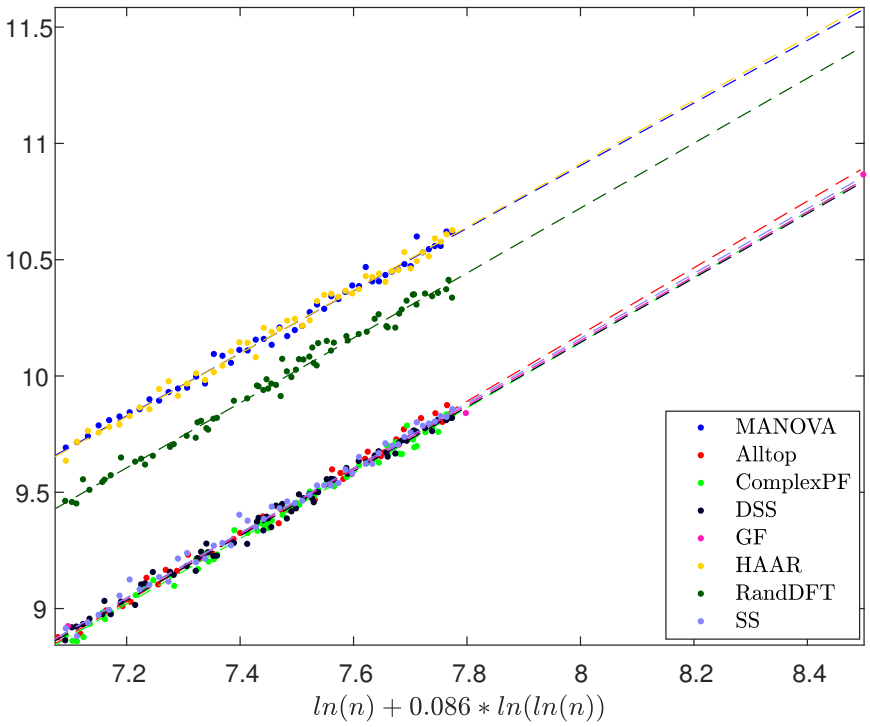

Figure 77: Test 2 for Ψ_{RIP}, complex frames $\gamma = 0.5$ and $\beta = 0.5$. Plot shows $-\ln \mathbb{E}_{K_n}(\Delta_\Psi(X_{K_n}^{(n)}; n, m_n, k_n)^2)$

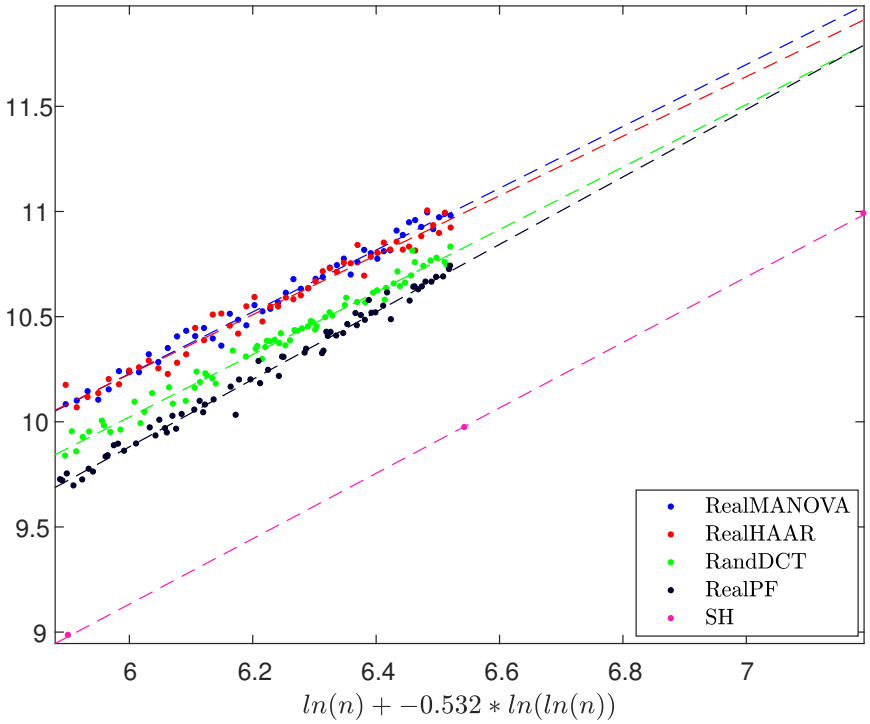

Figure 78: Test 2 for Ψ_{RIP}, real frames $\gamma = 0.5$ and $\beta = 0.5$. Plot shows $-\ln \mathbb{E}_{K_n}(\Delta_\Psi(X_{K_n}^{(n)}; n, m_n, k_n)^2)$

Frame	R^2	$\hat{b}$	$SE(\hat{b})$	p-value $b = b_{MANOVA}$
MANOVA	0.99097	1.34583	0.01855	1
DSS	0.99167	1.38541	0.01563	0.10551
GF	0.99892	1.38508	0.04556	0.42884
ComplexPF	0.99232	1.40459	0.01521	0.01583
Alltop	0.99232	1.43513	0.02134	0.00222
SS	0.99200	1.39393	0.01807	0.06631
HAAR	0.98923	1.36011	0.02048	0.60663
RandDFT	0.98709	1.39582	0.01965	0.06692
RealMANOVA	0.98361	1.47043	0.02740	1
RealPF	0.98804	1.60428	0.02189	2.2133e-04
SH	0.99996	1.55534	0.00972	0.00527
RealHAAR	0.96952	1.41522	0.03622	0.22706
RandDCT	0.98346	1.48602	0.02372	0.66788

Table 45: Results of Test 2 for Ψ_{RIP}, $\gamma = 0.5$ and $\beta = 0.5$

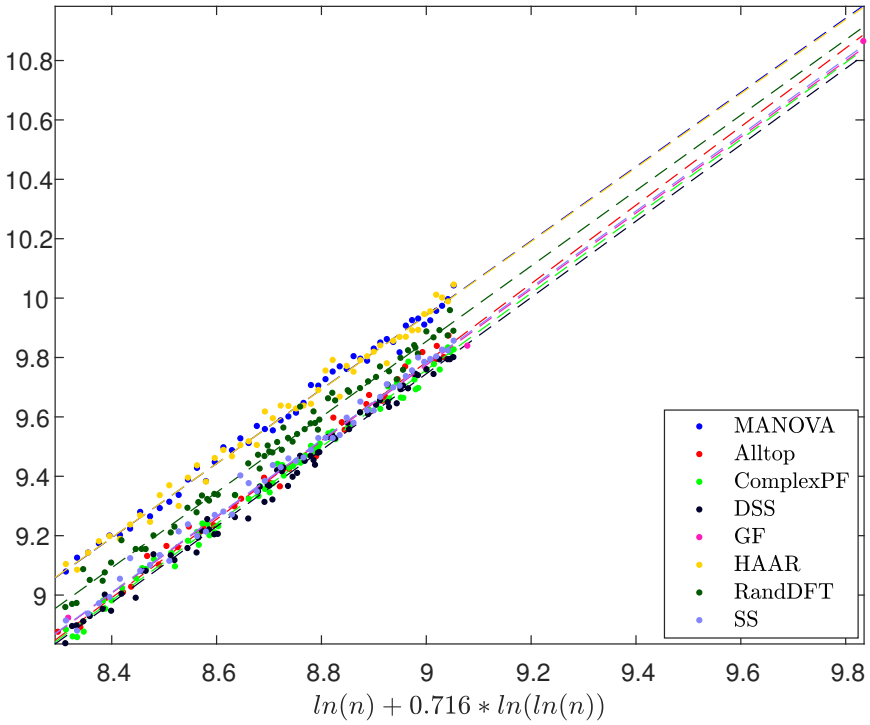

Figure 79: Test 2 for Ψ_{max}, complex frames $\gamma = 0.5$ and $\beta = 0.5$. Plot shows $-\ln \mathbb{E}_{K_n}(\Delta_\Psi(X_{K_n}^{(n)}; n, m_n, k_n)^2)$

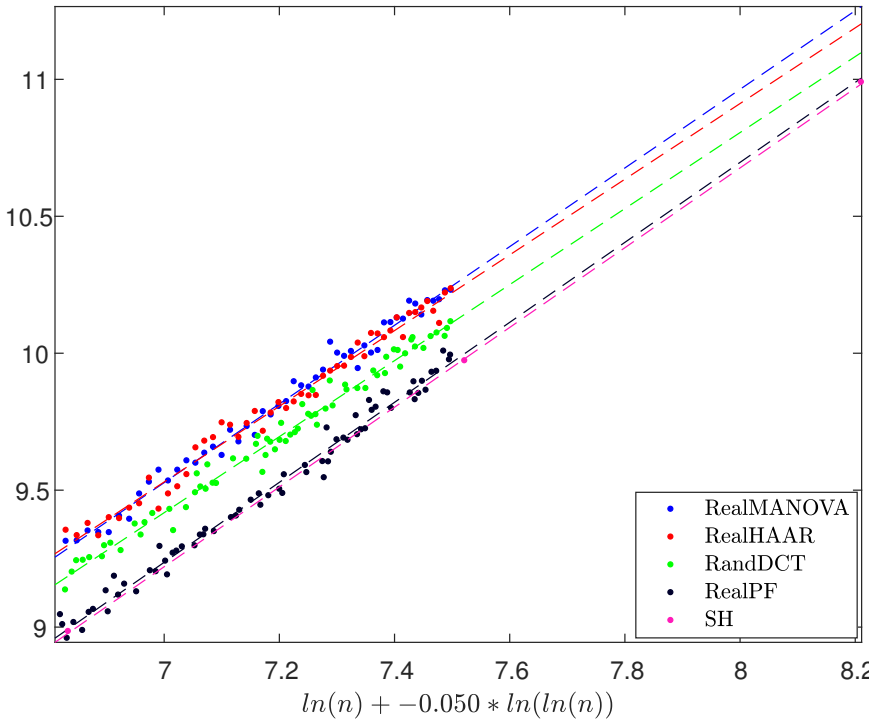

Figure 80: Test 2 for Ψ_{max}, real frames $\gamma = 0.5$ and $\beta = 0.5$. Plot shows $-\ln \mathbb{E}_{K_n}(\Delta_\Psi(X_{K_n}^{(n)}; n, m_n, k_n)^2)$

Frame	R^2	$\hat{b}$	$SE(\hat{b})$	p-value $b = b_{MANOVA}$
MANOVA	0.99381	1.24983	0.01424	1
DSS	0.99198	1.28493	0.01422	0.08385
GF	0.99879	1.28006	0.04463	0.52169
ComplexPF	0.99236	1.29373	0.01397	0.02979
Alltop	0.99229	1.32193	0.01969	0.00393
SS	0.99200	1.28399	0.01664	0.12211
HAAR	0.98758	1.24563	0.02016	0.86548
RandDFT	0.98870	1.27007	0.01671	0.35861
RealMANOVA	0.98757	1.43603	0.02326	1
RealPF	0.98640	1.46036	0.02127	0.44172
SH	0.99994	1.45616	0.01173	0.44326
RealHAAR	0.98180	1.38177	0.02715	0.13239
RandDCT	0.98322	1.38786	0.02232	0.13786

Table 46: Results of Test 2 for Ψ_{max}, $\gamma = 0.5$ and $\beta = 0.5$

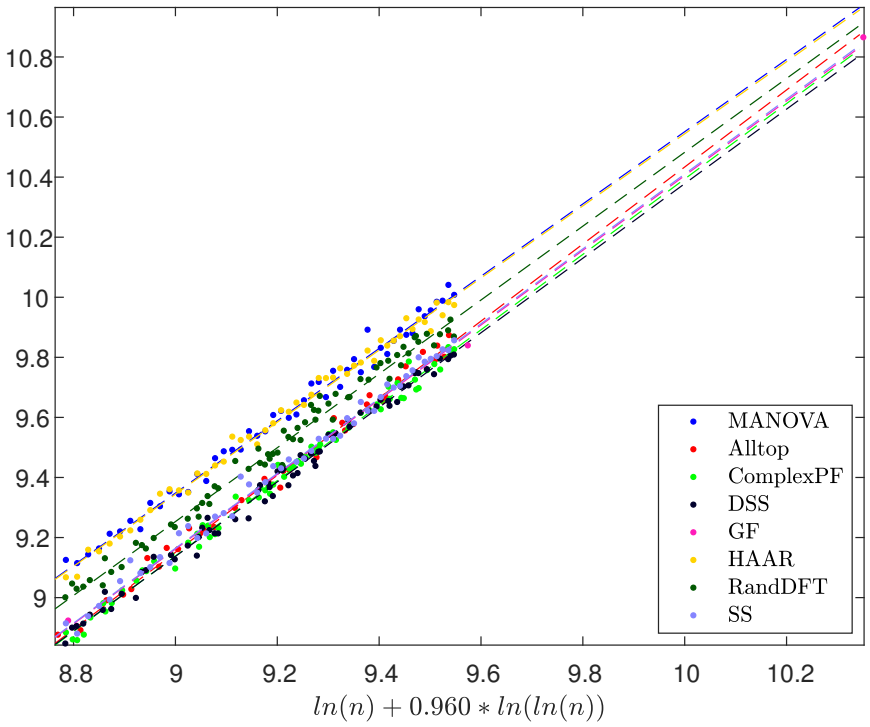

Figure 81: Test 2 for Ψ_{min}, complex frames $\gamma = 0.5$ and $\beta = 0.5$. Plot shows $-\ln \mathbb{E}_{K_n}(\Delta_\Psi(X_{K_n}^{(n)}; n, m_n, k_n)^2)$

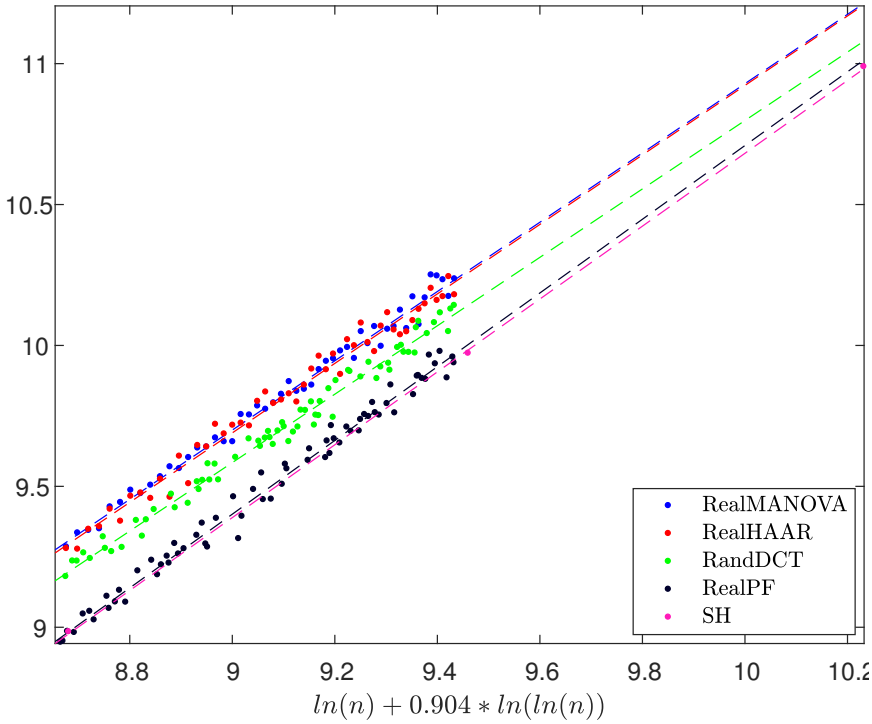

Figure 82: Test 2 for Ψ_{min}, real frames $\gamma = 0.5$ and $\beta = 0.5$. Plot shows $-\ln \mathbb{E}_{K_n}(\Delta_\Psi(X_{K_n}^{(n)}; n, m_n, k_n)^2)$

Frame	R^2	$\hat{b}$	$SE(\hat{b})$	p-value $b = b_{MANOVA}$
MANOVA	0.98988	1.20307	0.01755	1
DSS	0.99177	1.24084	0.01391	0.09447
GF	0.99874	1.24354	0.04421	0.39902
ComplexPF	0.99238	1.25535	0.01354	0.02008
Alltop	0.99228	1.28274	0.01912	0.00290
SS	0.99201	1.24593	0.01614	0.07550
HAAR	0.99241	1.20011	0.01515	0.89859
RandDFT	0.98884	1.22955	0.01608	0.26850
RealMANOVA	0.98832	1.22924	0.01929	1
RealPF	0.98769	1.30824	0.01812	0.00348
SH	0.99988	1.29280	0.01425	0.01079
RealHAAR	0.97981	1.23286	0.02554	0.91014
RandDCT	0.98499	1.21397	0.01844	0.56838

Table 47: Results of Test 2 for Ψ_{min}, $\gamma = 0.5$ and $\beta = 0.5$

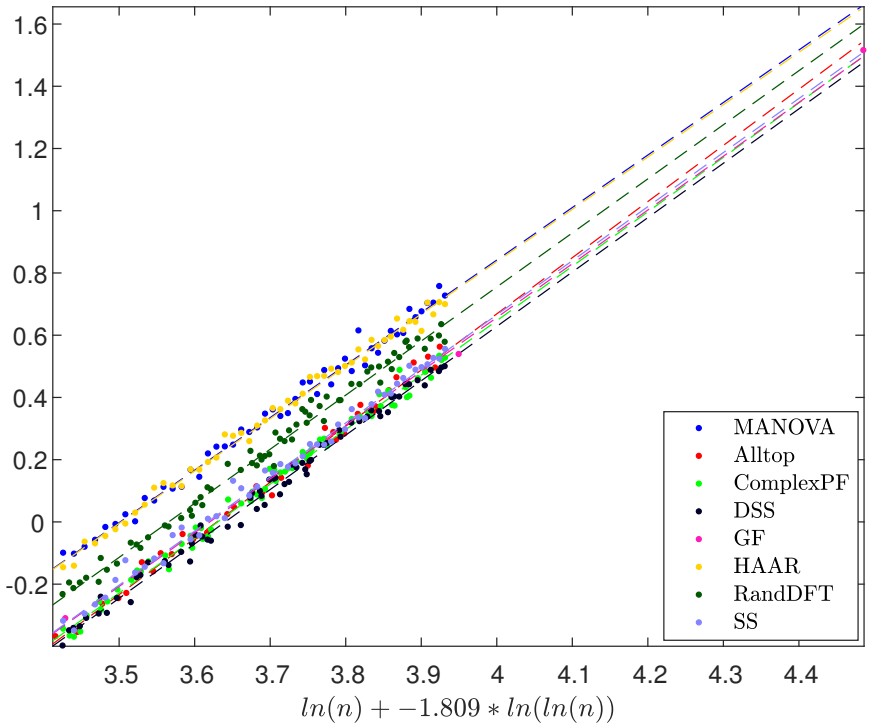

Figure 83: Test 2 for Ψ_{cond}, complex frames $\gamma = 0.5$ and $\beta = 0.5$. Plot shows $-\ln \mathbb{E}_{K_n}(\Delta_\Psi(X^{(n)}_{K_n}; n, m_n, k_n)^2)$

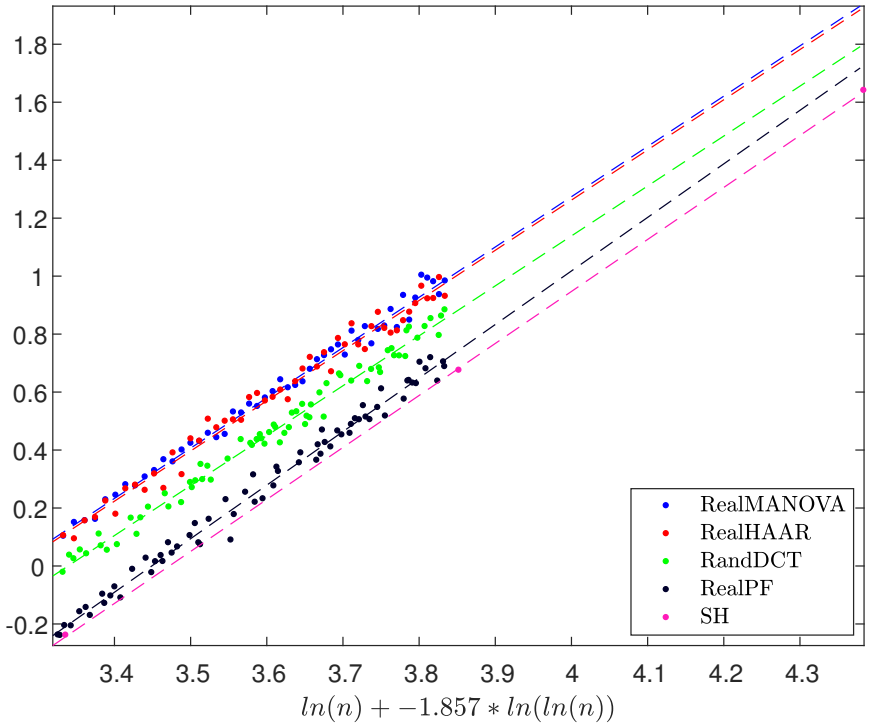

Figure 84: Test 2 for Ψ_{cond}, real frames $\gamma = 0.5$ and $\beta = 0.5$. Plot shows $-\ln \mathbb{E}_{K_n}(\Delta_\Psi(X_{K_n}^{(n)}; n, m_n, k_n)^2)$

Frame	R^2	$\hat{b}$	$SE(\hat{b})$	p-value $b = b_{MANOVA}$
MANOVA	0.99051	1.68782	0.02384	1
DSS	0.99173	1.74755	0.01965	0.05566
GF	0.99897	1.72825	0.05553	0.50661
ComplexPF	0.99200	1.75015	0.01935	0.04470
Alltop	0.99214	1.80445	0.02714	0.00179
SS	0.99187	1.73781	0.02270	0.13220
HAAR	0.99262	1.68219	0.02093	0.85951
RandDFT	0.98967	1.73777	0.02185	0.12525
RealMANOVA	0.98979	1.73479	0.02544	1
RealPF	0.98846	1.84732	0.02476	0.00196
SH	0.99995	1.79389	0.01320	0.04450
RealHAAR	0.98053	1.73126	0.03521	0.93544
RandDCT	0.98586	1.72284	0.02540	0.74025

Table 48: Results of Test 2 for Ψ_{cond}, $\gamma = 0.5$ and $\beta = 0.5$

Frame	R^2	$\hat{b}$	$SE(\hat{b})$	p-value $b = b_{MANOVA}$
MANOVA	0.99874	0.95877	0.00492	1
DSS	0.99955	0.90196	0.01910	0.00589
Alltop	0.99718	0.90835	0.01080	6.7123e-05
HAAR	0.99768	0.96836	0.00674	0.25358
RandDFT	0.99617	0.92578	0.00829	9.1113e-04
RealMANOVA	0.99876	0.96657	0.00491	1
RealHAAR	0.99718	0.96245	0.00739	0.64367
RandDCT	0.99753	0.96236	0.00590	0.58418

Table 49: Results of Test 1 for $\gamma = 0.25$ and $\beta = 0.8$.

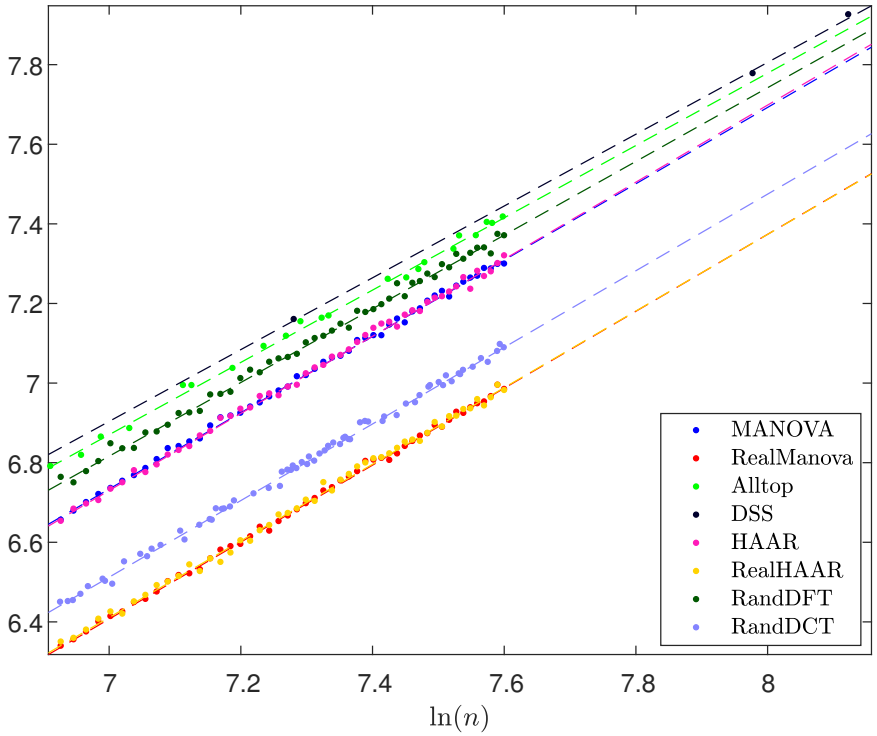

Figure 85: Test 1 for $\gamma = 0.25$ and $\beta = 0.8$. Plot shows $-\frac{1}{2}\ln Var_{K_n}(\Delta_{KS}(X_{K_n}^{(n)}; n, m_n, k_n))$ over $\ln(n)$.

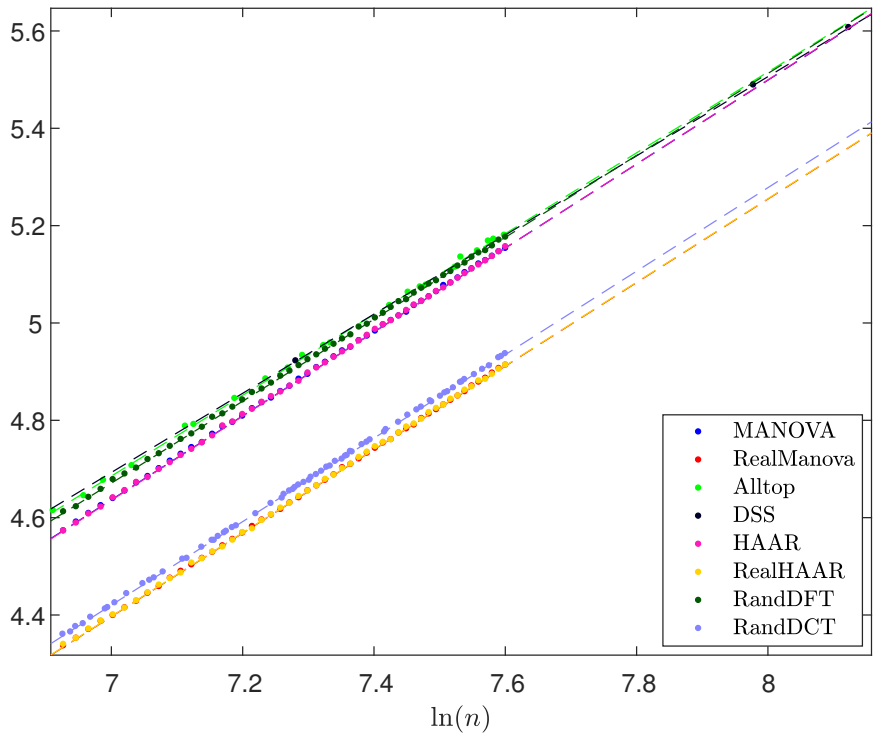

Figure 86: Test 1 for $\gamma = 0.25$ and $\beta = 0.8$. Plot shows $-\frac{1}{2}\ln \mathbb{E}_{K_n}(\Delta_{KS}(X_{K_n}^{(n)}; n, m_n, k_n)^2)$ over $\ln(n)$.

Frame	R^2	$\hat{b}$	$SE(\hat{b})$	p-value $b = b_{MANOVA}$
MANOVA	0.99994	0.86216	0.00095	1
DSS	1.00000	0.81326	0.00007	2.2697e-44
Alltop	0.99942	0.83030	0.00448	1.6634e-09
HAAR	0.99991	0.86372	0.00121	0.31297
RandDFT	0.99986	0.84177	0.00144	2.0468e-20
RealMANOVA	0.99994	0.85799	0.00097	1
RealHAAR	0.99986	0.85811	0.00149	0.94493
RandDCT	0.99991	0.85771	0.00100	0.83880

Table 50: Results of Test 1 (MSE) for $\gamma = 0.25$ and $\beta = 0.8$.

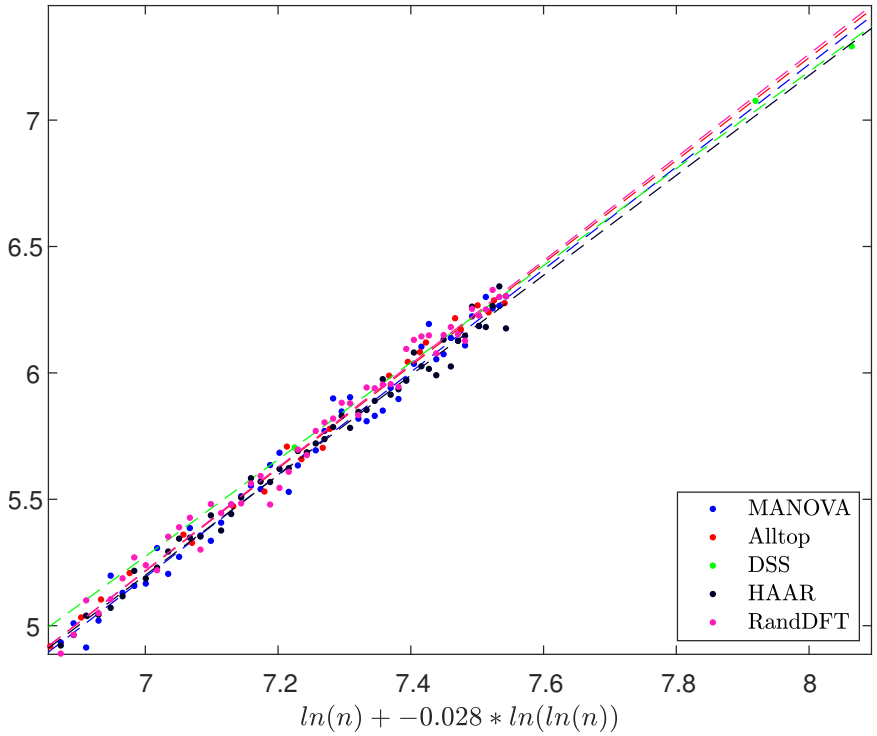

Figure 87: Test 2 for Ψ_{AC}, complex frames $\gamma = 0.25$ and $\beta = 0.8$. Plot shows $-\ln \mathbb{E}_{K_n}(\Delta_\Psi(X_{K_n}^{(n)}; n, m_n, k_n)^2)$

Frame	R^2	$\hat{b}$	$SE(\hat{b})$	p-value $b = b_{MANOVA}$
MANOVA	0.98158	2.02891	0.04011	1
DSS	0.99868	1.91793	0.06979	0.17423
Alltop	0.99426	2.03145	0.03451	0.96187
HAAR	0.98969	1.97723	0.02913	0.29977
RandDFT	0.98504	2.04319	0.03635	0.79246
RealMANOVA	0.98708	1.11400	0.01840	1
RealHAAR	0.98754	1.10152	0.01786	0.62771
RandDCT	0.98710	1.10769	0.01559	0.79411

Table 51: Results of Test 2 for Ψ_{AC}, $\gamma = 0.25$ and $\beta = 0.8$

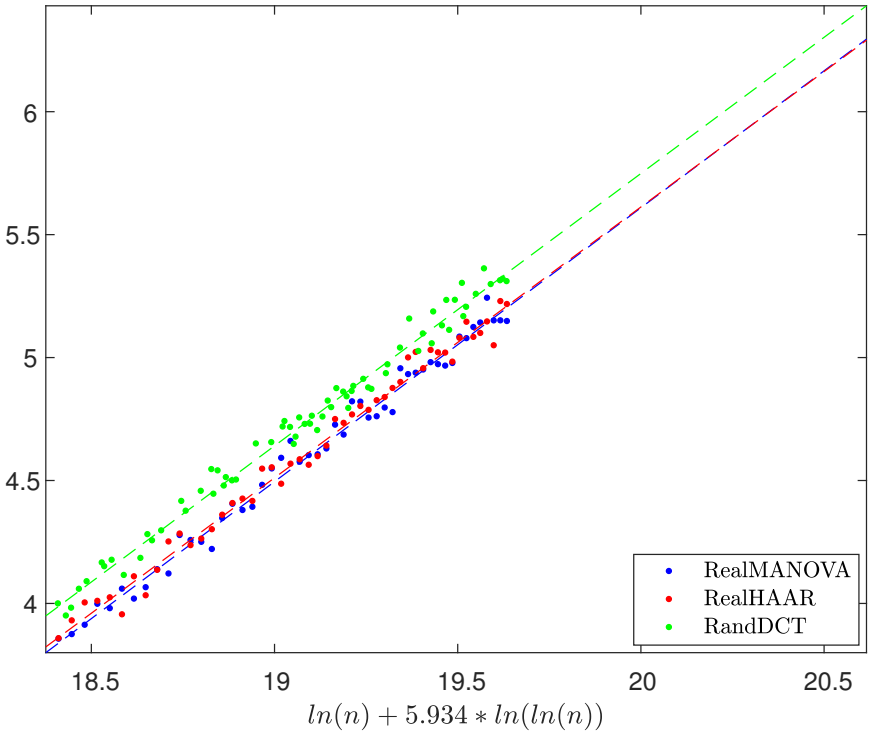

Figure 88: Test 2 for Ψ_{AC}, real frames $\gamma = 0.25$ and $\beta = 0.8$. Plot shows $-\ln \mathbb{E}_{K_n}(\Delta_\Psi(X_{K_n}^{(n)}; n, m_n, k_n)^2)$

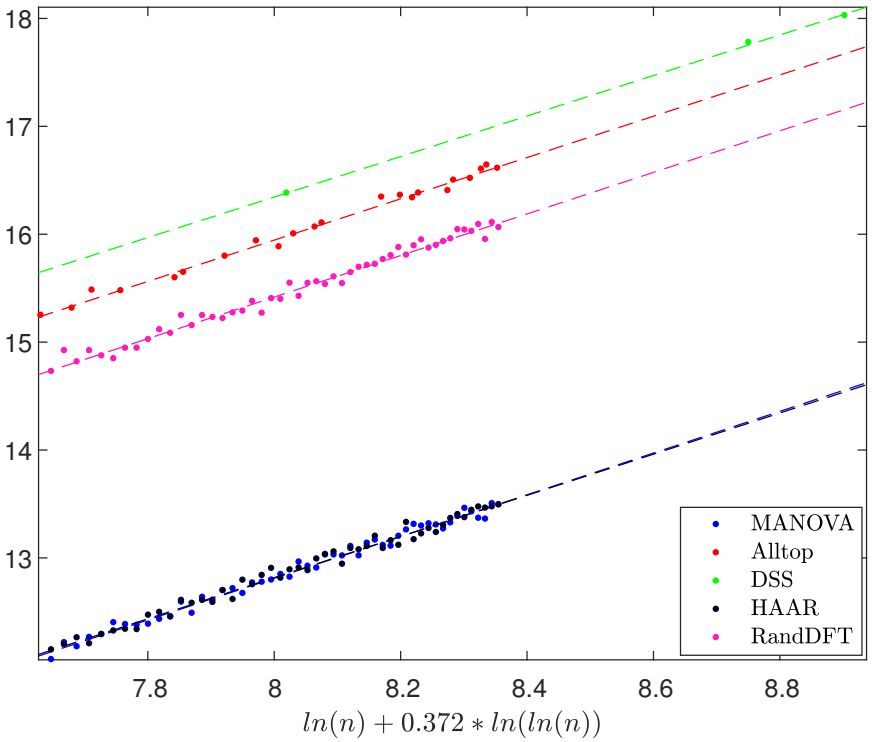

Figure 89: Test 2 for $\Psi_{Shannon}$, complex frames $\gamma = 0.25$ and $\beta = 0.8$. Plot shows $-\ln \mathbb{E}_{K_n}(\Delta_\Psi(X_{K_n}^{(n)}; n, m_n, k_n)^2)$

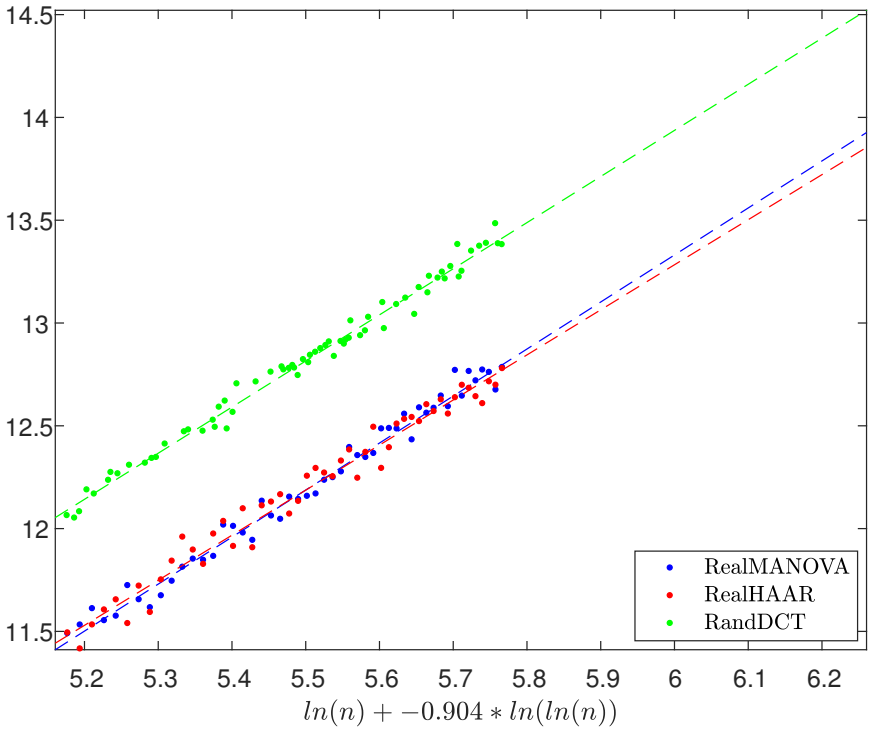

Figure 90: Test 2 for $\Psi_{Shannon}$, real frames $\gamma = 0.25$ and $\beta = 0.8$. Plot shows $-\ln \mathbb{E}_{K_n}(\Delta_\Psi(X_{K_n}^{(n)}; n, m_n, k_n)^2)$

Frame	R^2	$\hat{b}$	$SE(\hat{b})$	p-value $b = b_{MANOVA}$
MANOVA	0.98788	1.93331	0.03091	1
DSS	0.99952	1.87770	0.04097	0.28385
Alltop	0.99156	1.91367	0.03948	0.69644
HAAR	0.98603	1.90768	0.03278	0.57068
RandDFT	0.98354	1.92636	0.03597	0.88379
RealMANOVA	0.98368	2.28690	0.04251	1
RealHAAR	0.97130	2.19227	0.05439	0.17362
RandDCT	0.98792	2.24315	0.03053	0.40492

Table 52: Results of Test 2 for $\Psi_{Shannon}$, $\gamma = 0.25$ and $\beta = 0.8$

Frame	R^2	$\hat{b}$	$SE(\hat{b})$	p-value $b = b_{MANOVA}$
MANOVA	0.99020	1.30582	0.01876	1
DSS	0.99999	1.31908	0.00374	0.49120
Alltop	0.99753	1.34522	0.01497	0.10524
HAAR	0.98990	1.24633	0.01817	0.02494
RandDFT	0.99176	1.29581	0.01705	0.69378
RealMANOVA	0.98625	1.53609	0.02618	1
RealHAAR	0.97894	1.49241	0.03160	0.28979
RandDCT	0.99024	1.63612	0.01999	0.00296

Table 53: Results of Test 2 for Ψ_{RIP}, $\gamma = 0.25$ and $\beta = 0.8$

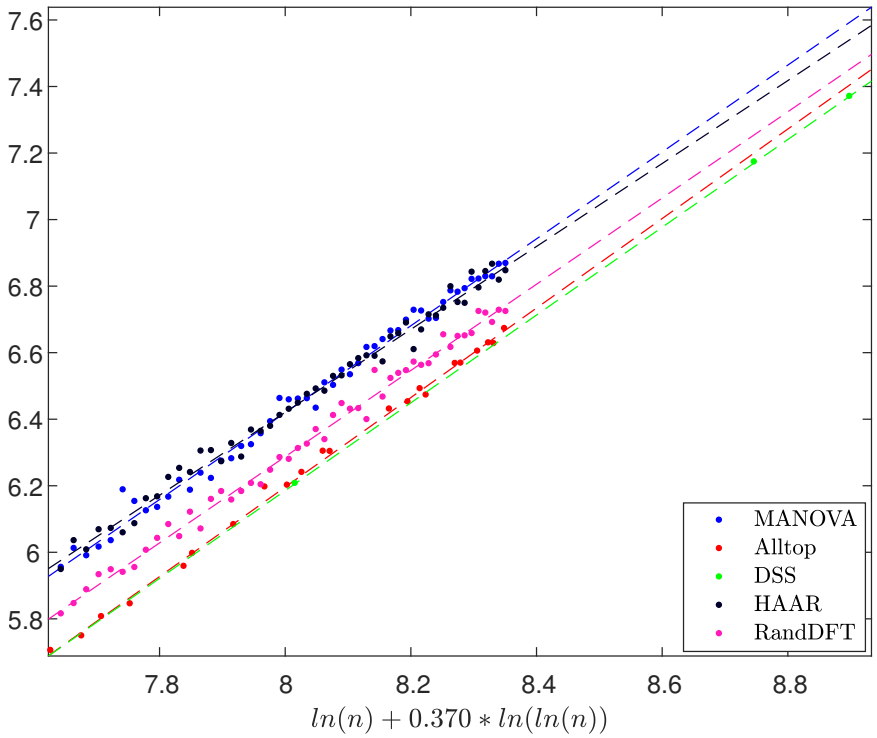

Figure 91: Test 2 for Ψ_{RIP}, complex frames $\gamma = 0.25$ and $\beta = 0.8$. Plot shows $-\ln \mathbb{E}_{K_n}(\Delta_\Psi(X_{K_n}^{(n)}; n, m_n, k_n)^2)$

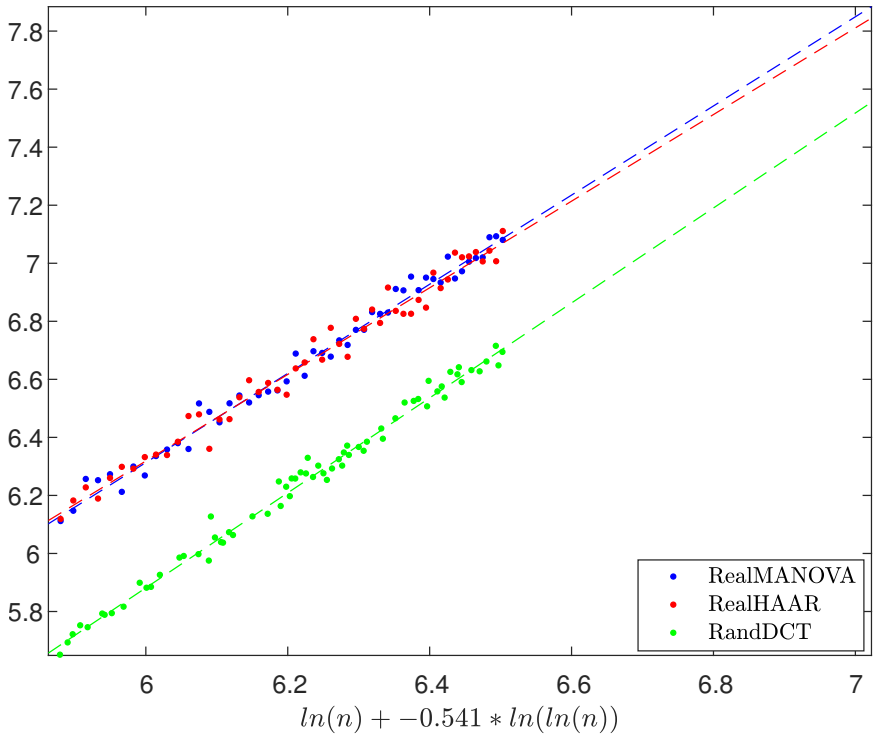

Figure 92: Test 2 for Ψ_{RIP}, real frames $\gamma = 0.25$ and $\beta = 0.8$. Plot shows $-\ln \mathbb{E}_{K_n}(\Delta_\Psi(X_{K_n}^{(n)}; n, m_n, k_n)^2)$

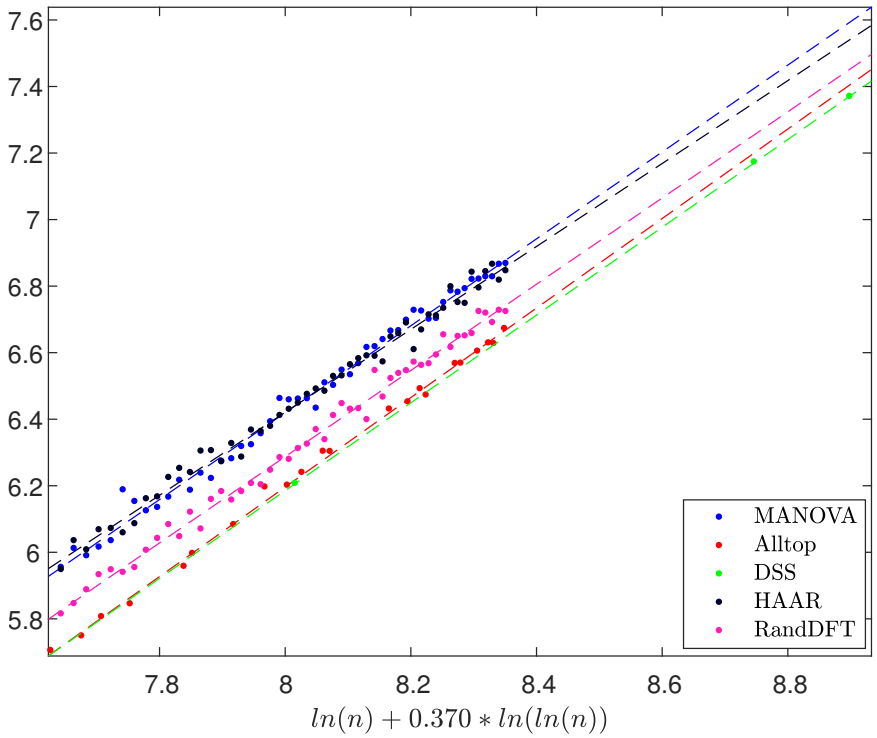

Figure 93: Test 2 for Ψ_{max}, complex frames $\gamma = 0.25$ and $\beta = 0.8$. Plot shows $-\ln \mathbb{E}_{K_n}(\Delta_\Psi(X_{K_n}^{(n)}; n, m_n, k_n)^2)$

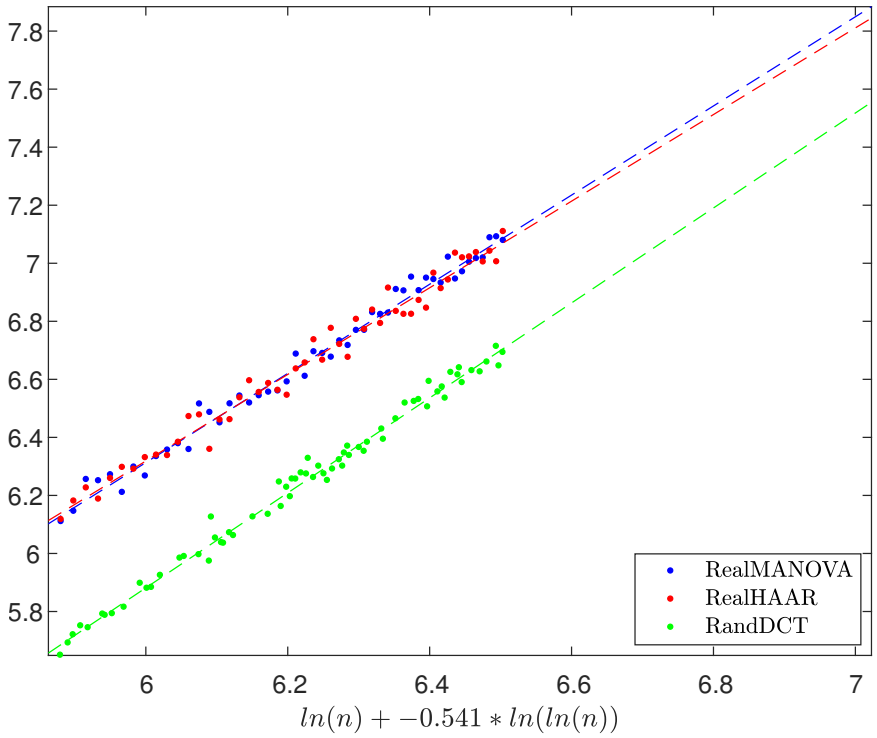

Figure 94: Test 2 for Ψ_{max}, real frames $\gamma = 0.25$ and $\beta = 0.8$. Plot shows $-\ln \mathbb{E}_{K_n}(\Delta_\Psi(X_{K_n}^{(n)}; n, m_n, k_n)^2)$

Frame	R^2	$\hat{b}$	$SE(\hat{b})$	p-value $b = b_{MANOVA}$
MANOVA	0.99020	1.30582	0.01876	1
DSS	0.99999	1.31908	0.00374	0.49120
Alltop	0.99753	1.34522	0.01497	0.10524
HAAR	0.98990	1.24633	0.01817	0.02494
RandDFT	0.99176	1.29581	0.01705	0.69378
RealMANOVA	0.98625	1.53609	0.02618	1
RealHAAR	0.97894	1.49241	0.03160	0.28979
RandDCT	0.99024	1.63612	0.01999	0.00296

Table 54: Results of Test 2 for Ψ_{max}, $\gamma = 0.25$ and $\beta = 0.8$

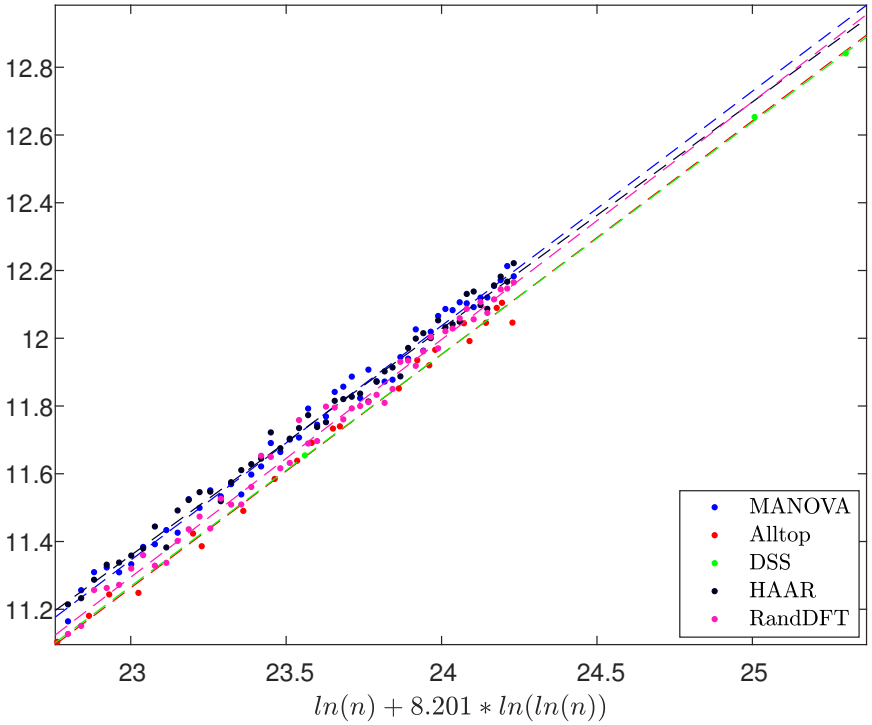

Figure 95: Test 2 for Ψ_{min}, complex frames $\gamma = 0.25$ and $\beta = 0.8$. Plot shows $-\ln \mathbb{E}_{K_n}(\Delta_\Psi(X^{(n)}_{K_n}; n, m_n, k_n)^2)$

Frame	R^2	$\hat{b}$	$SE(\hat{b})$	p-value $b = b_{MANOVA}$
MANOVA	0.99069	0.69211	0.00968	1
DSS	0.99989	0.68481	0.00707	0.54549
Alltop	0.99361	0.68938	0.01236	0.86252
HAAR	0.99118	0.66928	0.00911	0.08921
RandDFT	0.99015	0.70167	0.01010	0.49586
RealMANOVA	0.98338	0.50871	0.00955	1
RealHAAR	0.98410	0.51233	0.00940	0.78729
RandDCT	0.97513	0.52982	0.01042	0.13787

Table 55: Results of Test 2 for Ψ_{min}, $\gamma = 0.25$ and $\beta = 0.8$

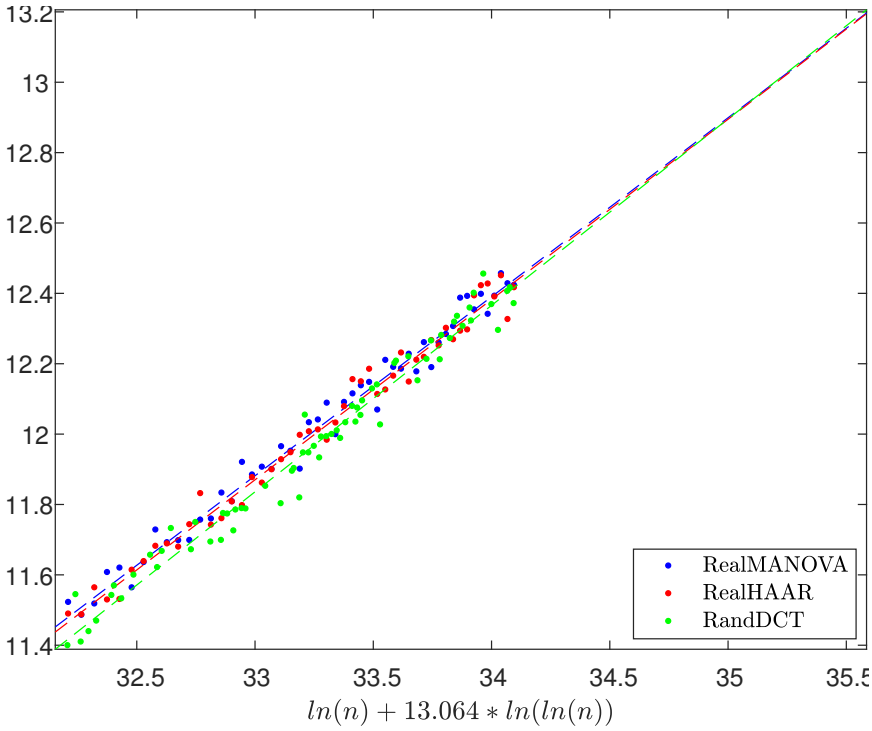

Figure 96: Test 2 for Ψ_{min}, real frames $\gamma = 0.25$ and $\beta = 0.8$. Plot shows $-\ln \mathbb{E}_{K_n}(\Delta_\Psi(X_{K_n}^{(n)}; n, m_n, k_n)^2)$

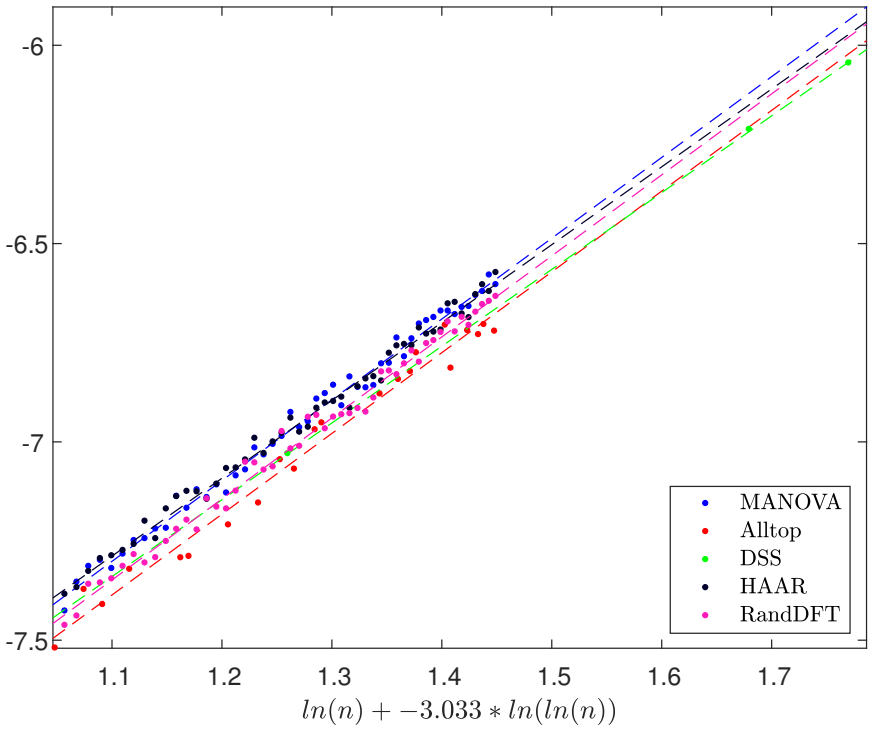

Figure 97: Test 2 for Ψ_{cond}, complex frames $\gamma = 0.25$ and $\beta = 0.8$. Plot shows $-\ln \mathbb{E}_{K_n}(\Delta_\Psi(X_{K_n}^{(n)}; n, m_n, k_n)^2)$

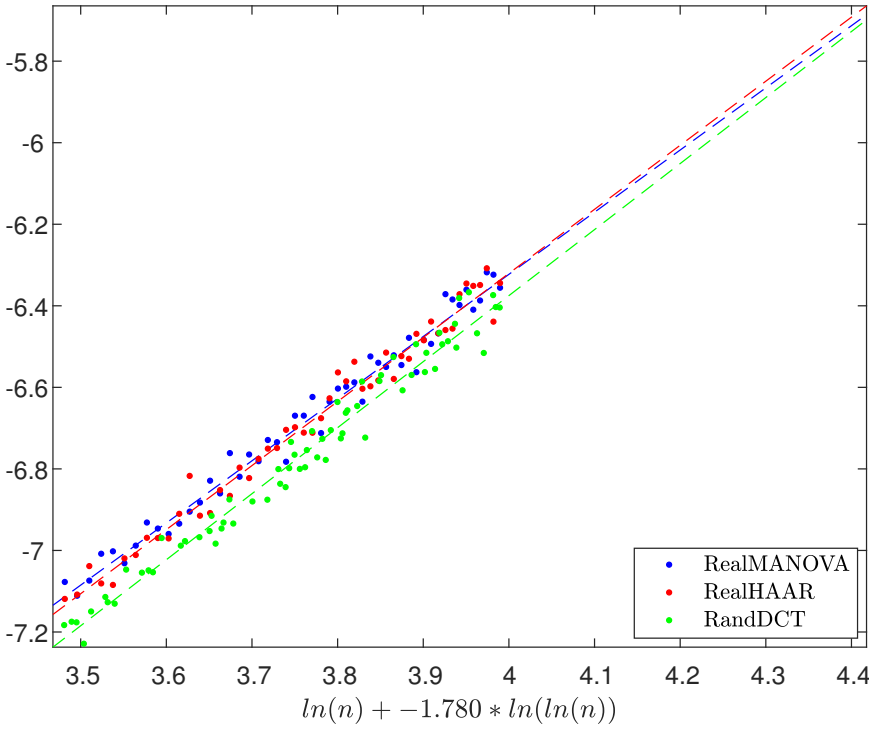

Figure 98: Test 2 for Ψ_{cond}, real frames $\gamma = 0.25$ and $\beta = 0.8$. Plot shows $-\ln \mathbb{E}_{K_n}(\Delta_\Psi(X^{(n)}_{K_n}; n, m_n, k_n)^2)$

Frame	R^2	$\hat{b}$	$SE(\hat{b})$	p-value $b = b_{MANOVA}$
MANOVA	0.99091	2.03679	0.02815	1
DSS	0.99994	1.93609	0.01469	0.00262
Alltop	0.98003	2.03648	0.06500	0.99658
HAAR	0.99124	1.96294	0.02663	0.05971
RandDFT	0.99059	2.04277	0.02873	0.88199
RealMANOVA	0.98096	1.52444	0.03066	1
RealHAAR	0.97965	1.57117	0.03269	0.29973
RandDCT	0.97458	1.61929	0.03219	0.03502

Table 56: Results of Test 2 for Ψ_{cond}, $\gamma = 0.25$ and $\beta = 0.8$

Frame	R^2	$\hat{b}$	$SE(\hat{b})$	p-value $b = b_{MANOVA}$
MANOVA	0.99856	0.96986	0.00532	1
DSS	0.99946	0.90177	0.02101	0.00285
Alltop	0.99859	0.93852	0.00788	0.00155
HAAR	0.99683	0.96243	0.00784	0.43495
RandDFT	0.99416	0.94482	0.01045	0.03528
RealMANOVA	0.99820	0.97742	0.00599	1
RealHAAR	0.99756	0.96389	0.00688	0.14130
RandDCT	0.99772	0.96618	0.00568	0.17634

Table 57: Results of Test 1 for $\gamma = 0.25$ and $\beta = 0.6$.

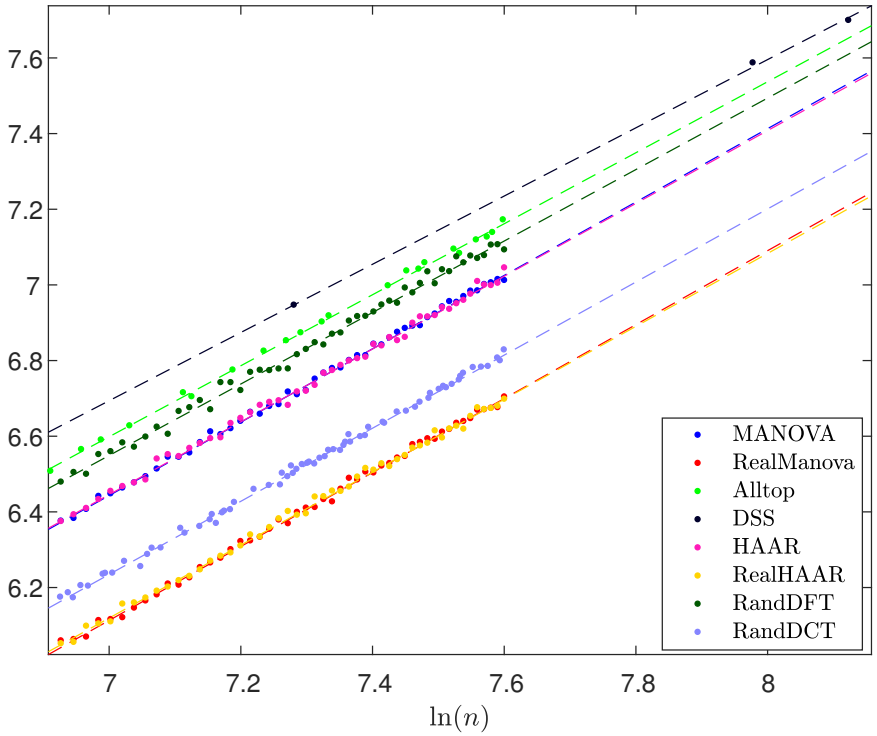

Figure 99: Test 1 for $\gamma = 0.25$ and $\beta = 0.6$. Plot shows $-\frac{1}{2}\ln Var_{K_n}(\Delta_{KS}(X_{K_n}^{(n)}; n, m_n, k_n))$ over $\ln(n)$.

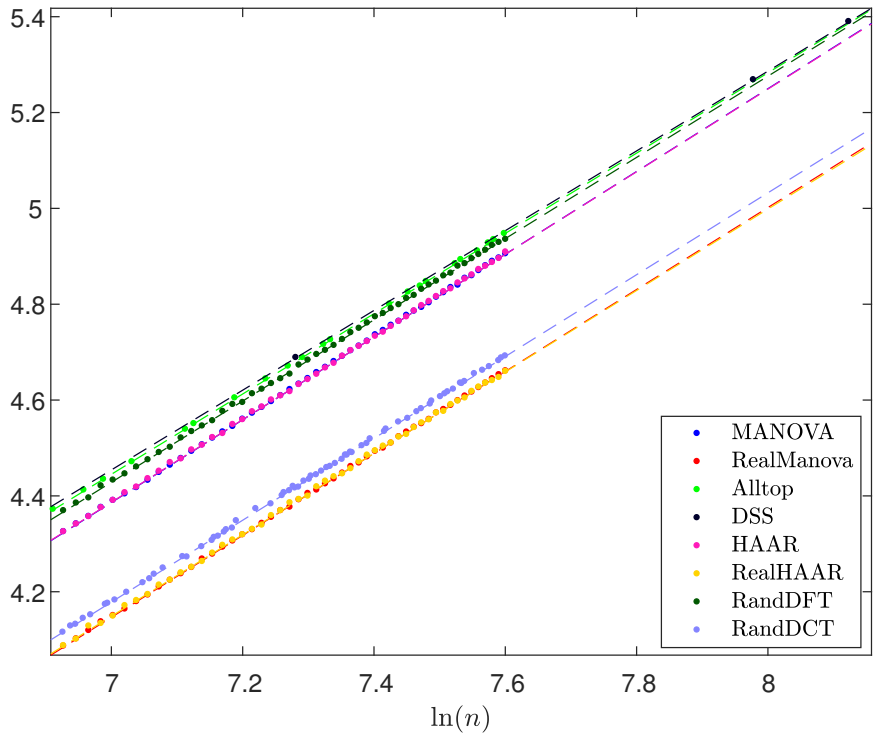

Figure 100: Test 1 for $\gamma = 0.25$ and $\beta = 0.6$. Plot shows $-\frac{1}{2}\ln \mathbb{E}_{K_n}(\Delta_{KS}(X_{K_n}^{(n)}; n, m_n, k_n)^2)$ over $\ln(n)$.

Frame	R^2	$\hat{b}$	$SE(\hat{b})$	p-value $b = b_{MANOVA}$
MANOVA	0.99995	0.86361	0.00088	1
DSS	1.00000	0.83218	0.00055	2.1430e-33
Alltop	0.99997	0.83782	0.00107	1.9002e-28
HAAR	0.99986	0.86226	0.00148	0.43162
RandDFT	0.99981	0.84749	0.00167	1.8150e-13
RealMANOVA	0.99993	0.85513	0.00103	1
RealHAAR	0.99971	0.84973	0.00209	0.02256
RandDCT	0.99980	0.85404	0.00149	0.54873

Table 58: Results of Test 1 (MSE) for $\gamma = 0.25$ and $\beta = 0.6$.

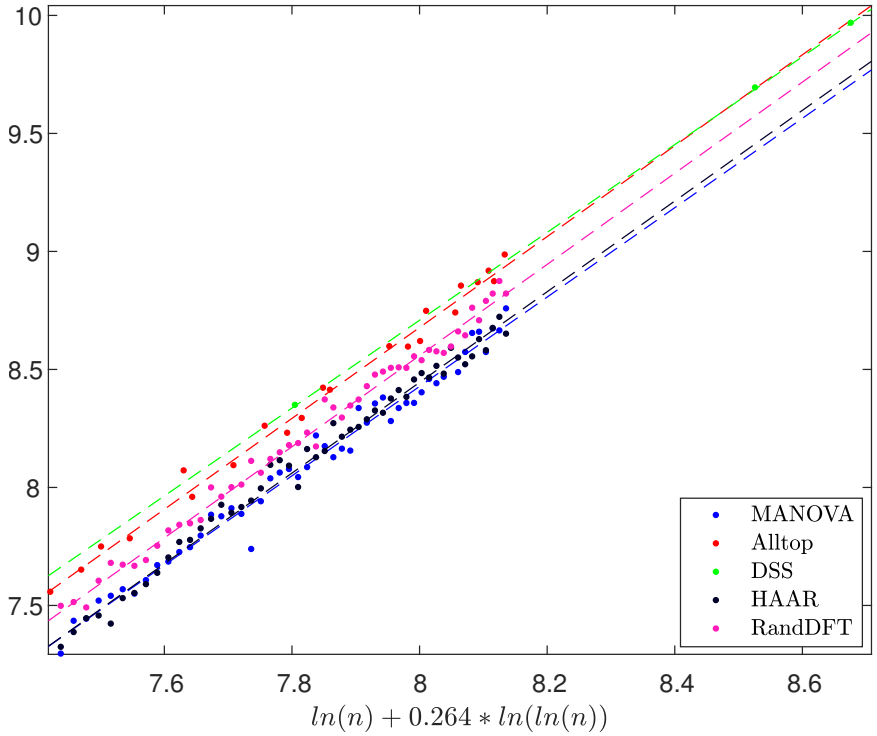

Figure 101: Test 2 for Ψ_{AC}, complex frames $\gamma = 0.25$ and $\beta = 0.6$. Plot shows $-\ln \mathbb{E}_{K_n}(\Delta_\Psi(X_{K_n}^{(n)}; n, m_n, k_n)^2)$

Frame	R^2	$\hat{b}$	$SE(\hat{b})$	p-value $b = b_{MANOVA}$
MANOVA	0.98243	1.89351	0.03655	1
DSS	0.99999	1.86080	0.00561	0.38065
Alltop	0.99071	1.92582	0.04170	0.56201
HAAR	0.98878	1.92117	0.02954	0.55743
RandDFT	0.99112	1.93144	0.02639	0.40216
RealMANOVA	0.99088	1.53352	0.02123	1
RealHAAR	0.97957	1.46262	0.03049	0.05935
RandDCT	0.97619	1.47286	0.02831	0.08926

Table 59: Results of Test 2 for Ψ_{AC}, $\gamma = 0.25$ and $\beta = 0.6$

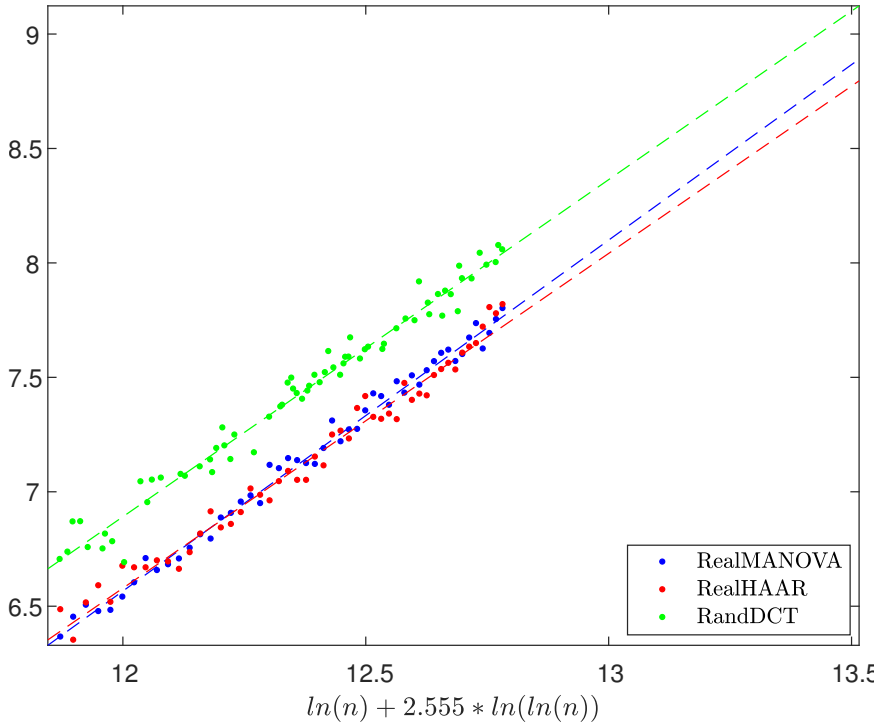

Figure 102: Test 2 for Ψ_{AC}, real frames $\gamma = 0.25$ and $\beta = 0.6$. Plot shows $-\ln \mathbb{E}_{K_n}(\Delta_\Psi(X_{K_n}^{(n)}; n, m_n, k_n)^2)$

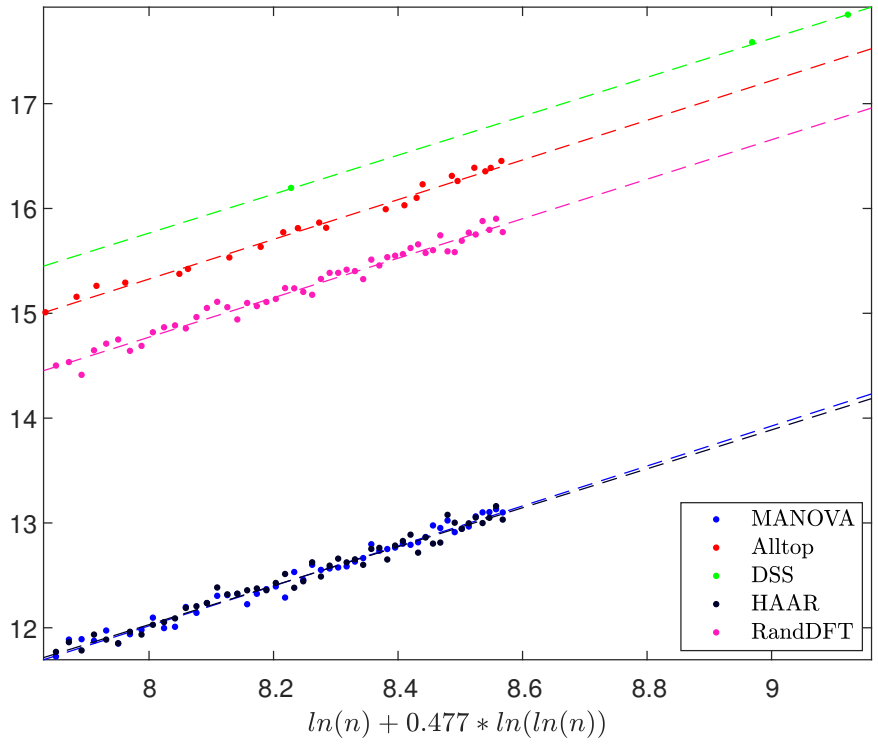

Figure 103: Test 2 for $\Psi_{Shannon}$, complex frames $\gamma = 0.25$ and $\beta = 0.6$. Plot shows $-\ln \mathbb{E}_{K_n}(\Delta_\Psi(X_{K_n}^{(n)}; n, m_n, k_n)^2)$

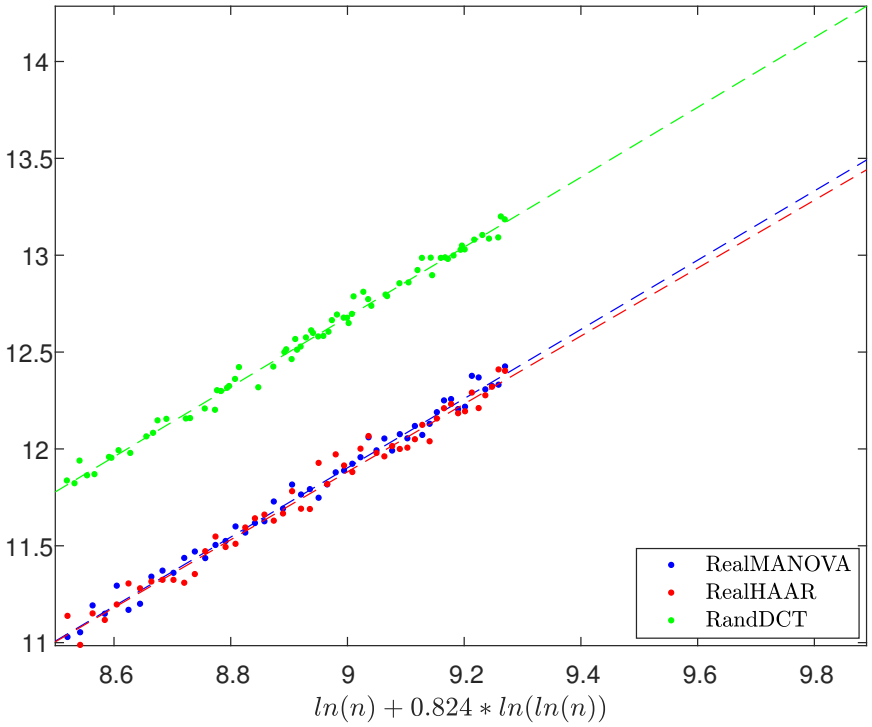

Figure 104: Test 2 for $\Psi_{Shannon}$, real frames $\gamma = 0.25$ and $\beta = 0.6$. Plot shows $-\ln \mathbb{E}_{K_n}(\Delta_\Psi(X_{K_n}^{(n)}; n, m_n, k_n)^2)$

Frame	R^2	$\hat{b}$	$SE(\hat{b})$	p-value $b = b_{MANOVA}$
MANOVA	0.98123	1.90661	0.03806	1
DSS	0.99982	1.85725	0.02489	0.28313
Alltop	0.98847	1.89320	0.04572	0.82235
HAAR	0.97592	1.85769	0.04212	0.39097
RandDFT	0.97595	1.88367	0.04268	0.68930
RealMANOVA	0.98856	1.78680	0.02774	1
RealHAAR	0.97955	1.75288	0.03656	0.46169
RandDCT	0.99173	1.80394	0.02028	0.61890

Table 60: Results of Test 2 for $\Psi_{Shannon}$, $\gamma = 0.25$ and $\beta = 0.6$

Frame	R^2	$\hat{b}$	$SE(\hat{b})$	p-value $b = b_{MANOVA}$
MANOVA	0.99092	1.31345	0.01815	1
DSS	0.99799	1.39998	0.06277	0.19159
Alltop	0.99492	1.36593	0.02183	0.06882
HAAR	0.99322	1.28966	0.01538	0.31990
RandDFT	0.99005	1.35857	0.01965	0.09494
RealMANOVA	0.98124	1.31460	0.02624	1
RealHAAR	0.98790	1.31414	0.02099	0.98897
RandDCT	0.99110	1.44101	0.01681	9.1562e-05

Table 61: Results of Test 2 for Ψ_{RIP}, $\gamma = 0.25$ and $\beta = 0.6$

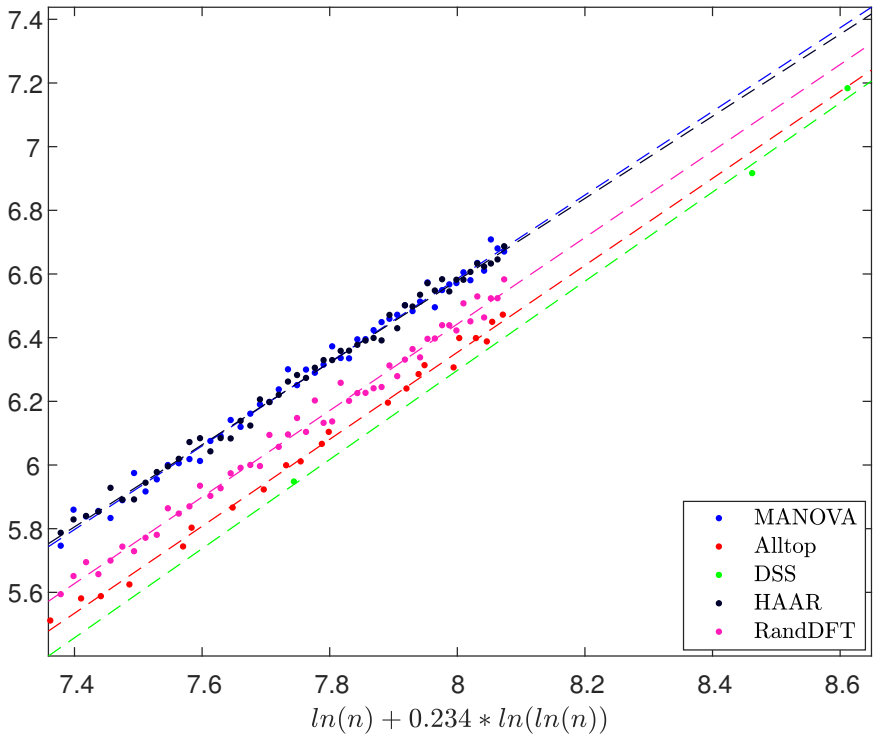

Figure 105: Test 2 for Ψ_{RIP}, complex frames $\gamma = 0.25$ and $\beta = 0.6$. Plot shows $-\ln \mathbb{E}_{K_n}(\Delta_\Psi(X_{K_n}^{(n)}; n, m_n, k_n)^2)$

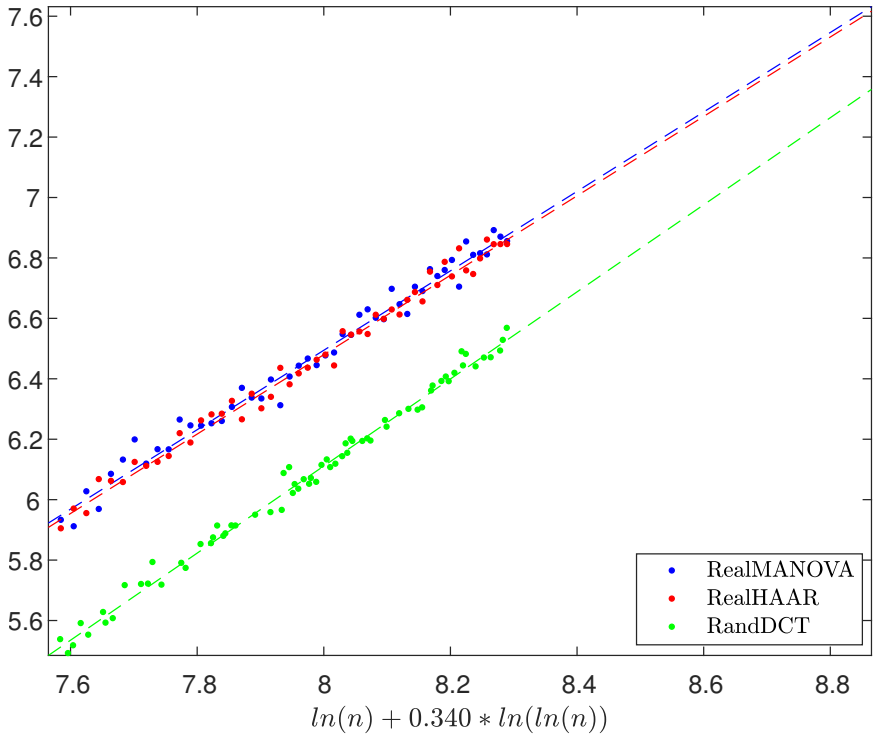

Figure 106: Test 2 for Ψ_{RIP}, real frames $\gamma = 0.25$ and $\beta = 0.6$. Plot shows $-\ln \mathbb{E}_{K_n}(\Delta_\Psi(X_{K_n}^{(n)}; n, m_n, k_n)^2)$

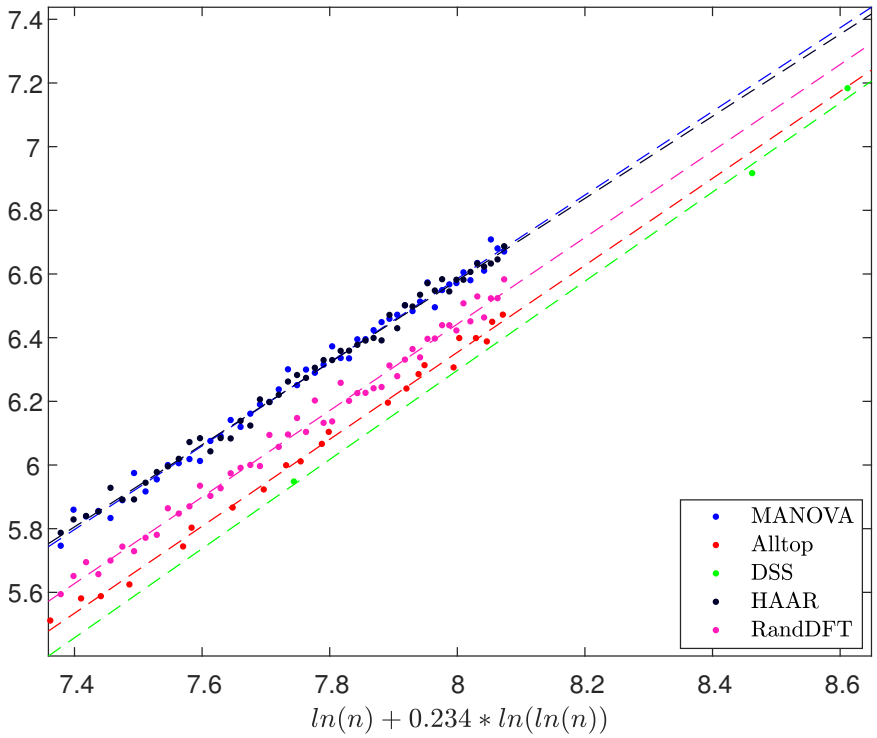

Figure 107: Test 2 for Ψ_{max}, complex frames $\gamma = 0.25$ and $\beta = 0.6$. Plot shows $-\ln \mathbb{E}_{K_n}(\Delta_\Psi(X_{K_n}^{(n)}; n, m_n, k_n)^2)$

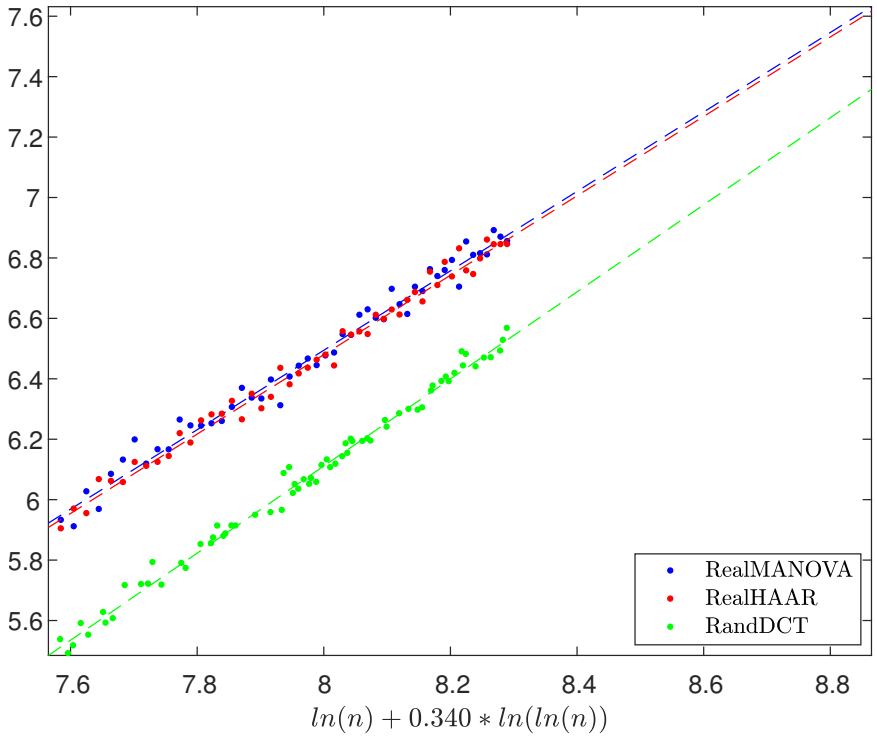

Figure 108: Test 2 for Ψ_{max}, real frames $\gamma = 0.25$ and $\beta = 0.6$. Plot shows $-\ln \mathbb{E}_{K_n}(\Delta_\Psi(X_{K_n}^{(n)}; n, m_n, k_n)^2)$

Frame	R^2	$\hat{b}$	$SE(\hat{b})$	p-value $b = b_{MANOVA}$
MANOVA	0.99092	1.31345	0.01815	1
DSS	0.99799	1.39998	0.06277	0.19159
Alltop	0.99492	1.36593	0.02183	0.06882
HAAR	0.99322	1.28966	0.01538	0.31990
RandDFT	0.99005	1.35857	0.01965	0.09494
RealMANOVA	0.98124	1.31460	0.02624	1
RealHAAR	0.98790	1.31414	0.02099	0.98897
RandDCT	0.99110	1.44101	0.01681	9.1562e-05

Table 62: Results of Test 2 for Ψ_{max}, $\gamma = 0.25$ and $\beta = 0.6$

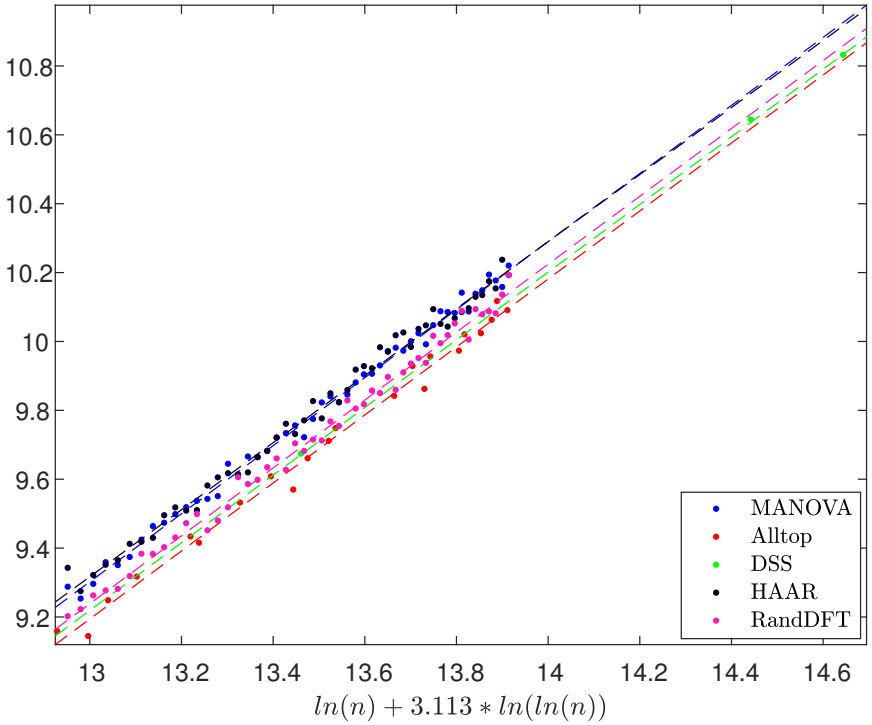

Figure 109: Test 2 for Ψ_{min}, complex frames $\gamma = 0.25$ and $\beta = 0.6$. Plot shows $-\ln \mathbb{E}_{K_n}(\Delta_\Psi(X^{(n)}_{K_n}; n, m_n, k_n)^2)$

Frame	R^2	$\hat{b}$	$SE(\hat{b})$	p-value $b = b_{MANOVA}$
MANOVA	0.99503	0.98800	0.01008	1
DSS	0.99993	0.98227	0.00825	0.66190
Alltop	0.99131	0.98723	0.02066	0.97357
HAAR	0.99098	0.97317	0.01340	0.37865
RandDFT	0.99265	0.98587	0.01224	0.89369
RealMANOVA	0.98207	0.92557	0.01805	1
RealHAAR	0.98914	0.93239	0.01410	0.76670
RandDCT	0.97997	0.96050	0.01690	0.16054

Table 63: Results of Test 2 for Ψ_{min}, $\gamma = 0.25$ and $\beta = 0.6$

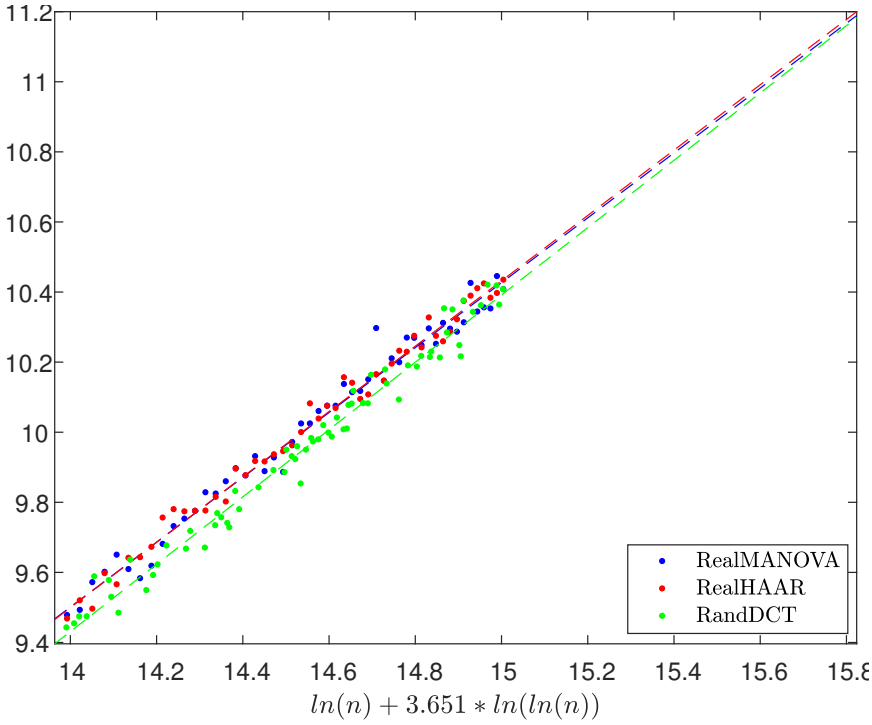

Figure 110: Test 2 for Ψ_{min}, real frames $\gamma = 0.25$ and $\beta = 0.6$. Plot shows $-\ln \mathbb{E}_{K_n}(\Delta_\Psi(X_{K_n}^{(n)}; n, m_n, k_n)^2)$

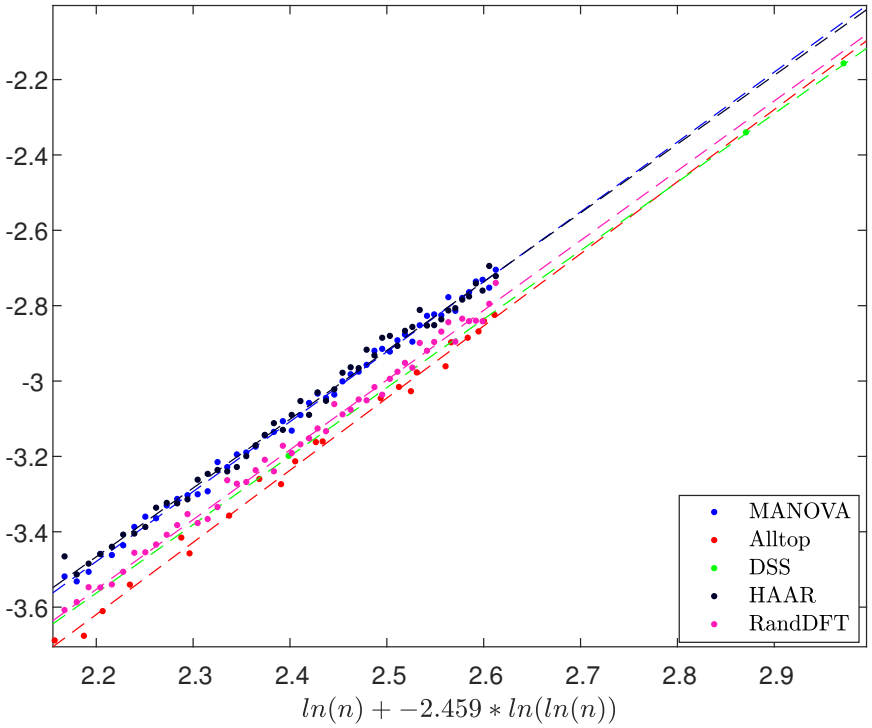

Figure 111: Test 2 for Ψ_{cond}, complex frames $\gamma = 0.25$ and $\beta = 0.6$. Plot shows $-\ln \mathbb{E}_{K_n}(\Delta_\Psi(X_{K_n}^{(n)}; n, m_n, k_n)^2)$

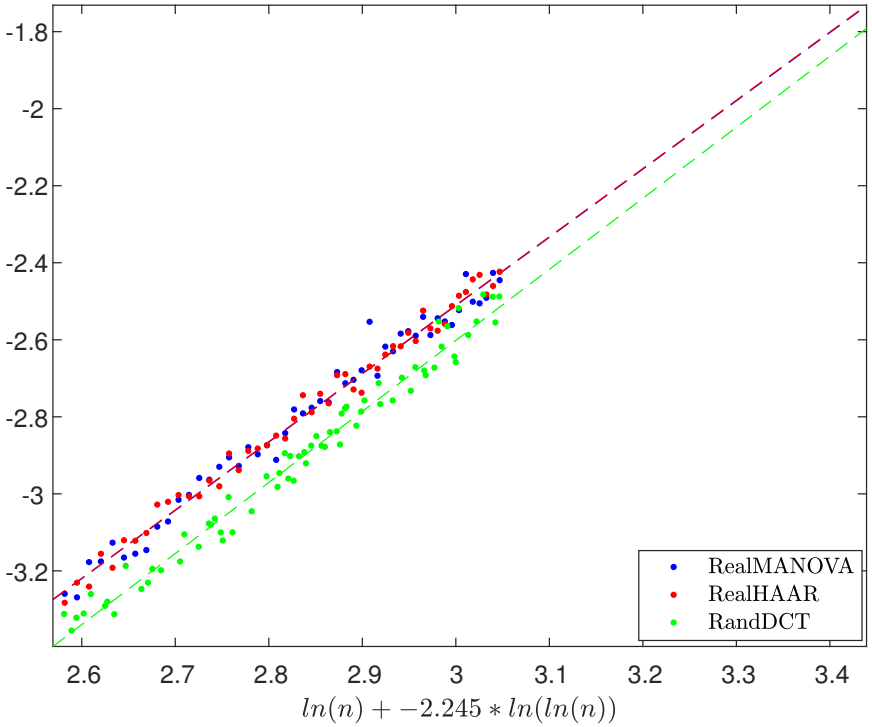

Figure 112: Test 2 for Ψ_{cond}, real frames $\gamma = 0.25$ and $\beta = 0.6$. Plot shows $-\ln \mathbb{E}_{K_n}(\Delta_\Psi(X_{K_n}^{(n)}; n, m_n, k_n)^2)$

Frame	R^2	$\hat{b}$	$SE(\hat{b})$	p-value $b = b_{MANOVA}$
MANOVA	0.99630	1.85529	0.01632	1
DSS	1.00000	1.81781	0.00044	0.02598
Alltop	0.99497	1.91434	0.03043	0.09181
HAAR	0.99271	1.82527	0.02258	0.28394
RandDFT	0.99379	1.85176	0.02113	0.89494
RealMANOVA	0.98234	1.77223	0.03430	1
RealHAAR	0.98912	1.77294	0.02684	0.98709
RandDCT	0.98002	1.84466	0.03242	0.12767

Table 64: Results of Test 2 for Ψ_{cond}, $\gamma = 0.25$ and $\beta = 0.6$

Table 65: Summary of Hypotheses Acceptance

Frame	H1	H2	H3	H4	H5	H6
Deterministic frames						
DSS	+	+	+	$(0.5, 0.5)$ $(0.5, 0.9)$	+	$(0.5, 0.3)$ Ψ_{RIP}, Ψ_{max}, Ψ_{min}, Ψ_{cond}
GF	+	+	+	$(0.5, 0.6)$ $(0.5, 0.9)$	+	$(0.5, 0.3)$ Ψ_{RIP}
RealPF	+	+	+	$(0.5, 0.8)$	+	$(0.5, 0.3)$ Ψ_{RIP}, Ψ_{max}, Ψ_{min}, Ψ_{cond} $(0.5, 0.7)$ Ψ_{max} $(0.5, 0.5)$ Ψ_{RIP}
ComplexPF	+	+	+	$(0.5, 0.7)$ $(0.5, 0.9)$ $(0.25, 0.8)$	+	$(0.5, 0.3)$ Ψ_{RIP}, Ψ_{max}
Alltop	+	+	+		+	$(0.5, 0.3)$ Ψ_{RIP}, Ψ_{max}, Ψ_{cond}
SS	+	+	+		+	$(0.5, 0.3)$ Ψ_{RIP}
SH	+	+	+		+	$(0.5, 0.9)$ Ψ_{RIP}, Ψ_{max}
Random frames						
HAAR	+	+	+	+	+	+
RealHAAR	+	+	+	+	+	+
RandDFT	+	+	+	$(0.25, 0.8)$	+	$(0.5, 0.3)$ Ψ_{RIP}, Ψ_{max}, Ψ_{cond}
RandDCT	+	+	+	+	+	$(0.5, 0.9)$ Ψ_{RIP} $(0.25, 0.6)$ Ψ_{RIP}, Ψ_{max}

Table 65 gives a summary of which hypotheses are accepted/rejected for the particular frame of interest. + means that the hypothesis was accepted for all 8 tested points in the (γ, β) phase space (and all functional from H5, H6), without any exceptions. Otherwise, the values for which the hypothesis was rejected for a certain frame are listed in the relevant cell. Empty cells correspond to frames which are irrelevant to the hypothesis.

A frame that does not satisfy the Universality Hypotheses

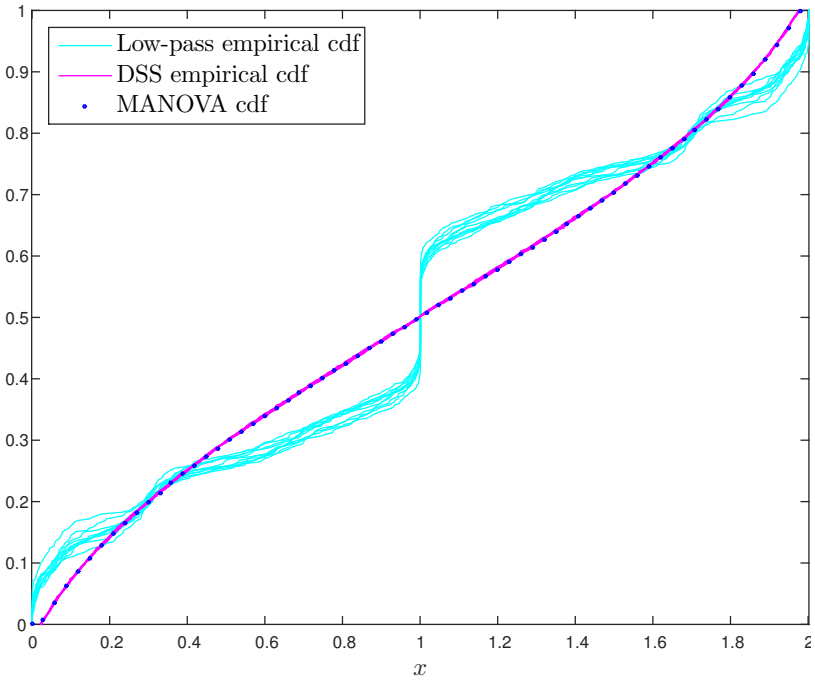

Figure 113: Empirical CDFs for 10 submatrices X_K of lowpass and DSS frames, $(n, m, k) = (947, 473, 394)$.

It is evident from Figure 113 that for low-pass frame, the limiting distribution of $\lambda(G_K)$, if exists, is not the MANOVA density. In contrast, the concentration of DSS frame example about the limiting spectrum is notable. In order to verify existence of limiting spectral distribution for low-pass frame, we performed the two-sample Kolmogorov-Smirnov test for pairs of submatrices and evaluated the mean squared KS-distance. Figure 114 shows the vanishing MSE for $T = 100$ pairs from each dimension. A submatrix of a low-pass frame

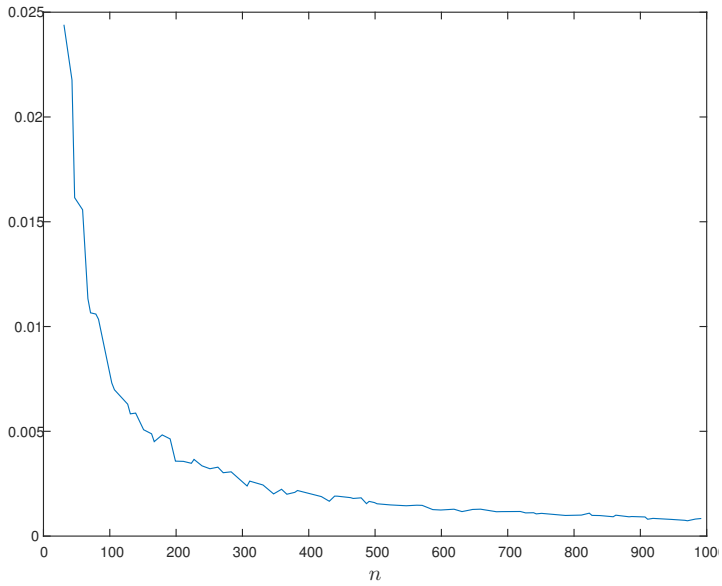

Figure 114: $\overline{\Delta^2}_{KS}(X_{K_1}, X_{K_2}; n, m, k)$, low-pass frame, $\gamma = 0.5$, $\beta = 0.8$.

can be considered as an k by m Vandermonde matrix with unit magnitude complex entries. The work in [1] and [2] establishes the existence of the empirical eigenvalue distribution in the large matrix limit on a wide range of independently and identically distributed phases for Vandermonde matrices. In our case the phases

correspond to the rows from a uniformly distributed random subset of size k which induces a non independant, though almost uniform distribution on the interval $[-\pi, \pi]$.

The case $\beta > 1$

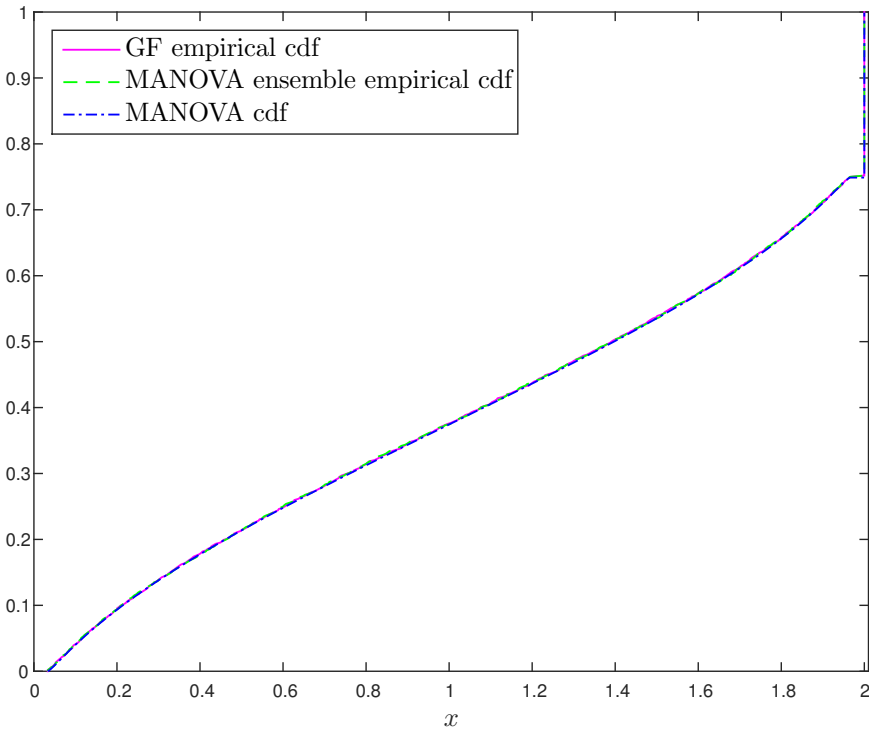

Figure 115: Distributions of non-zero eigenvalues, $\gamma = 0.5$, $\beta = 1.25$, $n = 1024$.

Figure 115 shows that also for $\beta > 1$ the following CDFs coincide: empirical spectral distribution of X_K from a Grassmannian frame (non-zero eigenvalues), empirical spectral distribution of a random matrix $\beta \cdot Y_{n,m,k,\mathbb{C}}$ and the theoretical density $\beta f_{\beta,\gamma}^{MANOVA}(x)$. Same fit to the limiting density is observed for all deterministic frames under study and nonstandard aspect ratio.

Data Deposition

The data have been deposited in mat files as well as json files in a folder named 'results' at `https://purl.stanford.edu/qg138qm8653`. This folder contains a subfolder for each configuration of parameters, ($\beta = 0.3, \gamma = 0.5$), ($\beta = 0.5, \gamma = 0.5$), ($\beta = 0.6, \gamma = 0.5$), ($\beta = 0.7, \gamma = 0.5$), ($\beta = 0.8, \gamma = 0.5$), ($\beta = 0.9, \gamma = 0.5$), ($\beta = 0.6, \gamma = 0.25$), ($\beta = 0.8, \gamma = 0.25$). Each one contains a folder named 'func' with results of functionals tests and a folder named 'KS' with results of Kolmogorov-Smirnov test. The results of each type are organized in 3 folders: 'all' with results of all frames, 'complex' with results of complex frames and 'real' with results of real frame. Every file is a struct with the following fields:

FrameName_KStest

- n_vec - vector of frame 'n' dimensions on which simulations were preformed.
- Niters - T - number of iterations.
- ks_var - N-dimensional vector with variances of KS-distances (over the iterations); N - length of n_vec.
- MSE - N-dimensional vector with MSEs of KS-distances.
- ks_max - N-dimensional vector with the maximal KS-distances.
- ks_mean - N-dimensional vector with the average KS-distances.
- p_var - N-dimensional vector with variances of p-values.
- p_mean - N-dimensional vector with the average p-values.
- beta - $\frac{1}{\beta}$ (the accurate $\frac{m}{k}$).
- name - string with the frame name (or the MANOVA ensemble).
- time - time that simulation on the frame/MANOVA ensemble lasted.
- num_workers - number of worker in the aws cluster.
- num_nodes - number of machines in the aws cluster.
- inds - indices of 'n' vector for which $\frac{k}{m}$ is as close to β as possible (depends on a frame, the subset of valid n's and m_n, for some exactly β can be achieved and for some it is not possible at all and the indices are the whole vector). Implemented only for ($\beta = 0.6, \gamma = 0.5$), ($\beta = 0.8, \gamma = 0.5$), the rest (with different grid) use the entire vector.

FrameName_functionalTest

- n_vec - vector of frame 'n' dimensions on which simulations were preformed.
- Niters - T - number of iterations.
- RIPBias - bias of RIP functional
- RIPVar - empirical variance of RIP functional
- RIPMse - MSE of RIP functional
- scoreBias - bias of AC (analog coding) functional
- scoreVar - empirical variance of AC functional
- scoreMse - MSE of AC functional
- scoreShannonBias - bias of Shannon functional

- scoreShannonVar - empirical variance of Shannon functional
- scoreShannonMse - MSE of Shannon functional
- minBias - bias of minimal eigenvalue functional
- minVar - empirical variance of minimal eigenvalue functional
- minMse - MSE of minimal eigenvalue functional
- maxBias - bias of maximal eigenvalue functional
- maxVar - empirical variance of maximal eigenvalue functional
- maxMse - MSE of maximal eigenvalue functional
- condBias - bias of condition number functional
- condVar - empirical variance of condition number functional
- condMse - MSE of condition number functional
- beta - $\frac{1}{\beta}$.
- name - string with the frame name (or the MANOVA ensemble).
- time - time that simulation on the frame/MANOVA ensemble lasted.
- num_workers - number of worker in the aws cluster.
- num_nodes - number of machines in the aws cluster.
- inds - indices of 'n' vector for which $\frac{k}{m}$ is as close to β as possible (deppends on a frame, the subset of valid n's and m_n, for some exctly β can be achieved and for some it is not possible at all and the indices are the whole vector).

"FrameNames" in file names:

- SS - Spikes and Sines
- SH - Spikes and Hadamard
- RS - Random Fourier transform (RandDFT)
- RHF - Orthogonal Haar frame (RealHAAR)
- RealPF - Real Paley's construction
- Rdct - Random Cosine transform (RandDCT)
- HF - Unitary Haar frame (HAAR)
- GF - Grassmannian frame
- DSS - Difference-set spectrum
- ComplexPF - Complex Paley's construction
- Alltop - Quadratic Phase Chirp
- AARManova - real MANOVA ensemble
- AAManova - complex MANOVA ensemble

Code Deposition

The code deposition consists of two folders 'Simulations' and 'TestingAndVisualizing' at `https://purl.stanford.edu/qg138qm8653`.

'Simulations' contains all scripts and functions used to produce the files with the results of the simulations.

- The script 'runKSTests.m' runs the Kolmogorov-Smirnov test on the entire spectrum for all frames and MANOVA ensemble and saves the results. Reproducibility nuance - results for $(\beta = 0.8, \gamma = 0.5)$ were produced with 'runKSTests1.m', results for $(\beta = 0.6, \gamma = 0.5)$ were produced with 'runKSTests.m', rest of the results for $\gamma = 0.5$ were produced with 'runKSTests2.m' and results for $\gamma = 0.25$ were produced with 'runKSTestsGamma4.m'. (In order to keep reproducability, new similar scripts and functions were added instead of generalizing the old ones.)
- The script 'runFuncTests.m' runs the functionals tests for all frames and MANOVA ensemble and saves the results. Reproducibility nuance - results for $(\beta = 0.8, \gamma = 0.5)$ and $(\beta = 0.6, \gamma = 0.5)$ were produced with 'runFuncTests.m', rest of the results for $\gamma = 0.5$ were produced with 'runFuncTests2.m' and results for $\gamma = 0.25$ were produced with 'runFuncTestsGamma4.m'.
- The script 'ParamsSelection.m' adds the vector of most accurate indices to structs of results.

'TestingAndVisualizing' contains all analysis scripts and functions used to generate all figures and tables from results files.

- The script 'mainTestAndPlot' presents the analyzed results of Kolmogorov-Smirnov and functional tests - plots and saves figures and tables of results. One should choose folder with .mat files with results (β value, ks/functionals,complexity) and follow the examples in the script.

(All scripts and functions are documented.)

References

[1] Debbah, M. (2008). Asymptotic Behaviour of Random Vandermonde Matrices with Entries on the Unit Circle. *arXiv preprint arXiv:0802.3570.*

[2] Tucci, G. H., Whiting, P. A. (2011). Eigenvalue results for large scale random vandermonde matrices with unit complex entries. *IEEE Transactions on Information Theory*, 57(6), 3938-3954.